

OPTIMIZED DELAY DIVERSITY FOR SUBOPTIMUM EQUALIZATION

by

YIU, SIMON TIK-KONG

B.A.Sc., The University of British Columbia, 2002

A THESIS SUBMITTED IN PARTIAL FULFILLMENT OF
THE REQUIREMENTS FOR THE DEGREE OF
MASTER OF APPLIED SCIENCE

in

THE FACULTY OF GRADUATE STUDIES

(Department of Electrical and Computer Engineering)

We accept this thesis as conforming
to the required standard

THE UNIVERSITY OF BRITISH COLUMBIA

April 2004

© Yiu, Simon Tik-Kong, 2004

Library Authorization

In presenting this thesis in partial fulfillment of the requirements for an advanced degree at the University of British Columbia, I agree that the Library shall make it freely available for reference and study. I further agree that permission for extensive copying of this thesis for scholarly purposes may be granted by the head of my department or by his or her representatives. It is understood that copying or publication of this thesis for financial gain shall not be allowed without my written permission.

Yiu, Simon Tik-Kong
Name of Author (please print)

08/04/2004
Date (dd/mm/yyyy)

Title of Thesis: Optimized Delay Diversity for
Suboptimum Equalization.

Degree: MASC.

Year: 2004

Department of Electrical & Computer Engineering.

The University of British Columbia

Vancouver, BC Canada

Abstract

Two novel optimized delay diversity (ODD) schemes for suboptimum equalization are proposed in this thesis. In [1, 2], an ODD scheme was proposed based on the Chernoff bound on the pairwise error probability (PEP) for maximum-likelihood sequence estimation (MLSE) [3]. It was shown that the ODD scheme outperforms the generalized delay diversity (GDD) scheme proposed in [4] in frequency-selective fading channels. However, the MLSE scheme is too complex for most practical applications. Therefore, low-complexity equalization schemes such as decision-feedback equalization (DFE) [5] or even linear equalization (LE) [6] have to be used. In this work, two novel ODD schemes are investigated. The ODD transmit filters of the two novel schemes are optimized for correlated multiple-input multiple-output (MIMO) frequency-selective Rayleigh fading channels with suboptimum DFE or LE employed at the receiver, respectively. An equivalent discrete-time channel model containing the DD transmit filters, the pulse shaping filters, the mobile channel, and the receiver input filters is first given. Then, the worst-case pairwise error probabilities (PEPs) for both DFE and LE are derived based on the discrete-time channel model and the error variances of the two schemes. Finally, a stochastic gradient algorithm for optimization of the ODD filter coefficients is proposed. The algorithm assumes knowledge of the channel impulse response (CIR) at the receiver while only the statistics of the CIRs are required at the transmitter. The proposed algorithm takes into account the equivalent discrete-time channel, the operating signal-to-noise ratio (SNR), the modulation scheme, the length of the ODD transmit filters as well as the correlations

of the transmit and receive antennas. The resulting ODD filters are applied to GSM¹ [7, 8] and EDGE² [9, 10]. Simulation results show that the ODD filters obtained in this work achieve a lower bit error rate (BER) than those obtained in [1, 2, 4] when DFE and LE are used at the receiver, respectively. The results of this thesis have been summarized in [11, 12].

¹GSM: Global System for Mobile Communication

²EDGE: Enhanced Data Rates for GSM Evolution

Contents

Abstract	ii
Contents	iv
List of Tables	viii
List of Figures	ix
List of Abbreviations and Symbols	xii
Acknowledgments	xv
1 Introduction	1
2 Transmission System	5
2.1 Channel Model	5
2.2 Correlation of CIR Coefficients	9
2.3 Complete Equivalent Baseband Model	11
2.4 Equivalent Discrete-Time Model	14
3 Delay Diversity (DD)	17
3.1 Diversity Techniques	17
3.2 Generalized Delay Diversity (GDD)	18
3.3 Optimized DD (ODD) for MLSE	19
4 Decision-Feedback Equalization and Linear Equalization	23

4.1	Decision-Feedback Equalization (DFE)	24
4.2	Linear Equalization (LE)	29
4.3	Performance of DFE and LE	31
5	PEP Estimation	33
5.1	SNR for DFE	34
5.2	SNR for LE	36
5.3	Pairwise Error Probability	37
6	Stochastic Gradient Algorithm	39
6.1	Gradient Vector	39
6.2	Gradient Vector for DFE-ODD	40
6.3	Gradient Vector for LE-ODD	41
6.4	Adaptive Algorithm	43
6.5	Convergence of the ODD Schemes	44
6.6	The Influence of δ	45
6.7	The Influence of \bar{N}	47
6.8	The Influence of the Initial ODD Filter Coefficients	51
6.9	The Influence of N	55
7	Simulation Results	59
7.1	Decision-Feedback Equalization	59
7.2	Linear Equalization	64
7.3	Future Work	66
8	Conclusions	75
	Bibliography	77
A	Optimized Filters	84
A.1	Filters for 2-PSK	85
A.1.1	DFE, EQ, $L = 7$, $N_T = 2$, $N_R = 1$, $\rho_t = [0.5]$	85
A.1.2	LE, EQ, $L = 7$, $N_T = 2$, $N_R = 1$, $\rho_t = [0.5]$	85

A.1.3	DFE, HT, $L = 7, N_T = 2, N_R = 1, \rho_t = [0.5]$	86
A.1.4	LE, HT, $L = 7, N_T = 2, N_R = 1, \rho_t = [0.5]$	86
A.1.5	DFE, TU, $L = 5, N_T = 2, N_R = 1, \rho_t = [0.7]$	87
A.1.6	LE, TU, $L = 5, N_T = 2, N_R = 1, \rho_t = [0.7]$	87
A.1.7	DFE, EQ, $L = 7, N_T = 2, N_R = 2, \rho_t = [0.5], \rho_r = [0.7]$.	88
A.1.8	LE, EQ, $L = 7, N_T = 2, N_R = 2, \rho_t = [0.5], \rho_r = [0.7]$. .	88
A.1.9	DFE, HT, $L = 7, N_T = 2, N_R = 2, \rho_t = [0.5], \rho_r = [0.7]$.	89
A.1.10	LE, HT, $L = 7, N_T = 2, N_R = 2, \rho_t = [0.5], \rho_r = [0.7]$. .	89
A.1.11	DFE, TU, $L = 5, N_T = 2, N_R = 2, \rho_t = [0.7], \rho_r = [0.7]$.	90
A.1.12	LE, TU, $L = 5, N_T = 2, N_R = 2, \rho_t = [0.7], \rho_r = [0.7]$. .	90
A.1.13	DFE, EQ, $L = 7, N_T = 3, N_R = 1, \rho_t = [0.5, 0.5, 0.5]$. .	91
A.1.14	LE, EQ, $L = 7, N_T = 3, N_R = 1, \rho_t = [0.5, 0.5, 0.5]$. . .	91
A.1.15	DFE, HT, $L = 7, N_T = 3, N_R = 1, \rho_t = [0.2, 0.5, 0.2]$. .	92
A.1.16	LE, HT, $L = 7, N_T = 3, N_R = 1, \rho_t = [0.2, 0.5, 0.2]$. . .	92
A.1.17	DFE, TU, $L = 5, N_T = 3, N_R = 1, \rho_t = [0.7, 0.5, 0.7]$. .	93
A.1.18	LE, TU, $L = 5, N_T = 3, N_R = 1, \rho_t = [0.7, 0.5, 0.7]$. . .	93
A.1.19	DFE, EQ, $L = 7, N_T = 3, N_R = 2, \rho_t = [0.5, 0.7, 0.5],$ $\rho_r = [0.7]$	94
A.1.20	LE, EQ, $L = 7, N_T = 3, N_R = 2, \rho_t = [0.5, 0.7, 0.5],$ $\rho_r = [0.7]$	94
A.1.21	DFE, HT, $L = 7, N_T = 3, N_R = 2, \rho_t = [0.5, 0.5, 0.5],$ $\rho_r = [0.7]$	95
A.1.22	LE, HT, $L = 7, N_T = 3, N_R = 2, \rho_t = [0.5, 0.5, 0.5],$ $\rho_r = [0.7]$	95
A.1.23	DFE, TU, $L = 5, N_T = 3, N_R = 2, \rho_t = [0.5, 0.2, 0.5],$ $\rho_r = [0.7]$	96
A.1.24	LE, TU, $L = 5, N_T = 3, N_R = 2, \rho_t = [0.5, 0.2, 0.5],$ $\rho_r = [0.7]$	96
A.2	Filters for 8-PSK	97
A.2.1	DFE, EQ, $L = 7, N_T = 2, N_R = 1, \rho_t = [0.5]$	97

A.2.2	LE, EQ, $L = 7, N_T = 2, N_R = 1, \rho_t = [0.5]$	97
A.2.3	DFE, HT, $L = 7, N_T = 2, N_R = 1, \rho_t = [0.5]$	98
A.2.4	LE, HT, $L = 7, N_T = 2, N_R = 1, \rho_t = [0.5]$	98
A.2.5	DFE, TU, $L = 5, N_T = 2, N_R = 1, \rho_t = [0.7]$	99
A.2.6	LE, TU, $L = 5, N_T = 2, N_R = 1, \rho_t = [0.7]$	99
A.2.7	DFE, EQ, $L = 7, N_T = 2, N_R = 2, \rho_t = [0.5], \rho_r = [0.7]$.	100
A.2.8	LE, EQ, $L = 7, N_T = 2, N_R = 2, \rho_t = [0.5], \rho_r = [0.7]$. .	100
A.2.9	DFE, HT, $L = 7, N_T = 2, N_R = 2, \rho_t = [0.5], \rho_r = [0.7]$.	101
A.2.10	LE, HT, $L = 7, N_T = 2, N_R = 2, \rho_t = [0.5], \rho_r = [0.7]$. .	101
A.2.11	DFE, TU, $L = 5, N_T = 2, N_R = 2, \rho_t = [0.7], \rho_r = [0.7]$.	102
A.2.12	LE, TU, $L = 5, N_T = 2, N_R = 2, \rho_t = [0.7], \rho_r = [0.7]$. .	102
A.2.13	DFE, EQ, $L = 7, N_T = 3, N_R = 1, \rho_t = [0.5, 0.5, 0.5]$. .	103
A.2.14	LE, EQ, $L = 7, N_T = 3, N_R = 1, \rho_t = [0.5, 0.5, 0.5]$. . .	103
A.2.15	DFE, HT, $L = 7, N_T = 3, N_R = 1, \rho_t = [0.2, 0.5, 0.2]$. .	104
A.2.16	LE, HT, $L = 7, N_T = 3, N_R = 1, \rho_t = [0.2, 0.5, 0.2]$. . .	104
A.2.17	DFE, TU, $L = 5, N_T = 3, N_R = 1, \rho_t = [0.7, 0.5, 0.7]$. .	105
A.2.18	LE, TU, $L = 5, N_T = 3, N_R = 1, \rho_t = [0.7, 0.5, 0.7]$. . .	105
A.2.19	DFE, EQ, $L = 7, N_T = 3, N_R = 2, \rho_t = [0.5, 0.7, 0.5],$ $\rho_r = [0.7]$	106
A.2.20	LE, EQ, $L = 7, N_T = 3, N_R = 2, \rho_t = [0.5, 0.7, 0.5],$ $\rho_r = [0.7]$	106
A.2.21	DFE, HT, $L = 7, N_T = 3, N_R = 2, \rho_t = [0.5, 0.5, 0.5],$ $\rho_r = [0.7]$	107
A.2.22	LE, HT, $L = 7, N_T = 3, N_R = 2, \rho_t = [0.5, 0.5, 0.5],$ $\rho_r = [0.7]$	107
A.2.23	DFE, TU, $L = 5, N_T = 3, N_R = 2, \rho_t = [0.5, 0.2, 0.5],$ $\rho_r = [0.7]$	108
A.2.24	LE, TU, $L = 5, N_T = 3, N_R = 2, \rho_t = [0.5, 0.2, 0.5],$ $\rho_r = [0.7]$	108

List of Tables

7.1	MLSE-ODD and DFE-ODD comparison: 2-PSK, EQ, $L = 7$, $N_T = 2$, $N_R = 1$, and $\rho_t = [0.5]$	61
7.2	DFE-ODD filter coefficients: 2-PSK, EQ, $L = 7$, $N_T = 2$, $N_R =$ 2 , $\rho_t = [0.5]$, and $\rho_r = [0.7]$	62
7.3	MLSE-ODD and DFE-ODD comparison: 8-PSK, EQ, $L = 7$, $N_T = 3$, $N_R = 2$, $\rho_t = [0.5, 0.7, 0.5]$, and $\rho_r = [0.7]$	63
7.4	LE-ODD filter coefficients: 2-PSK, EQ, $L = 7$, $N_T = 2$, $N_R = 1$, $\rho_t = [0.5]$	65
7.5	LE-ODD filter coefficients: 2-PSK, HT, $L = 7$, $N_T = 3$, $N_R = 1$, $\rho_t = [0.2, 0.5, 0.2]$	65

List of Figures

2.1	Frequency selective MIMO channel.	7
2.2	Overall transmission system.	11
2.3	DD transmit filters.	12
3.1	Discrete-time block diagram of generalized delay diversity.	19
4.1	Block diagram of DFE with N_R receive antennas.	24
4.2	Block diagram of LE with N_R receive antennas.	30
6.1	$\mathcal{E}\{\text{PEP}_{\text{DFE}}(\mathbf{h}, \mathbf{g})\}$ vs. number of iterations for 2-PSK transmission over EQ channel with $L = 7$, $N_T = N_R = 2$, $N = 3$, $\bar{N} = 10$, $\boldsymbol{\rho}_t = [0.5]$, $\boldsymbol{\rho}_r = [0.7]$, and DFE at the receiver.	46
6.2	$\mathcal{E}\{\text{PEP}_{\text{DFE}}(\mathbf{h}, \mathbf{g})\}$ vs. number of iterations for 8-PSK transmission over EQ channel with $L=7$, $N_T = 2$, $N_R = 1$, $N = 3$, $\bar{N} = 10$, $\boldsymbol{\rho}_t = [0.5]$, and DFE at the receiver.	47
6.3	$\mathcal{E}\{\text{PEP}_{\text{LE}}(\mathbf{h}, \mathbf{g})\}$ vs. number of iterations for 2-PSK transmission over EQ channel with $L = 7$, $N_T = N_R = 2$, $N = 3$, $\bar{N} = 10$, $\boldsymbol{\rho}_t = [0.5]$, $\boldsymbol{\rho}_r = [0.7]$, and LE at the receiver.	48
6.4	$\mathcal{E}\{\text{PEP}_{\text{LE}}(\mathbf{h}, \mathbf{g})\}$ vs. number of iterations for 8-PSK transmission over EQ channel with $L = 7$, $N_T = 2$, $N_R = 1$, $N = 3$, $\bar{N} = 10$, $\boldsymbol{\rho}_t = [0.5]$, and LE at the receiver.	49
6.5	Simulated BER vs. \bar{N} for DFE and LE.	50

6.6	PEP _{DFE} ($\mathbf{h}[i], \mathbf{g}$) vs. i for 8-PSK transmission over EQ profile with $N_T = 2, N_R = 1, N = 3, \boldsymbol{\rho}_t = [0.5]$, and DFE employed at receiver. Solid line: $\bar{N} = 5$. Dashed line: $\bar{N} = 100$	51
6.7	$\mathcal{E}\{\text{PEP}_{\text{DFE}}(\mathbf{h}, \mathbf{g})\}$ vs. number of iterations for 2-PSK transmission over EQ channel with $L = 7, N_T = N_R = 2, N = 3, \delta = 10, \boldsymbol{\rho}_t = [0.5], \boldsymbol{\rho}_r = [0.7]$, and DFE at the receiver. Circles: $\mathbf{g}[0] = [1\ 0\ 0\ 0\ 0\ 1]^T$. Triangles: $\mathbf{g}[0] = 1/\sqrt{3}[1\ 1\ 1\ 1\ 1\ 1]^T$	53
6.8	$\mathcal{E}\{\text{PEP}_{\text{DFE}}(\mathbf{h}, \mathbf{g})\}$ vs. number of iterations for 8-PSK transmission over EQ channel with $L = 7, N_T = 2, N_R = 1, N = 3, \delta = 0.1, \boldsymbol{\rho}_t = [0.5]$, and DFE at the receiver. Circles: $\mathbf{g}[0] = [1\ 0\ 0\ 0\ 0\ 1]^T$. Triangles: $\mathbf{g}[0] = 1/\sqrt{3}[1\ 1\ 1\ 1\ 1\ 1]^T$	54
6.9	$\mathcal{E}\{\text{PEP}_{\text{LE}}(\mathbf{h}, \mathbf{g})\}$ vs. number of iterations for 8-PSK transmission over EQ channel with $L = 7, N_T = N_R = 2, N = 3, \delta = 10, \boldsymbol{\rho}_t = [0.5], \boldsymbol{\rho}_r = [0.7]$, and LE at the receiver. Circles: $\mathbf{g}[0] = [1\ 0\ 0\ 0\ 0\ 1]^T$. Triangles: $\mathbf{g}[0] = 1/\sqrt{3}[1\ 1\ 1\ 1\ 1\ 1]^T$	55
6.10	$\mathcal{E}\{\text{PEP}_{\text{LE}}(\mathbf{h}, \mathbf{g})\}$ vs. number of iterations for 8-PSK transmission over EQ channel with $L = 7, N_T = 2, N_R = 1, N = 3, \delta = 0.05, \boldsymbol{\rho}_t = [0.5]$, and LE at the receiver. Circles: $\mathbf{g}[0] = [1\ 0\ 0\ 0\ 0\ 1]^T$. Triangles: $\mathbf{g}[0] = 1/\sqrt{3}[1\ 1\ 1\ 1\ 1\ 1]^T$	56
6.11	Simulated BER of DFE vs. N for 2-PSK transmission over EQ channel with $L = 7, N_T = 2, N_R = 1$ and $\boldsymbol{\rho}_t = [0.5]$	57
6.12	Simulated BER of LE vs. N for 2-PSK transmission over EQ channel with $L = 7, N_T = 2, N_R = 1$ and $\boldsymbol{\rho}_t = [0.5]$	58
7.1	2-PSK simulations for GDD, MLSE-ODD, and DFE-ODD filters.	67
7.2	2-PSK simulations for GDD, MLSE-ODD, and DFE-ODD filters.	68
7.3	8-PSK simulations for GDD, MLSE-ODD, and DFE-ODD filters.	69
7.4	8-PSK simulations for GDD, MLSE-ODD, and DFE-ODD filters.	70
7.5	2-PSK simulations for GDD, MLSE-ODD, and LE-ODD filters.	71
7.6	2-PSK simulations for GDD, MLSE-ODD, and LE-ODD filters.	72
7.7	8-PSK simulations for GDD, MLSE-ODD, and LE-ODD filters.	73

List of Abbreviations and Symbols

Acronyms

AWGN	Additive white Gaussian noise
BER	Bit error rate
BT	Time-bandwidth
CIR	Channel impulse response
CSI	Channel state information
DD	Delay diversity
DFE	Decision-feedback equalization
DFSE	Decision feedback sequence estimation
EDGE	Enhanced data rates for GSM evolution
FBF	Feedback filter
FFF	Feed-forward filter
GDD	Generalized delay diversity
GMSK	Gaussian minimum shift keying
GSM	Global system for mobile communication
ISI	Intersymbol interference
LE	Linear equalization
LOS	Line-of-sight
LSSE	Least sum of squared errors
MIMO	Multiple-input multiple-output

MLSE	Maximum-likelihood sequence estimation
MMSE	Minimum mean-square error
MSE	Mean-square error
ODD	Optimized delay diversity
OFDM	Orthogonal frequency division multiplexing
pdf	probability density function
PEP	Pairwise error probability
PSK	Phase shift keying
QAM	Quadrature amplitude modulation
SDD	Standard delay diversity
SIMO	Single-input multiple-output
SISO	Single-input single-output
SNR	Signal-to-noise ratio
SRC	Square-root raised cosine
STBC	Space-time block codes
STTC	Space-time trellis codes
VA	Viterbi algorithm
WMF	Whitened matched filter
ZF	Zero forcing

Operators and Notation

$ \cdot $	Absolute value of a complex number
$\cdot * \cdot$	Convolution
$\cdot \otimes \cdot$	Kronecker product
$\delta(\cdot)$	Dirac delta function
$\mathcal{E}\{\cdot\}$	Expectation
$\det(\cdot)$	Determinant
$\text{tr}(\cdot)$	Trace

$[\cdot]^*$	Complex conjugate
$[\cdot]^T$	Matrix or vector transposition
$[\cdot]^H$	Matrix or vector hermitian transposition
$\mathbf{0}_m$	Zero vector with m elements
$\mathbf{I}_{m \times m}$	Identity matrix with dimension $m \times m$

Acknowledgments

I would like to extend my sincere thanks to my supervisor Professor Robert Schober for his invaluable guidance and for giving me invaluable insight into my research. Professor Schober provided much of the initial motivation for pursuing this investigation and also provided invaluable feedback that has improved this work in nearly every aspect.

I would also like to extend my thanks to Thorsten Hehn for his detailed explanation on the simulation program that I use for this work. Furthermore, I am also very thankful to Dr. Lampe Lutz for his comments on my presentation to the communications group.

Finally, I would like to thank my parents, brother and sister who have always encouraged me in my quest for higher education and especially Amy Lau for encouraging me and listening to my occasional whining and sighing.

Chapter 1

Introduction

Multiple-input multiple-output (MIMO) wireless systems [13, 14, 15] have recently gained much interest due to the increasing demand for higher data rates in wireless communications systems. Space-time coding is the subject of current research activities. Space-time trellis codes (STTCs) and space-time block codes (STBCs) constructed for the flat-fading channel are discussed in [16] and [17, 18], respectively. STTC proposed in [16] can be used in frequency-selective channels as well, however, the coding gain diminishes due to the effect of multipath fading [19].

Although most of the initial research on space-time codes assumed flat fading channels, more recently it has been shown that space-time codes can also lead to significant improvements for frequency-selective fading channels. Space-time coding schemes designed for frequency-selective fading channels that require processing of an entire burst of data have been proposed in [20, 21, 22, 23, 24]. The scheme in [20] is a generalization of Alamouti's STBC in [17], whereas the schemes in [21, 22] and [23, 24] are based on orthogonal frequency division multiplexing (OFDM) and single-carrier transmission combined with frequency domain equalization, respectively.

These burst-based space-time coding schemes achieve good performance. However, the channel is required to be constant over the entire data burst. In addition, if these schemes are used to upgrade existing systems from single an-

tenna transmission to multiple antenna transmission, the burst structure and the receiver have to be modified. These disadvantages may make burst-based space-time codes less attractive for the upgrade of existing systems.

Delay diversity (DD), which can be regarded as the simplest special case of a STTC, was proposed in [25]. It uses multiple transmit antennas to achieve transmit diversity for flat fading channels. DD has the advantage that the overall channel can be modeled as a single-input multiple-output (SIMO) system. Therefore, the same channel estimation, channel tracking, and equalization techniques as in the single transmit antenna case can be used. As a consequence, existing mobile communication systems can be upgraded easily with DD since the current burst structure does not have to be modified. A generalized delay diversity (GDD) scheme suitable for frequency-selective channels was proposed in [4]. At high signal-to-noise ratios (SNRs), GDD achieves full diversity by delaying the transmitted data stream on transmit antenna n_t , $1 \leq n_t \leq N_T$, by $(n_t - 1)L$ symbols where N_T and L are the number of transmit antennas and the length of the discrete-time channel impulse response (CIR), respectively. However, the resulting overall CIR may be excessively long implying high equalizer complexity.

Based on a Chernoff bound on the pairwise error probability (PEP) for maximum-likelihood sequence estimation (MLSE), optimized delay diversity (ODD) filters for correlated MIMO frequency-selective fading channels were obtained in [1, 2]. For the realistic case of low-to-moderate SNR, the resulting MLSE-ODD filters significantly outperform the GDD filters. In addition, the optimized filters do not only outperform the GDD filters of the same length but perform often better than GDD filters of larger length. As shorter filters lead to an equalizer with lower complexity at the receiver, the MLSE-ODD filters are preferable.

However, in many situations the complexity of optimum MLSE is still too high even with the shorter MLSE-ODD filters [3, 26]. This is especially true when higher order modulation schemes, such as 8-ary phase-shift keying (PSK) [27],

are employed since the computational complexity of MLSE grows as M^{L-1} , where M is size of the modulation alphabet [27]. Therefore, in practice, sub-optimum equalization strategies such as decision-feedback equalization (DFE) [5] or linear equalization (LE) [6] have to be adopted at the receiver. It is the aim of this work to obtain the ODD filters for correlated MIMO frequency-selective fading channels assuming DFE or LE being used at the receiver.

Based on an approximation of the worst-case PEP of the respective equalizer, a cost function that is suitable for the optimization of the ODD filter coefficients is derived for both DFE and LE, respectively. Since a closed-form solution for the optimization problem is not feasible, a stochastic gradient algorithm is used for the filter search. The resulting schemes are referred to as DFE-ODD and LE-ODD, respectively. We consider transmissions in the downlink direction and we adopt the system parameters of the global system for mobile communication (GSM) [7, 8] and enhanced data rates for GSM evolution system (EDGE) [9, 10] for numerical results. Simulation results show that when DFE or LE are employed at the receiver, the filters optimized for DFE and LE outperform the GDD filters proposed in [4] and MLSE-ODD filters proposed in [1, 2].

The outline of this work is as follows. In Chapter 2, we describe the adopted correlated MIMO frequency-selective Rayleigh fading model, and the GSM and EDGE power delay profiles. The DD filters, the GDD filters, and the ODD filters optimized for MLSE are briefly discussed in Chapter 3. In Chapter 4, we give a review on the finite-length DFE and LE and explain how to obtain the equalizer filter coefficients based on the minimum mean-square error (MMSE) criterion. In Chapter 5, we explain how the expected worst-case PEP is calculated by using the output error variance of DFE and LE with infinite-length filters. We use the expected worst-case PEP obtained in Chapter 5 to derive a stochastic gradient algorithm for optimization of the ODD filter coefficients in Chapter 6. In Chapter 7, we present the simulation results for the optimization and compare the proposed DFE-ODD filters and LE-ODD

filters with the MLSE-ODD filters and GDD filters. Finally, we summarize this work and draw some conclusions in Chapter 8. In Appendix A, DFE-ODD filters and LE-ODD filters for some typical GSM and EDGE channels are presented.

Chapter 2

Transmission System

In this chapter, the overall transmission system consisting of signal mapper, DD filters, pulse shaping filters, correlated MIMO channel, receiver input filters, equalizer, and demapper will be discussed. It will be first shown that the correlated MIMO channel with N_T transmit antennas and N_R receive antennas can be modeled by matrices with dimension $N_R \times N_T$. We will then show that the overall channel model, continuous in time, can be obtained by convolving the correlated MIMO channel with the pulse shaping filters, and the receiver input filters. Furthermore, an overall discrete-time channel model is obtained by sampling and truncating the continuous-time CIR. Finally, an equivalent channel model containing the combined effect of the overall discrete-time channel and DD filters is derived.

2.1 Channel Model

The correlated MIMO frequency-selective Rayleigh fading channel model is adopted in this work. In a MIMO wireless link, the data stream is broken into separate signals and sent over different transmit antennas. The frequency

non-selective MIMO channel can be modeled by the following matrix [13]:

$$\mathbf{H}_C(t) = \begin{bmatrix} h_C^{11}(t) & h_C^{12}(t) & \dots & h_C^{1N_T}(t) \\ h_C^{21}(t) & h_C^{22}(t) & \dots & h_C^{2N_T}(t) \\ \vdots & & & \vdots \\ h_C^{N_R1}(t) & h_C^{N_R2}(t) & \dots & h_C^{N_RN_T}(t) \end{bmatrix}. \quad (2.1)$$

$h_C^{n_r n_t}(t)$ is the continuous-time Rayleigh fading channel gain between transmit antenna n_t , $1 \leq n_t \leq N_T$, and receive antenna n_r , $1 \leq n_r \leq N_R$, where N_T and N_R are the total number of transmit and receive antennas, respectively. The complex gain $h_C^{n_r n_t}(t)$ is a continuous-time zero mean Gaussian random process

$$h_C^{n_r n_t}(t) = h_I^{n_r n_t}(t) + j h_Q^{n_r n_t}(t), \quad (2.2)$$

where $h_I^{n_r n_t}(t)$ and $h_Q^{n_r n_t}(t)$ are the real and imaginary parts of $h_C^{n_r n_t}(t)$, respectively [27]. The envelope of the process, $\zeta^{n_r n_t}(t) = |h_C^{n_r n_t}(t)|$, is Rayleigh distributed with probability density function (pdf)

$$p_\zeta(x) = \begin{cases} \frac{x}{\sigma_0^2} e^{-\frac{x^2}{2\sigma_0^2}}, & \text{for } x \geq 0 \\ 0, & \text{for } x < 0 \end{cases}, \quad (2.3)$$

where σ_0^2 is the variance of the two quadrature channels. Since $h_I^{n_r n_t}(t)$ and $h_Q^{n_r n_t}(t)$ are assumed to be independent, the variance of $h_C^{n_r n_t}(t)$ is equal to $2\sigma_0^2$.

The frequency non-selective model described by (2.1) is only valid when the signal bandwidth is much smaller than the coherence bandwidth of the channel. If the signal has a bandwidth greater than the coherence bandwidth, the transmitted signal is subjected to different gains and phase shifts across the band. In such a case, the channel is said to be frequency-selective [27]. A frequency-selective channel causes intersymbol interference (ISI). The received signal will be the superposition of several transmitted signals. ISI can be mitigated by employing an equalizer at the receiver side. MLSE, DFE, and LE are some of the equalization methods which are commonly used in practice. More details about equalizers will be discussed in Chapter 4.

A frequency-selective MIMO model with L multipath components is shown in Figure 2.1. $x_{n_t}(t)$ represents the signal transmitted by transmit antenna

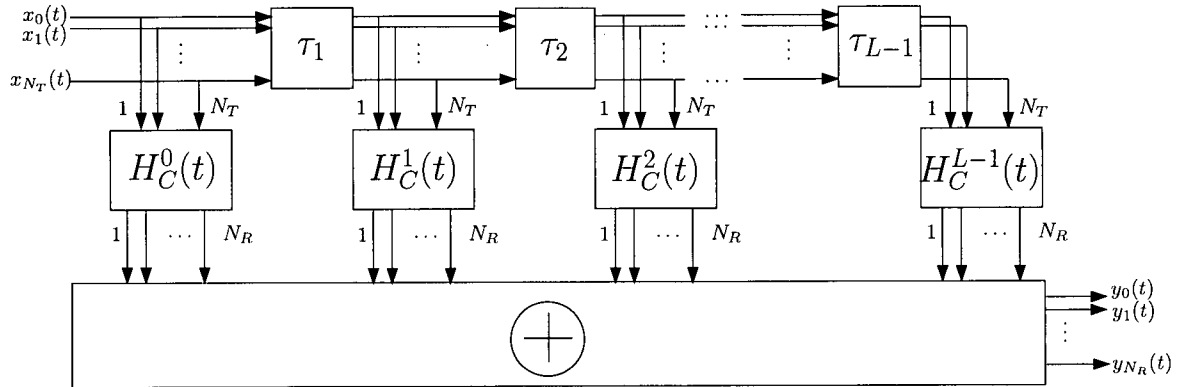


Figure 2.1: Frequency selective MIMO channel.

n_t , while $y_{n_r}(t)$ represents the signal received by receive antenna n_r . τ_l , $l = 1, \dots, L-1$, represents the delay of the multipath component l . Each matrix, $\mathbf{H}_C^l(t)$, $l = 0, \dots, L-1$, has dimension $N_R \times N_T$ and its elements can be written as [13, 27]

$$\mathbf{H}_C^l(t) = \begin{bmatrix} h_C^{11,l}(t) & h_C^{12,l}(t) & \dots & h_C^{1N_T,l}(t) \\ h_C^{21,l}(t) & h_C^{22,l}(t) & \dots & h_C^{2N_T,l}(t) \\ \vdots & \vdots & \ddots & \vdots \\ h_C^{N_R1,l}(t) & h_C^{N_R2,l}(t) & \dots & h_C^{N_RN_T,l}(t) \end{bmatrix}. \quad (2.4)$$

The matrices $\mathbf{H}_C^l(t)$ are independent for different l s, $l = 0, \dots, L-1$, and their elements, $h_C^{n_r n_t, l}(t)$, are continuous-time zero mean Gaussian random processes as defined in (2.2).

The overall MIMO channel impulse response $\mathbf{H}_C(\tau, t)$ is also a matrix with dimension $N_R \times N_T$. It relates to the matrices $\mathbf{H}_C^l(t)$ in the following way

$$\mathbf{H}_C(\tau, t) = \sum_{l=0}^{L-1} \mathbf{H}_C^l(t) \delta(\tau - \tau_l), \quad (2.5)$$

where $\delta(\cdot)$ is the Dirac delta function [28] and τ_0 is equal to zero.

Therefore, the matrix elements in (2.4) and (2.5) are related by the following

equation:

$$h_C^{n_r n_t}(\tau, t) = \sum_{l=0}^{L-1} h_C^{n_r n_t, l}(t) \delta(\tau - \tau_l). \quad (2.6)$$

The power delay profile [29] of the channel is defined as

$$p(\tau) = \sum_{l=0}^{L-1} (\sigma_C^{n_r n_t, l})^2 \delta(\tau - \tau_l), \quad (2.7)$$

where $(\sigma_C^{n_r n_t, l})^2$ is the variance of $h_C^{n_r n_t, l}(t)$,

$$(\sigma_C^{n_r n_t, l})^2 = \mathcal{E} \left\{ \left| h_C^{n_r n_t, l}(t) \right|^2 \right\}. \quad (2.8)$$

In practice, $(\sigma_C^{n_r n_t, l})^2$ are normalized such that

$$\sum_{l=0}^{L-1} (\sigma_C^{n_r n_t, l})^2 = 1 \quad (2.9)$$

is true.

For GSM and EDGE system, four different power delay profiles are specified [7]: rural area (RA), hilly terrain (HT), typical urban area (TU) and equalizer test (EQ). For EQ, HT, and TU, it is assumed that the amplitudes of all propagation paths, $h_C^{n_r n_t, l}(t)$, are continuous-time zero mean Gaussian random processes as described by (2.2). Their envelopes are Rayleigh distributed with pdf as defined in (2.3). For RA, it is assumed that the amplitudes of all propagation paths are continuous-time non-zero mean Gaussian random processes. The mean value is due to the line-of-sight (LOS) path between a transmit antenna and a receive antenna. This results in a Rician fading channel. In this work, the EQ, HT, and TU profiles are considered.

Finally, it should be noted that if N_T and N_R are both equal to one, the MIMO channel in (2.4) reduces to a single-input single-output (SISO) frequency-selective Rayleigh fading channel. Furthermore, if $L = 1$, the channel reduces to a frequency non-selective channel resulting in only scalar multiplicative distortion of the transmitted signals.

2.2 Correlation of CIR Coefficients

In general, an i.i.d. model assuming rich uniform scattering will not be an accurate description of real-world multi-antenna channels [30], since in practice, insufficient antenna spacing and a lack of scattering cause the individual antennas to be correlated. Therefore, spatial correlation is assumed to occur at both the transmit and receive antennas in this work. Under this assumption, the matrix taps in (2.4) can be written as [30]

$$\mathbf{H}_C^l(t) = \mathbf{R}^{1/2} \mathbf{H}^l(t) (\mathbf{S}^{1/2})^H, \quad (2.10)$$

where $\mathbf{H}^l(t)$, $\mathbf{R} = \mathbf{R}^{1/2}(\mathbf{R}^{1/2})^H$, and $\mathbf{S} = \mathbf{S}^{1/2}(\mathbf{S}^{1/2})^H$ are the uncorrelated channel matrix taps, the receive correlation matrix and the transmit correlation matrix, respectively. The superscripts $1/2$ and H denote the matrix square-root and Hermitian transposition, respectively. Although not completely general, this simple correlation model has been validated through recent field measurements as a sufficiently accurate representation of the fade correlations seen in actual cellular systems [30, 31]. \mathbf{S} and \mathbf{R} are positive definite matrices with dimensions $N_T \times N_T$ and $N_R \times N_R$, respectively.

From now on, we assume the MIMO model defined in (2.5) to be a spatially correlated frequency-selective MIMO channel with matrix taps described by (2.10). For simplicity, we assume that the spatial correlation is identical for all matrix taps. Setups with up to three transmit and two receive antennas are considered in this work. Since matrices \mathbf{S} and \mathbf{R} have the same form, we will concentrate on the transmit correlation matrix in the following discussion.

There is only one correlation factor for the two antennas case. The correlation matrix \mathbf{S} can be written as

$$\mathbf{S} = \begin{bmatrix} 1 & \rho_{12}^t \\ \rho_{12}^t & 1 \end{bmatrix}, \quad (2.11)$$

where ρ_{12}^t is the correlation factor between transmit antenna one and transmit

antenna two and it is defined by

$$\rho_{12}^t = \frac{\mathcal{E} \{ h_C^{n_r,1,l}(t) h_C^{n_r,2,l^*}(t) \}}{\sqrt{(\sigma_C^{n_r,1,l})^2 (\sigma_C^{n_r,2,l})^2}}. \quad (2.12)$$

There are three correlation factors for the three antennas case, ρ_{12}^t , ρ_{23}^t , and ρ_{13}^t . They represent the correlation between transmit antenna one and transmit antenna two, between transmit antenna two and transmit antenna three, and between transmit antenna one and transmit antenna three, respectively. The resulting correlation matrix is a 3×3 matrix with elements

$$\mathbf{S} = \begin{bmatrix} 1 & \rho_{12}^t & \rho_{13}^t \\ \rho_{12}^t & 1 & \rho_{23}^t \\ \rho_{13}^t & \rho_{23}^t & 1 \end{bmatrix}. \quad (2.13)$$

The square root of the correlation matrix can be calculated by using Cholesky decomposition such that $\mathbf{S}^{1/2}$ and $\mathbf{R}^{1/2}$ are lower triangular whereas $(\mathbf{S}^{1/2})^H$ and $(\mathbf{R}^{1/2})^H$ are upper triangular [32]. $\mathbf{S}^{1/2}$ for the two and three transmit antennas case can be written as

$$\mathbf{S}^{1/2} = \begin{bmatrix} 1 & 0 \\ \rho_{12}^t & \sqrt{1 - (\rho_{12}^t)^2} \end{bmatrix}, \quad (2.14)$$

and

$$\mathbf{S}^{1/2} = \begin{bmatrix} 1 & 0 & 0 \\ \rho_{12}^t & \sqrt{1 - (\rho_{12}^t)^2} & 0 \\ \rho_{13}^t & \frac{\rho_{23}^t - \rho_{12}^t \rho_{13}^t}{\sqrt{1 - (\rho_{12}^t)^2}} & \sqrt{1 - (\rho_{13}^t)^2 - \frac{(\rho_{23}^t - \rho_{12}^t \rho_{13}^t)^2}{1 - (\rho_{12}^t)^2}} \end{bmatrix}, \quad (2.15)$$

respectively. Similar results can be obtained for the receive antennas by replacing the correlation factors in the above matrices with the respective receive correlation factors. For future convenience,

$$\boldsymbol{\rho}_t = \begin{bmatrix} \rho_{12}^t & \rho_{13}^t & \rho_{23}^t \end{bmatrix} \quad (2.16)$$

and

$$\boldsymbol{\rho}_r = \begin{bmatrix} \rho_{12}^r & \rho_{13}^r & \rho_{23}^r \end{bmatrix} \quad (2.17)$$

are defined, where $\boldsymbol{\rho}_t$ and $\boldsymbol{\rho}_r$ are the correlation vectors for the transmit and receive antennas, respectively.

2.3 Complete Equivalent Baseband Model

The channel model presented in the previous section is only a part of the overall mobile communications transmission model. The other parts of the model are discussed in this section. A block diagram of the equivalent baseband system model is shown in Figure 2.2.

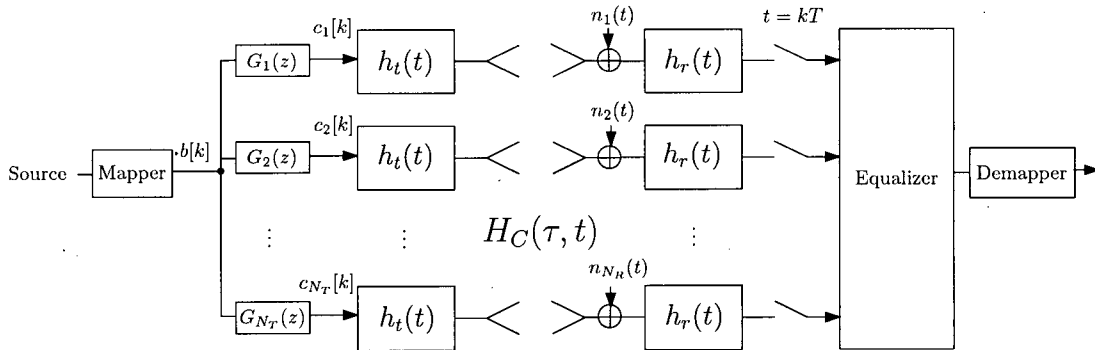


Figure 2.2: Overall transmission system.

The binary input data sequence is first mapped to symbols belong to a linear modulation format such as M -ary phase-shift keying (PSK) or quadrature amplitude modulation (QAM) symbol. We consider GSM and EDGE in this work. Therefore, the mapped symbol is either a 2-PSK or an 8-PSK symbol depending on whether GSM or EDGE is used. Note that GSM uses binary Gaussian minimum-shift keying (GMSK), which can be approximated as filtered 2-PSK. EDGE improves spectral efficiency by employing 8-PSK modulation instead. However, other system parameters such as symbol rate and burst duration remain unchanged in order to enable a smooth transition from GSM to EDGE [33].

Before transmit pulse shaping, the modulated symbols, $b[k]$, are first filtered by the DD transmit filters, $G_{n_t}(z)$. The DD transmit filters depicted in Figure 2.2 are discrete-time filters, which can be realized as tapped delay lines. The filtering process is shown in Figure 2.3.

The filter is defined by

$$G_{n_t}(z) = \sqrt{\frac{E_s}{N_T}} \sum_{n=0}^{N-1} g_{n_t}[n] z^{-n}, \quad n_t = 1, \dots, N_T \quad (2.18)$$

where $g_{n_t}[n]$ is the n th filter tap of the DD filter of transmit antenna n_t . All DD filters have length N . In order to keep the total transmitted energy E_s constant, a factor $\sqrt{E_s/N_T}$ is applied to each transmit antenna branch. As a result, the filtered symbols $c_{n_t}[k]$ of antenna n_t can be obtained from the modulated symbols $b[k]$ by

$$c_{n_t}[k] = \sqrt{\frac{E_s}{N_T}} \cdot (b[k] * g_{n_t}[k]), \quad (2.19)$$

where $*$ refers to convolution.

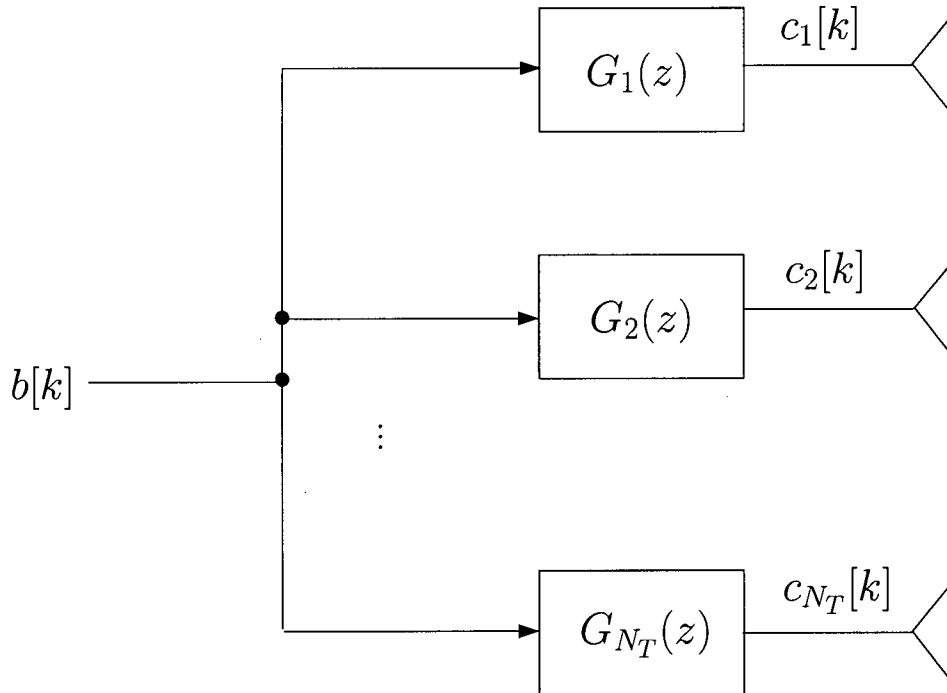


Figure 2.3: DD transmit filters.

For transmit pulse shaping, the linearized impulse $h_t(t)$ corresponding to Gaussian Minimum Shift Keying (GMSK) with time-bandwidth (BT) product 0.3 is employed [27]. Therefore, the transmit filter impulse response is given by

[33, 34, 35]

$$h_t(t) = \begin{cases} \prod_{k=0}^3 s(t + kT), & 0 \leq t \leq 5T \\ 0, & \text{else} \end{cases} \quad (2.20)$$

with

$$s(t) = \begin{cases} \sin\left(\pi \int_0^t g(\tau) d\tau\right), & 0 \leq t \leq 4T \\ \sin\left(\frac{\pi}{2} - \pi \int_0^{t-4T} g(\tau) d\tau\right), & 4T \leq t \leq 8T \\ 0, & \text{else} \end{cases} \quad (2.21)$$

where $T = 3.69\mu\text{s}$ is the symbol duration. The impulse $g(t)$ of duration $4T$ is given by

$$g(t) = \frac{1}{2T} \left(Q\left(2\pi \cdot 0.3 \frac{t - \frac{5T}{2}}{T\sqrt{\ln(2)}}\right) - Q\left(2\pi \cdot 0.3 \frac{t - \frac{3T}{2}}{T\sqrt{\ln(2)}}\right) \right), \quad 0 \leq t \leq 4T, \quad (2.22)$$

where $Q(\cdot)$ denotes the complementary Gaussian error integral [27],

$$Q(t) = \frac{1}{\sqrt{2\pi}} \int_t^{+\infty} e^{-\tau^2/2} d\tau. \quad (2.23)$$

The continuous-time signals are transmitted over the correlated MIMO channel $\mathbf{H}_C(\tau, t)$ discussed in the last section. At the receiver, the continuous-time received signal at antenna n_r is impaired by additive white Gaussian noise (AWGN) $n_{n_r}(t)$. The choice of the receiver input filter, $h_r(t)$, is up to the receiver designer. We assume a filter with square-root Nyquist frequency response. This allows us to model the channel noise after sampling as a spatially and temporally white discrete-time Gaussian random process. More will be said about the discrete-time channel model in Section 2.4.

Two filters which have a square-root Nyquist frequency response are the whitened matched filter (WMF) [27], which belongs to the class of optimum receiver input filters [3], and the square-root raised cosine (SRC) filter [27, 29]. We use a fixed filter in this work, namely the SRC receive filter with roll-off

factor 0.3 [29]. This filter offers a similar performance as the optimum WMF. However, the implementation of the SRC filter is simpler because, in contrast to the WMF, it does not have to be adapted to a particular channel impulse response [33]. The discrete-time received signals are obtained by sampling the output of the receiver input filters at times $t = kT$. Finally, the receiver, assumed to have perfect knowledge of the overall CIR, performs equalization of the received signals and the demapper converts the detected symbols back to binary data.

It should be noted that the DD transmit filters $G_{n_t}(z)$, the pulse shaping filters $h_t(t)$, and the receiver input filters $h_r(t)$, introduce additional ISI to the MIMO channel. In addition, the pulse shaping filters and receiver input filters introduce temporal correlation to the channel.

2.4 Equivalent Discrete-Time Model

The overall channel model discussed in the previous section is in continuous-time and contains different blocks including the pulse shaping filters $h_t(t)$, the physical channel $\mathbf{H}(\tau, t)$, and the receiver input filters $h_r(t)$. It is convenient to derive an equivalent discrete-time model containing the combined effects of all these blocks. In this section, we will show how the discrete-time model can be obtained.

In this work, block fading is assumed. That is, the wireless channel coefficients $h_C^{n_r n_t, l}(t)$ defined in (2.4) are approximately constant during one burst but vary from burst to burst. In other words, the coefficients $h_C^{n_r n_t, l}(t)$ are time-invariant within each burst. This assumption is valid for small-to-moderate burst lengths and low vehicle speeds. With this assumption, the time dependence of $h_C^{n_r n_t, l}(t)$

can be dropped and (2.4) reduces to

$$\mathbf{H}_C^l = \begin{bmatrix} h_C^{11,l} & h_C^{12,l} & \dots & h_C^{1N_T,l} \\ h_C^{21,l} & h_C^{22,l} & \dots & h_C^{2N_T,l} \\ \vdots & \vdots & \ddots & \vdots \\ h_C^{N_R1,l} & h_C^{N_R2,l} & \dots & h_C^{N_RN_T,l} \end{bmatrix}. \quad (2.24)$$

Now, the overall CIR can be obtained from

$$h_{n_r n_t}(t) = h_t(t) * h_C^{n_r n_t}(t) * h_r(t), \quad (2.25)$$

where

$$h_C^{n_r n_t}(t) = \sum_{l=0}^{L-1} h_C^{n_r n_t, l} \delta(t - \tau_l). \quad (2.26)$$

One can also obtain the above equation from (2.6). Since the channel is time-invariant, t in (2.6) is fixed and can be dropped from the equation. Therefore, the only variable left is τ . Replacing τ with t yields $h_C^{n_r n_t}(t)$.

In principle, the overall CIR is of infinite length. However, in practice, it can be sampled and truncated to L consecutive taps which exhibit maximum energy [36]. Therefore, the sampled and truncated overall CIR can be written as

$$h_{n_r n_t}[l] = h_C^{n_r n_t}(lT + t_0), \quad l = 0, \dots, L - 1 \quad (2.27)$$

where t_0 is a small time delay. L and t_0 are chosen so that only a negligible amount of power is disregarded.

With this discrete-time channel model, the T -spaced, sampled version of the received signal at receive antenna n_r is

$$r_{n_r}[k] = \sum_{n_t=1}^{N_T} \sum_{l=0}^{L-1} h_{n_r n_t}[l] c_{n_t}[k-l] + n_{n_r}[k], \quad (2.28)$$

where $c_{n_t}[k]$ is defined in (2.19). Note that $n_{n_r}[k] = n_{n_r}(kT + t_0)$ in (2.28) is spatially and temporally white because the SRC receive filter autocorrelation function fulfills the first Nyquist criterion [27].

Furthermore, (2.28) can be written as

$$\begin{aligned}
r_{n_r}[k] &= \sqrt{\frac{E_s}{N_T}} \sum_{n_t=1}^{N_T} h_{n_r n_t}[k] * b[k] * g_{n_t}[k] + n_{n_r}[k] \\
&= h_{n_r}^{\text{eq}}[k] * b[k] + n_{n_r}[k] \\
&= \sum_{l=0}^{L+N-2} h_{n_r}^{\text{eq}}[l] b[k-l] + n_{n_r}[k],
\end{aligned} \tag{2.29}$$

where $h_{n_r}^{\text{eq}}[k]$ is the equivalent CIR with length $L_{\text{eq}} = L + N - 1$ corresponding to receive antenna n_r and is defined as

$$h_{n_r}^{\text{eq}}[k] = \sqrt{\frac{E_s}{N_T}} \sum_{n_t=1}^{N_T} h_{n_r n_t}[k] * g_{n_t}[k]. \tag{2.30}$$

Therefore, the overall discrete-time channel can be modeled as a SIMO system with equivalent CIR, $h_{n_r}^{\text{eq}}[k]$.

The discussions in this chapter are valid for both GSM and EDGE systems because they use the same frequency bands, transmit pulse shaping filters, and receiver input filters [7]. It should also be noted that the model is not restricted to GSM and EDGE systems, but is applicable to any system that employs linear single-carrier modulation.

Chapter 3

Delay Diversity (DD)

A key feature of a MIMO system is its ability to use multipath propagation to increase data rate or to improve spatial diversity [13, 14, 15]. In this work it is not intended to use the MIMO channel to increase the capacity but for diversity reasons. In this chapter, we will review the different diversity techniques briefly and we will then concentrate on delay diversity, which is the form of diversity investigated in this work.

3.1 Diversity Techniques

Diversity means that the receiver is provided with independently faded versions of the same information. If several replicas of the same information signal are transmitted over independently fading channels, the probability that all the signal components will fade simultaneously is very small [27]. In wireless communications, there are three main forms of diversity techniques which are widely used: frequency diversity, time diversity, and spatial diversity.

Frequency diversity creates redundancy in the frequency domain by transmitting the same information-bearing signal on multiple carriers. This is reasonable because the multipath structure in different frequency bands is different for a frequency-selective channel. The drawback of frequency diversity is the extra spectrum required to achieve the diversity. This limits the number of

mobile users and the amount of bandwidth available to each user at a given time.

Time diversity creates redundancy in the time domain by transmitting the same information signal at different points in time. It uses the fact that in a time-variant channel, the fading in different time intervals is different. The major drawbacks of time diversity are the waste of bandwidth due to repetition and the delay constraints making it hard to exploit.

The final type of diversity which is commonly used is spatial diversity. Spatial diversity creates redundancy in the spatial domain by using more than one antenna either at the transmitter or receiver side. It uses the fact that different antennas see different multipath characteristics. This form of diversity can be further broken into transmit diversity and receive diversity. One major drawback of spatial diversity is the requirement of deploying multiple antennas at either the transmitter or receiver side, which is not always possible due to size constraints or economic reasons. However, spatial diversity is attractive because no bandwidth expansion is required to achieve diversity. DD is a form of spatial diversity because the information signal is transmitted by different antennas. DD basically transforms spatial diversity into frequency diversity by increasing the length of the overall channel by N .

3.2 Generalized Delay Diversity (GDD)

As we have already mentioned in the last section, DD for MIMO systems introduces redundancy in the spatial domain to provide diversity. The block diagram of a DD transmitter with N_T transmit antennas is shown in Figure 3.1.

In GDD, the filtered symbols $c_{n_t}[k]$ are delayed versions of the data symbols, $b[k]$. The delay is achieved by employing N_T discrete-time DD filters with $g_{n_t}[k]=1$ for $k = (n_t - 1)D$ and $g_{n_t}[k]=0$ for $k \neq (n_t - 1)D$. When $D = 1$, standard delay diversity (SDD) [37] results where the source symbol is delayed

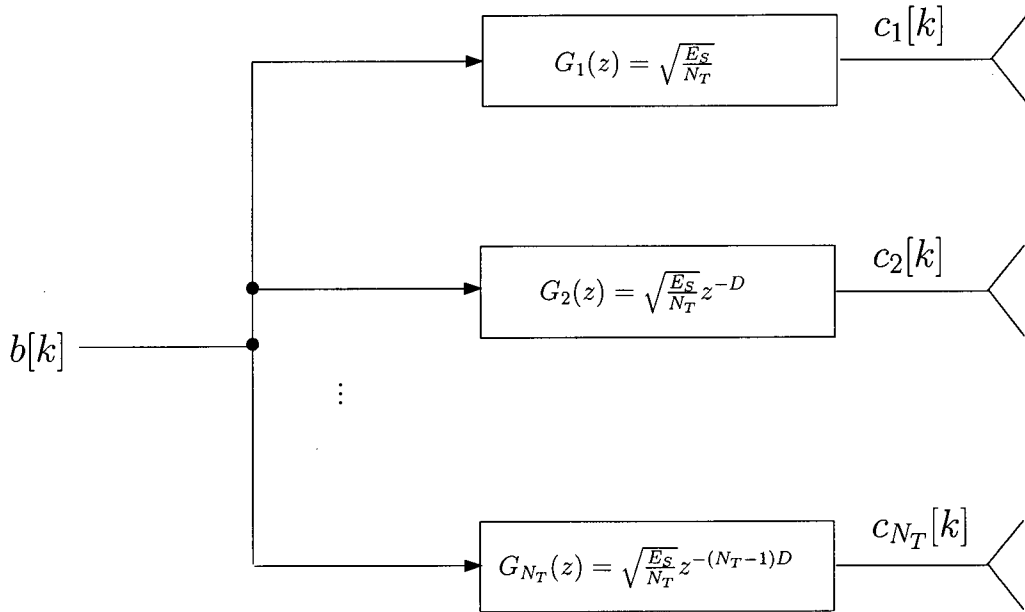


Figure 3.1: Discrete-time block diagram of generalized delay diversity.

by one symbol period for each antenna. SDD achieves full spatio-temporal diversity in flat-fading channels [37]. However, it has been shown that SDD fails to exploit full diversity over frequency-selective channels [4]. There has been some effort to improve the performance of SDD on frequency-selective channels in the context of channel equalization [38, 39, 40].

It has been shown in [4] that full spatio-temporal diversity can be achieved over frequency-selective channels if D is chosen to be equal to the length of the overall CIR L . The resulting GDD filters have a length of $N = (N_T - 1)L + 1$ and coefficients $g_{n_t}[k] = 1$ for $k = (n_t - 1)L$ and $g_{n_t}[k] = 0$ for $k \neq (n_t - 1)L$.

3.3 Optimized DD (ODD) for MLSE

Although full diversity can be achieved by GDD, the resulting equivalent channel is excessively long. In [1, 2], a cost function that is suitable for optimization of the DD transmit filter coefficients was derived based on a Chernoff upper bound on the PEP for optimum MLSE. It was shown that the shorter optimized DD filters achieve a better performance than the GDD filters at

low-to-moderate SNRs.

The PEP is the probability that the detector decides in favour of symbol $b_\alpha[k]$ although $b_\beta[k]$ has been transmitted. According to [1, 2], the PEP of MLSE can be approximated by

$$P_e(b_\alpha[k], b_\beta[k]) \approx \frac{1}{\det \left(\mathbf{I}_{L_{\text{eq}}N_R \times L_{\text{eq}}N_R} + d_{\min}^2 \frac{1}{4\sigma_n^2} \mathbf{C}_m \Phi \mathbf{C}_m^H \right)}, \quad (3.1)$$

where σ_n^2 is the noise variance of $n_{n_r}[k]$ in (2.28), $\mathbf{I}_{N \times N}$ is an identity matrix with dimension $N \times N$, $\det\{\cdot\}$ denotes the determinant of a matrix, and d_{\min} is the minimum Euclidean distance of two adjacent signal points which depends on the used modulation scheme. \mathbf{C}_m is called the modified code matrix in [1, 2] with dimension $L_{\text{eq}}N_R \times LN_TN_R$ and elements

$$\mathbf{C}_m = \mathbf{I}_{N_R \times N_R} \otimes \mathbf{C}'_m, \quad (3.2)$$

where \otimes represents the Kronecker product, and

$$\mathbf{C}'_m = \begin{bmatrix} g_1[0] & \dots & 0 & \dots & g_{N_T}[0] & \dots & 0 \\ g_1[1] & \ddots & 0 & \dots & g_{N_T}[1] & \ddots & 0 \\ \vdots & \ddots & 0 & \dots & \vdots & \ddots & 0 \\ g_1[N-1] & \ddots & g_1[0] & \dots & g_{N_T}[N-1] & \ddots & g_{N_T}[0] \\ 0 & \ddots & g_1[1] & \dots & 0 & \ddots & g_{N_T}[1] \\ \vdots & \ddots & \vdots & \dots & \vdots & \ddots & \vdots \\ 0 & \dots & g_1[N-1] & \dots & 0 & \dots & g_{N_T}[N-1] \end{bmatrix}. \quad (3.3)$$

In (3.1), Φ is the covariance matrix of the used channel with dimension $LN_TN_R \times LN_TN_R$ and is defined by

$$\Phi = \mathcal{E}\{\mathbf{h}\mathbf{h}^H\}, \quad (3.4)$$

where $\mathcal{E}\{\cdot\}$ is the expectation operator and \mathbf{h} is the channel vector with elements

$$\mathbf{h} = \left[\mathbf{h}_1^T \quad \mathbf{h}_2^T \quad \dots \quad \mathbf{h}_{N_R}^T \right]^T, \quad (3.5)$$

where

$$\mathbf{h}_{n_r} = \left[h_{n_r,1}[0] \ \dots \ h_{n_r,1}[L-1] \ \dots \ h_{n_r,N_T}[0] \ \dots \ h_{n_r,N_T}[L-1] \right]^T \quad (3.6)$$

with dimension $LN_T \times 1$. The superscript T in the above equations refers to vector or matrix transposition.

In order to minimize (3.1), the cost function

$$d = \det \left(\mathbf{I}_{L_{\text{eq}}N_R \times L_{\text{eq}}N_R} + d_{\min}^2 \frac{1}{4\sigma_n^2} \mathbf{C}_m \Phi \mathbf{C}_m^H \right) \quad (3.7)$$

has to be maximized subject to the power constraint,

$$\text{tr}(\mathbf{C}_m \mathbf{C}_m^H) = N_R N_T L, \quad (3.8)$$

where $\text{tr}(\cdot)$ refers to the trace operation.

The maximization of (3.7) does not have a closed-form solution and therefore, a steepest decent algorithm has to be used to solve the optimization problem.

With the following DD filter coefficient vector defined,

$$\mathbf{g} = \left[g_1[0] \ \dots \ g_1[N-1] \ \dots \ g_{N_T}[0] \ \dots \ g_{N_T}[N-1] \right]^T, \quad (3.9)$$

it was shown in [1, 2] that the gradient of (3.7), $\frac{\partial d}{\partial \mathbf{g}^*}$ is

$$\begin{bmatrix} \frac{\partial d}{\partial g_1^*[0]} \\ \frac{\partial d}{\partial g_1^*[1]} \\ \vdots \\ \vdots \\ \frac{\partial d}{\partial g_{N_T}^*[N-1]} \end{bmatrix} = \begin{bmatrix} \text{tr} \left(\left(\mathbf{I}_{L_{\text{eq}}N_R \times L_{\text{eq}}N_R} + \alpha \mathbf{C}_m \Phi \mathbf{C}_m^H \right)^{-1} \alpha \left(\mathbf{C}_m \Phi \mathbf{E}_{11}^H + \mathbf{E}_{11} \Phi \mathbf{C}_m^H \right) \right) \\ \text{tr} \left(\left(\mathbf{I}_{L_{\text{eq}}N_R \times L_{\text{eq}}N_R} + \alpha \mathbf{C}_m \Phi \mathbf{C}_m^H \right)^{-1} \alpha \left(\mathbf{C}_m \Phi \mathbf{E}_{12}^H + \mathbf{E}_{12} \Phi \mathbf{C}_m^H \right) \right) \\ \vdots \\ \vdots \\ \text{tr} \left(\left(\mathbf{I}_{L_{\text{eq}}N_R \times L_{\text{eq}}N_R} + \alpha \mathbf{C}_m \Phi \mathbf{C}_m^H \right)^{-1} \alpha \left(\mathbf{C}_m \Phi \mathbf{E}_{N_T N}^H + \mathbf{E}_{N_T N} \Phi \mathbf{C}_m^H \right) \right) \end{bmatrix}, \quad (3.10)$$

where

$$\alpha = d_{\min}^2 \frac{1}{4\sigma_n^2}. \quad (3.11)$$

It should be noted that it is the usual convention to calculate the derivative with respect to the complex-conjugate coefficient vector \mathbf{g}^* rather than derivative with respect to \mathbf{g} itself [41].

$\mathbf{E}_{n_t, k}$ in (3.10) can be obtained from \mathbf{C}_m by replacing element $g_{n_t}[k]$ of \mathbf{C}_m with 1 and the remaining elements with 0. The gradient vector shown in (3.10) has dimension $NN_T \times 1$.

For a pre-defined number of iterations, the gradient vector is multiplied with a step size δ and added to the current filter vector to obtain an improved vector $\mathbf{g}_0[i+1]$, where i is the iteration number,

$$\mathbf{g}_0[i+1] = \mathbf{g}[i] + \delta \cdot \begin{pmatrix} \frac{\partial d}{\partial g_1^*[0]} \\ \frac{\partial d}{\partial g_1^*[1]} \\ \vdots \\ \vdots \\ \frac{\partial d}{\partial g_{N_T}^*[N-1]} \end{pmatrix}. \quad (3.12)$$

At the end of each iteration, the normalization

$$\mathbf{g}[i+1] = \sqrt{\frac{N_T}{\mathbf{g}_0^H[i+1]\mathbf{g}_0[i+1]}} \mathbf{g}_0[i+1] \quad (3.13)$$

is performed to ensure that the vector \mathbf{g} has energy N_T .

The DD scheme that uses filters which were optimized by the method described above is called MLSE-ODD. Simulation results for 2-PSK and 8-PSK in [1, 2] show that MLSE-ODD yields a lower BER than GDD at low-to-moderate SNRs. This holds for MLSE decoding as well as suboptimum decoding including DFE [5] and decision feedback sequence estimation (DFSE) [42]. Also, the MLSE-ODD filters do not only outperform the GDD filters of the same length but perform often better than the longer GDD filters.

Chapter 4

Decision-Feedback Equalization and Linear Equalization

Although MLSE-ODD obtained in [1, 2] yields better performance than GDD, optimum equalization at the receiver based on the Viterbi algorithm (VA) [43] requires an excessive computational complexity and is not feasible in many situations. The computational complexity of MLSE is directly related to the number of states of the underlying trellis diagram, which is given by $Z = M^{L-1}$. Therefore, MLSE has a maximum complexity of $Z = 2^{(7-1)} = 64$ states for GSM as GSM uses binary GMSK and the longest channel specified is $L = 7$. In contrast, the complexity of MLSE is prohibitively high for EDGE, which uses 8-PSK as its modulation scheme. The TU channel is the shortest channel defined in the GSM and EDGE system with $L = 4$ and therefore, a full-state VA would require $Z = 8^{(4-1)} = 512$ states which is far too complex for a practical implementation. Therefore, alternative equalization strategies such as DFSE, DFE, or even LE have to be employed at the receiver in practice for EDGE. In this work, we will concentrate on DFE and LE. A brief review of the two suboptimum equalization schemes will be given in the following two subsections and a comparison of the two schemes will be given at the end of this chapter.

4.1 Decision-Feedback Equalization (DFE)

A block diagram of a DFE scheme with N_R receive antennas is shown in Figure 4.1. The equalizer consists of N_R discrete-time feed-forward filters (FFF) and one discrete-time feedback filter (FBF). The idea of DFE is to use previous decisions to cancel the ISI. The inputs to each of the FFFs are the received symbols $r_{n_r}[k]$ at each receive antenna. The inputs to the FBF are the previously detected symbols. At each time instant, the output of the FBF, which is a weighted linear combination of the previous symbol decisions, is subtracted from the sum of the outputs of the FFFs to produce an estimate, $\tilde{b}[k]$, of the current symbol, $b[k]$. This cancels the ISI produced by the previous symbols. The estimate $\tilde{b}[k]$ is then passed through a threshold device which generates the current symbol decision $\hat{b}[k]$.

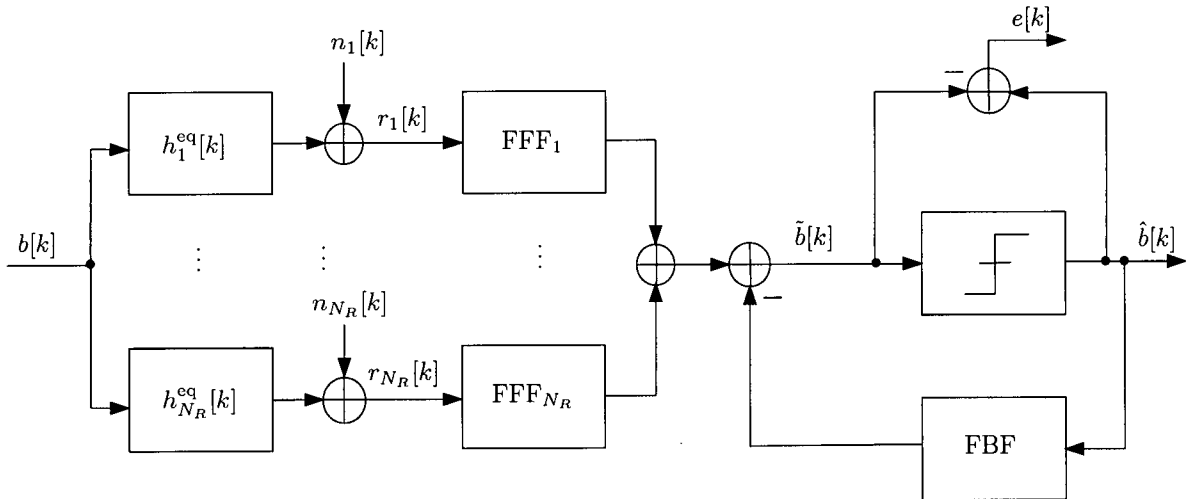


Figure 4.1: Block diagram of DFE with N_R receive antennas.

In theory, the FFFs of DFE are of infinite length. However, FFFs of finite length are employed in practice. We have tried FFFs of different lengths for simulations and found that FFFs with a filter length that is four times the overall CIR yield comparable performance to infinite-length FFFs. Therefore, FFFs in this work are designed such that their lengths are four times the CIR lengths.

Since the most meaningful measure of performance for a digital communication system is the average probability of error, it is desirable to choose the FFF and FBF coefficients to minimize this performance index. However, the probability of error is a highly non-linear function of the filter coefficients and therefore, using the probability of error as a performance index for optimizing the filter coefficients is computationally very complex. Two performance criteria have found widespread use in optimizing the DFE coefficients. One is the zero forcing (ZF) criterion and the other is the mean-square error (MSE) criterion [27]. The former completely eliminates the ISI under a ZF constraint while the later minimizes the MSE between the true sample $b[k]$ and the observed signal $\tilde{b}[k]$ just prior to the decision threshold. Since the MSE criterion is more prevalent in practice and results in a better performance [44], it is used in deriving the filter coefficients in this work. The optimization of the DFE filters is usually carried out assuming that the past decisions are correct, thus simplifying the mathematics involved [5]. The same assumption is made in this work. Therefore, according to Figure 4.1, $b[k] = \hat{b}[k]$ and $\tilde{b}[k]$ can be written as

$$\tilde{b}[k] = \sum_{n_r=1}^{N_R} \sum_{n=-(N_f-1)}^0 f_{n_r}[n] r_{n_r}[k-n] - \sum_{n=1}^{N_w} w[n] b[k-n], \quad (4.1)$$

where $f_{n_r}[n]$ and $w[n]$ are the coefficients of the FFF of receive antenna n_r and the FBF, respectively, and N_f and N_w are their respective lengths. N_w is equal to $L_{\text{eq}} - 1$ and therefore, the FBF is one tap shorter than the length of the equivalent CIR, $h_{n_r}^{\text{eq}}[k]$ [27].

$f_{n_r}[n]$ is an anti-casual filter meaning that its output depends on the future input values. Anti-casual filters are not realizable. However, this problem can be overcome by introducing a delay $(N_f - 1)$ to the received symbols, $r_{n_r}[k]$, at each receive antenna.

The error term, $e[k]$, denoted in Figure 4.1 can now be written compactly in vector form as

$$e[k] = b[k] - \tilde{b}[k] = b[k] + \mathbf{w}^H \mathbf{b}[k] - \mathbf{f}^H \mathbf{r}[k], \quad (4.2)$$

where the following definitions were used:

$$\begin{aligned}
\mathbf{f} &= \left[f_1[-(N_f - 1)] \quad \dots \quad f_1[0] \quad \dots \quad f_{N_R}[-(N_f - 1)] \quad \dots \quad f_{N_R}[0] \right]^H \\
\mathbf{r}[k] &= \left[r_1[k + (N_f - 1)] \quad \dots \quad r_1[k] \quad \dots \quad r_{N_R}[k + (N_f - 1)] \quad \dots \quad r_{N_R}[k] \right]^T \\
\mathbf{w} &= \left[w[1] \quad w[2] \quad \dots \quad w[N_w] \right]^H \\
\mathbf{b}[k] &= \left[b[k - 1] \quad b[k - 2] \quad \dots \quad b[k - N_w] \right]^T
\end{aligned} \tag{4.3}$$

The vectors \mathbf{f} , $\mathbf{r}[k]$, \mathbf{w} , and $\mathbf{b}[k]$ have dimensions $N_f N_R \times 1$, $N_f N_R \times 1$, $N_w \times 1$, and $N_w \times 1$, respectively.

Based on the assumption that the previous symbol decisions are correct, the MSE to be minimized is

$$\begin{aligned}
\sigma^2 &= \mathcal{E}\{e[k]e^*[k]\} \\
&= \mathcal{E}\{(b[k] + \mathbf{w}^H \mathbf{b}[k] - \mathbf{f}^H \mathbf{r}[k])(b^*[k] + \mathbf{b}^H[k] \mathbf{w} - \mathbf{r}^H[k] \mathbf{f})\} \\
&= \mathcal{E}\{|b[k]|^2\} + \mathcal{E}\{b[k] \mathbf{b}^H[k] \mathbf{w}\} - \mathcal{E}\{b[k] \mathbf{r}^H[k] \mathbf{f}\} \\
&\quad + \mathcal{E}\{\mathbf{w}^H \mathbf{b}[k] b^*[k]\} + \mathcal{E}\{\mathbf{w}^H \mathbf{b}[k] \mathbf{b}^H[k] \mathbf{w}\} - \mathbf{w}^H \mathbf{b}[k] \mathbf{r}^H[k] \mathbf{f}\} \\
&\quad - \mathcal{E}\{\mathbf{f}^H \mathbf{r}[k] b^*[k]\} - \mathcal{E}\{\mathbf{f}^H \mathbf{r}[k] \mathbf{b}^H[k] \mathbf{w}\} \\
&\quad + \mathcal{E}\{\mathbf{f}^H \mathbf{r}[k] \mathbf{r}^H[k] \mathbf{f}\}.
\end{aligned} \tag{4.4}$$

The above equation (4.4) can be simplified by recalling (2.29) and using the following facts.

- The input data are temporally uncorrelated, i.e., $\mathcal{E}\{b[j]b^*[k]\} = \sigma_b^2$ if $j = k$ and $\mathcal{E}\{b[j]b^*[k]\} = 0$, otherwise.
- The input data and noise are mutually uncorrelated.

The terms in (4.4) can now be simplified to

$$\begin{aligned}
\mathcal{E}\{b[k] \mathbf{b}^H[k] \mathbf{w}\} &= \mathcal{E}\{\mathbf{w}^H \mathbf{b}[k] b^*[k]\} = 0 \\
\mathcal{E}\{b[k] \mathbf{r}^H[k] \mathbf{f}\} &= \sigma_b^2 \mathbf{h}_f^H \mathbf{f} \\
\mathcal{E}\{\mathbf{w}^H \mathbf{b}[k] \mathbf{b}^H[k] \mathbf{w}\} &= \sigma_b^2 \mathbf{w}^H \mathbf{w}
\end{aligned}$$

$$\begin{aligned}
\mathcal{E}\{\mathbf{w}^H \mathbf{b}[k] \mathbf{r}^H[k] \mathbf{f}\} &= \sigma_b^2 \mathbf{w}^H \mathbf{A} \mathbf{f} \\
\mathcal{E}\{\mathbf{f}^H \mathbf{r}[k] \mathbf{b}^*[k]\} &= \sigma_b^2 \mathbf{f}^H \mathbf{h}_f \\
\mathcal{E}\{\mathbf{f}^H \mathbf{r}[k] \mathbf{b}^H[k] \mathbf{w}\} &= \sigma_b^2 \mathbf{f}^H \mathbf{A}^H \mathbf{w} \\
\mathcal{E}\{\mathbf{f}^H \mathbf{r}[k] \mathbf{r}^H[k] \mathbf{f}\} &= \sigma_b^2 \mathbf{f}^H [\mathbf{B} \mathbf{B}^H + \frac{\sigma_n^2}{\sigma_b^2} (\mathbf{I}_{(N_f N_R) \times (N_f N_R)})] \mathbf{f} \\
&= \sigma_b^2 \mathbf{f}^H \mathbf{\Gamma} \mathbf{f}
\end{aligned} \tag{4.5}$$

where \mathbf{h}_f , \mathbf{A} , \mathbf{B} , and $\mathbf{\Gamma}$ are defined as follows:

$$\mathbf{h}_f = \left[\mathbf{0}_{N_f - (N_w + 1)}^T \quad h_1^{\text{eq}}[N_w] \quad \dots \quad h_1^{\text{eq}}[0] \quad \dots \quad \mathbf{0}_{N_f - (N_w + 1)}^T \quad \dots \quad h_{N_R}^{\text{eq}}[0] \right]^T \tag{4.6}$$

$$\mathbf{A} = \left[\mathbf{A}_1 \quad \mathbf{A}_2 \quad \dots \quad \mathbf{A}_{N_R} \right] \tag{4.7}$$

with

$$\mathbf{A}_{n_r} = \begin{bmatrix} \mathbf{0}_{N_f - N_w}^T & h_{n_r}^{\text{eq}*}[N_w] & \dots & \dots & h_{n_r}^{\text{eq}*}[1] \\ \mathbf{0}_{N_f - N_w}^T & 0 & h_{n_r}^{\text{eq}*}[N_w] & \dots & h_{n_r}^{\text{eq}*}[2] \\ \vdots & \ddots & \ddots & \ddots & \vdots \\ \mathbf{0}_{N_f - N_w}^T & 0 & 0 & 0 & h_{n_r}^{\text{eq}*}[N_w] \end{bmatrix} \tag{4.8}$$

$$\mathbf{B} = \begin{bmatrix} h_1^{\text{eq}}[0] & \dots & h_1^{\text{eq}}[N_w] & 0 & \dots & 0 & 0 & 0 \\ 0 & h_1^{\text{eq}}[0] & \dots & h_1^{\text{eq}}[N_w] & \ddots & 0 & 0 & 0 \\ 0 & \ddots & \ddots & \ddots & \ddots & \ddots & \ddots & 0 \\ 0 & 0 & 0 & 0 & \ddots & h_1^{\text{eq}}[0] & \dots & h_1^{\text{eq}}[N_w] \\ \vdots & \ddots & \ddots & \ddots & \ddots & \ddots & \ddots & \vdots \\ h_{N_R}^{\text{eq}}[0] & \dots & h_{N_R}^{\text{eq}}[N_w] & 0 & \ddots & 0 & 0 & 0 \\ 0 & h_{N_R}^{\text{eq}}[0] & \dots & h_{N_R}^{\text{eq}}[N_w] & \ddots & 0 & 0 & 0 \\ 0 & \ddots & \ddots & \ddots & \ddots & \ddots & \ddots & 0 \\ 0 & 0 & 0 & 0 & \dots & h_{N_R}^{\text{eq}}[0] & \dots & h_{N_R}^{\text{eq}}[N_w] \end{bmatrix} \tag{4.9}$$

$$\mathbf{\Gamma} = \mathbf{B} \mathbf{B}^H + \frac{\sigma_n^2}{\sigma_b^2} (\mathbf{I}_{(N_f N_R) \times (N_f N_R)}). \tag{4.10}$$

$\mathbf{0}_N$ in (4.6) and (4.8) refers to the zero vector with dimension $N \times 1$. The dimensions of \mathbf{h}_f , \mathbf{A} , \mathbf{B} , and $\mathbf{\Gamma}$ are $N_f N_R \times 1$, $N_w \times N_f N_R$, $N_f N_R \times (N_f + N_w)$, and $N_f N_R \times N_f N_R$, respectively.

After substituting (4.5) into (4.4), (4.4) becomes

$$\begin{aligned} \sigma^2 = & \sigma_b^2 - \sigma_b^2 \mathbf{h}_f^H \mathbf{f} + \sigma_b^2 \mathbf{w}^H \mathbf{w} - \sigma_b^2 \mathbf{w}^H \mathbf{A} \mathbf{f} \\ & - \sigma_b^2 \mathbf{f}^H \mathbf{h}_f - \sigma_b^2 \mathbf{f}^H \mathbf{A}^H \mathbf{w} + \sigma_b^2 \mathbf{f}^H \mathbf{\Gamma} \mathbf{f}. \end{aligned} \quad (4.11)$$

The coefficients of \mathbf{w} can be obtained by differentiating (4.11) with respect to \mathbf{w}^* and setting the resulting expression to zero [41],

$$\frac{\partial \sigma^2}{\partial \mathbf{w}^*} = \sigma_b^2 \mathbf{w} - \sigma_b^2 \mathbf{A} \mathbf{f} = \mathbf{0}_{N_w}. \quad (4.12)$$

The resulting FBF coefficients are

$$\mathbf{w} = \mathbf{A} \mathbf{f}. \quad (4.13)$$

The coefficients of \mathbf{f} can be obtained in a similar way by differentiating (4.11) with respect to \mathbf{f}^* and setting the resulting expression to zero,

$$\frac{\partial \sigma^2}{\partial \mathbf{f}^*} = -\sigma_b^2 \mathbf{h}_f - \sigma_b^2 \mathbf{A}^H \mathbf{w} + \sigma_b^2 \mathbf{\Gamma} \mathbf{f} = \mathbf{0}_{N_f N_R}. \quad (4.14)$$

After substituting \mathbf{w} in the above equation (4.14) with (4.13), (4.14) reduces to

$$\begin{aligned} \mathbf{h}_f &= \mathbf{\Gamma} \mathbf{f} - \mathbf{A}^H \mathbf{A} \mathbf{f} \\ &= (\mathbf{\Gamma} - \mathbf{A}^H \mathbf{A}) \mathbf{f} \\ &= [\mathbf{B} \mathbf{B}^H + \frac{\sigma_n^2}{\sigma_b^2} (\mathbf{I}_{(N_f N_R) \times (N_f N_R)}) - \mathbf{A}^H \mathbf{A}] \mathbf{f} \\ &= [\mathbf{C} \mathbf{C}^H + \frac{\sigma_n^2}{\sigma_b^2} (\mathbf{I}_{(N_f N_R) \times (N_f N_R)})] \mathbf{f}, \end{aligned} \quad (4.15)$$

where

$$\mathbf{C} = \begin{bmatrix} h_1^{\text{eq}}[0] & \dots & h_1^{\text{eq}}[N_w] & 0 & \dots & 0 \\ 0 & h_1^{\text{eq}}[0] & \dots & h_1^{\text{eq}}[N_w] & \ddots & 0 \\ 0 & \ddots & \ddots & \ddots & \ddots & \ddots \\ 0 & 0 & 0 & 0 & \ddots & h_1^{\text{eq}}[0] \\ \vdots & \ddots & \ddots & \ddots & \ddots & \ddots \\ h_{N_R}^{\text{eq}}[0] & \dots & h_{N_R}^{\text{eq}}[N_w] & 0 & \ddots & 0 \\ 0 & h_{N_R}^{\text{eq}}[0] & \dots & h_{N_R}^{\text{eq}}[N_w] & \ddots & 0 \\ 0 & \ddots & \ddots & \ddots & \ddots & \ddots \\ 0 & 0 & 0 & 0 & \dots & h_{N_R}^{\text{eq}}[0] \end{bmatrix} \quad (4.16)$$

and its dimension is $N_f N_R \times N_f$.

Finally, the FFF coefficients can be computed from

$$\mathbf{f} = [\mathbf{C}\mathbf{C}^H + \frac{\sigma_n^2}{\sigma_b^2}(\mathbf{I}_{(N_f N_R) \times (N_f N_R)})]^{-1} \mathbf{h}_f, \quad (4.17)$$

and this result can be used to obtain the FBF coefficients from (4.13).

Al-Dhahir and Sayed obtained the same results in [45] using a different derivation.

4.2 Linear Equalization (LE)

LE is another suboptimum equalization technique that is commonly used in practice. It employs N_R linear transversal filters to compensate for the ISI. The filter structure has a computational complexity that is a linear function of the channel dispersion length L [27]. A block diagram of a LE scheme with N_R receive antennas is shown in Figure 4.2. Similar to DFE, the LE scheme consists of N_R discrete time FFFs. The inputs to the FFFs are the received symbols $r_{n_r}[k]$ at each receive antenna. The output of each FFF is a weighted linear combination of the received signals at the corresponding receive antenna n_r . These outputs are summed together to form an estimate $\tilde{b}[k]$ of the current symbol $b[k]$. The threshold device then uses this value to estimate the current symbol decision $\hat{b}[k]$.

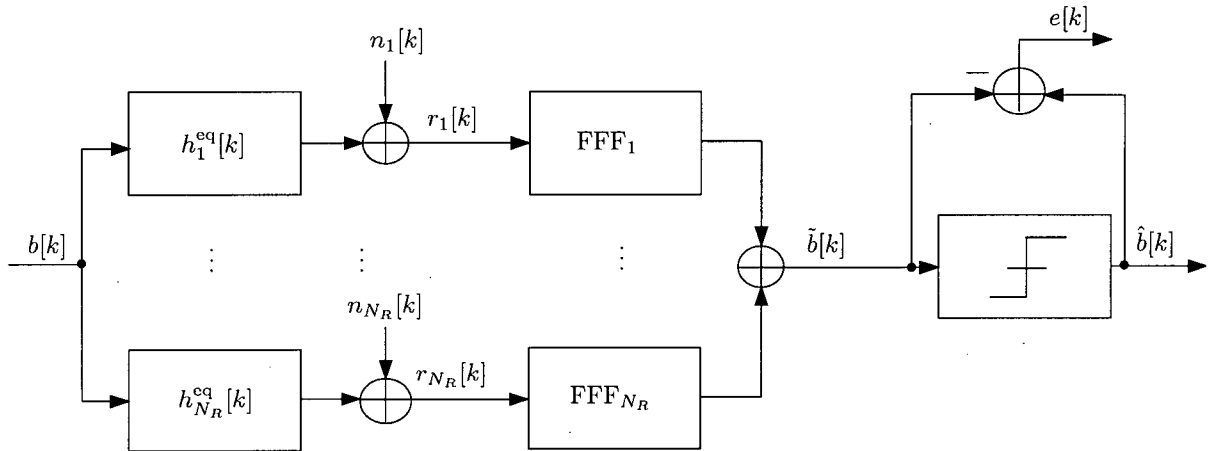


Figure 4.2: Block diagram of LE with N_R receive antennas.

Similar to DFE, the optimum FFFs of LE are of infinite-length. However, FFFs with length four times the overall CIR yield similar performance to the infinite-length FFFs. Therefore, the length of the FFF of LE in this work is assumed to be four times the overall CIR. The MSE criterion is used again for optimization.

$\tilde{b}[k]$ in Figure 4.2 can be written as

$$\tilde{b}[k] = \sum_{n_r=1}^{N_R} \sum_{n=-(N_f-1)}^0 f_{n_r}[n] r_{n_r}[k-n], \quad (4.18)$$

where $f_{n_r}[n]$ are the coefficients of the FFF of receive antenna n_r . The length of the FFF is N_f . Similar to the DFE case, the FFFs of LE are anti-causal filters as well. This again can be solved by introducing a delay of $(N_f - 1)$ at the input of each of the FFFs.

The error term denoted in Figure 4.2 as $e[k]$ can be written compactly in vector form as

$$e[k] = b[k] - \tilde{b}[k] = b[k] - \mathbf{f}^H \mathbf{r}[k], \quad (4.19)$$

where \mathbf{f} and $\mathbf{r}[k]$ were already defined in (4.3). The MSE can now be written as

$$\begin{aligned} \sigma^2 &= \mathcal{E}\{e[k]e^*[k]\} \\ &= \mathcal{E}\{(b[k] - \mathbf{f}^H \mathbf{r}[k])(b^*[k] - \mathbf{r}^H[k]\mathbf{f})\} \end{aligned}$$

$$\begin{aligned}
&= \mathcal{E}\{|b[k]|^2\} - \mathcal{E}\{b[k]\mathbf{r}^H[k]\mathbf{f}\} \\
&\quad - \mathcal{E}\{\mathbf{f}^H\mathbf{r}[k]b^*[k]\} + \mathcal{E}\{\mathbf{f}^H\mathbf{r}[k]\mathbf{r}^H[k]\mathbf{f}\}. \tag{4.20}
\end{aligned}$$

The above equation (4.20) can again be simplified by recalling (2.29) and using the same assumptions as in the DFE case.

The terms in (4.20) can now be simplified to

$$\begin{aligned}
\mathcal{E}\{b[k]\mathbf{r}^H[k]\mathbf{f}\} &= \sigma_b^2 \mathbf{h}_f^H \mathbf{f} \\
\mathcal{E}\{\mathbf{f}^H\mathbf{r}[k]b^*[k]\} &= \sigma_b^2 \mathbf{f}^H \mathbf{h}_f \\
\mathcal{E}\{\mathbf{f}^H\mathbf{r}[k]\mathbf{r}^H[k]\mathbf{f}\} &= \sigma_b^2 \mathbf{f}^H [\mathbf{B}\mathbf{B}^H + \frac{\sigma_n^2}{\sigma_b^2} (\mathbf{I}_{(N_f N_R) \times (N_f N_R)})] \mathbf{f} \\
&= \sigma_b^2 \mathbf{f}^H \mathbf{\Gamma} \mathbf{f}, \tag{4.21}
\end{aligned}$$

where \mathbf{h}_f , \mathbf{B} , and $\mathbf{\Gamma}$ were defined in (4.6), (4.9), and (4.10), respectively.

Substituting (4.21) into (4.20) yields

$$\sigma^2 = \sigma_b^2 - \sigma_b^2 \mathbf{h}_f^H \mathbf{f} - \sigma_b^2 \mathbf{f}^H \mathbf{h}_f + \sigma_b^2 \mathbf{f}^H \mathbf{\Gamma} \mathbf{f}. \tag{4.22}$$

Differentiating the above equation with respect to \mathbf{f}^* and setting the resulting equation to zero yields the solution for the FFF coefficients,

$$\mathbf{f} = \mathbf{\Gamma}^{-1} \mathbf{h}_f. \tag{4.23}$$

4.3 Performance of DFE and LE

For the suboptimum equalizers discussed in the last two sections, the location of the zeros of the Z-transform of the discrete-time equivalent CIR $h_{nr}^{\text{eq}}[k]$ is very important [46]. LE does not perform well when the equivalent channel has a spectral null since the noise power is enhanced at frequencies around the spectral null. In other words, if zeros are located close to the unit circle of the complex plane, the performance of LE degrades. DFE makes memoryless decisions and cancels the ISI caused by the previous symbols. Without the FFFs, its performance degrades if zeros are located outside the unit circle [46],

i.e., if the discrete-time equivalent CIR is not minimum phase. Therefore, allpass prefilters such as the FFFs depicted in Figure 4.1 which transform the equivalent CIR in its minimum phase equivalent should be employed if DFE is used at the receiver. Error propagation is another issue which needs to be considered when employing the DFE at the receiver. This is because when deriving the coefficients of the FFFs and FBF, the assumption that the past decisions are correct is usually made and this is certainly not true. However, despite error propagation, the performance of DFE is generally better than that of LE in wireless ISI channels.

Chapter 5

PEP Estimation

In this chapter, the approximate worst-case PEP of DFE and LE will be calculated. The calculation of the PEP requires the error variances of the two schemes. In principle, the error variance in (4.4) and (4.20) can be used for this purpose for DFE and LE, respectively. However, the resulting expressions to be optimized require the inverse of large matrices making this approach impractical because the optimization has to be carried out for a large number of samples. Since DFE and LE with FFF lengths four times the overall CIR yield comparable performances as their respective counterparts with infinite-length FFFs, the error variances of DFE and LE with infinite FFF lengths are used instead to estimate their respective PEP in this work.

In the next two sections, we will calculate the SNR for DFE and LE, respectively. It will be seen later that the resulting expressions cannot be evaluated in closed-form. Therefore, numerical methods will be used to approximate the SNRs. In the last section of this chapter, the obtained SNRs are used to approximate the worst-case PEPs of DFE and LE, respectively.

5.1 SNR for DFE

According to [47], the error variance of DFE with infinite-length FFFs and multiple receive antennas is

$$\sigma^2(\mathbf{h}, \mathbf{g}) = \sigma_b^2 \exp \left\{ -T \int_{-1/2T}^{1/2T} \ln \left[1 + \frac{\sigma_b^2}{\sigma_n^2} \sum_{n_r=1}^{N_R} |H_{n_r}^{\text{eq}}(e^{j2\pi fT})|^2 \right] df \right\}. \quad (5.1)$$

This error variance depends on the overall CIRs between all the transmit and receive antenna pairs \mathbf{h} , and the DD filter coefficients \mathbf{g} . $H_{n_r}^{\text{eq}}(e^{j2\pi fT})$ is the Fourier transform of $h_{n_r}^{\text{eq}}[k]$ and it is, therefore, the frequency response of the equivalent channel of receive antenna n_r [48]. It can be expressed as

$$\begin{aligned} H_{n_r}^{\text{eq}}(e^{j2\pi fT}) &= h_{n_r}^{\text{eq}}[0] + h_{n_r}^{\text{eq}}[1] \cdot \exp\{-j2\pi fT\} + \dots \\ &\quad + h_{n_r}^{\text{eq}}[L_{\text{eq}} - 1] \cdot \exp\{-j2\pi fT(L_{\text{eq}} - 1)\}. \end{aligned} \quad (5.2)$$

The SNR also depends on \mathbf{h} and \mathbf{g} and can be written as

$$\begin{aligned} \text{SNR}_{\text{DFE}}(\mathbf{h}, \mathbf{g}) &= \frac{\sigma_b^2}{\sigma^2(\mathbf{h}, \mathbf{g})} \\ &= \exp \left\{ \int_{-1/2}^{1/2} \ln \left[1 + \frac{\sigma_b^2}{\sigma_n^2} \sum_{n_r=1}^{N_R} |H_{n_r}^{\text{eq}}(e^{j2\pi x})|^2 \right] dx \right\} \\ &= \frac{\sigma_b^2}{\sigma_n^2} \exp \left\{ \int_{-1/2}^{1/2} \ln \left[\frac{\sigma_n^2}{\sigma_b^2} + \sum_{n_r=1}^{N_R} |H_{n_r}^{\text{eq}}(e^{j2\pi x})|^2 \right] dx \right\}. \end{aligned} \quad (5.3)$$

A closed-form solution to the above $\text{SNR}_{\text{DFE}}(\mathbf{h}, \mathbf{g})$ expression does not seem to be possible. Therefore, a numerical method is used to calculate $\text{SNR}_{\text{DFE}}(\mathbf{h}, \mathbf{g})$. The definite integral in (5.3) can be approximated by numerical integration. There are four main methods for evaluating definite integrals numerically [49]: the Trapezoid Rule, the Midpoint Rule, Simpson's Rule, and the Romberg Method. All of these methods can be easily implemented on a small computer. Also, all these techniques require to calculate the argument in the integral at a set of equally spaced points in interval $[a, b]$ where a and b are the lower and upper limits of the integral, respectively. In this work, the Midpoint Rule is used. The computational complexity for this method is slightly less than

those of the other three. It involves forming a Riemann sum of the areas of rectangles whose heights are taken at the midpoints of the subintervals [49].

The lower and upper limits of the integral in (5.3) are $-1/2$ and $1/2$, respectively. Let the number of points to be evaluated within this interval be $2\bar{N} + 1$.

Now the integral in (5.3) can be approximated by

$$\begin{aligned}
\text{SNR}_{\text{DFE}}(\mathbf{h}, \mathbf{g}) &\approx \frac{\sigma_b^2}{\sigma_n^2} \exp \left\{ \sum_{s=-\bar{N}}^{\bar{N}} \ln \left[\frac{\sigma_n^2}{\sigma_b^2} + \sum_{n_r=1}^{N_R} |H_{n_r}^{\text{eq}}(e^{j2\pi \frac{s}{2\bar{N}+1}})|^2 \right] \frac{1}{2\bar{N}+1} \right\} \\
&= \frac{\sigma_b^2}{\sigma_n^2} \left\{ \exp \left\{ \sum_{s=-\bar{N}}^{\bar{N}} \ln \left[\frac{\sigma_n^2}{\sigma_b^2} + \sum_{n_r=1}^{N_R} |H_{n_r}^{\text{eq}}(e^{j2\pi \frac{s}{2\bar{N}+1}})|^2 \right] \right\} \right\}^{\frac{1}{2\bar{N}+1}} \\
&= \frac{\sigma_b^2}{\sigma_n^2} \left\{ \prod_{s=-\bar{N}}^{\bar{N}} \left[\frac{\sigma_n^2}{\sigma_b^2} + \sum_{n_r=1}^{N_R} |H_{n_r}^{\text{eq}}(e^{j2\pi \frac{s}{2\bar{N}+1}})|^2 \right] \right\}^{\frac{1}{2\bar{N}+1}}.
\end{aligned} \tag{5.4}$$

The frequency response $H_{n_r}^{\text{eq}}(e^{j2\pi \frac{s}{2\bar{N}+1}})$ can be calculated by

$$H_{n_r}^{\text{eq}}(e^{j2\pi \frac{s}{2\bar{N}+1}}) = \sum_{k=0}^{L_{\text{eq}}-1} h_{n_r}^{\text{eq}}[k] \exp \left\{ -j2\pi \frac{s}{2\bar{N}+1} k \right\}. \tag{5.5}$$

Recall that $h_{n_r}^{\text{eq}}[k]$ is the equivalent CIR defined in (2.30) with length L_{eq} . The above equation can now be written compactly in vector form as

$$h_{n_r}^{\text{eq}}[k] = \sqrt{\frac{E_s}{N_T}} \mathbf{H}_{n_r} \mathbf{g}, \tag{5.6}$$

where

$$\mathbf{H}_{n_r} = \begin{bmatrix} h_{n_r1}[0] & \dots & 0 & \dots & h_{n_r N_T}[0] & \dots & 0 \\ h_{n_r1}[1] & \ddots & 0 & \dots & h_{n_r N_T}[1] & \ddots & 0 \\ \vdots & \ddots & 0 & \dots & \vdots & \ddots & 0 \\ h_{n_r1}[L-1] & \ddots & h_{n_r1}[0] & \dots & h_{n_r N_T}[L-1] & \ddots & h_{n_r N_T}[0] \\ 0 & \ddots & h_{n_r1}[1] & \dots & 0 & \ddots & h_{n_r N_T}[1] \\ \vdots & \ddots & \vdots & \dots & \vdots & \ddots & \vdots \\ 0 & \dots & h_{n_r1}[L-1] & \dots & 0 & \dots & h_{n_r N_T}[L-1] \end{bmatrix} \tag{5.7}$$

with dimension $(L + N - 1) \times NN_T$.

Now (5.5) can be written as

$$H_{n_r}^{\text{eq}}(e^{j2\pi\frac{s}{2\bar{N}+1}}) = \sqrt{\frac{E_s}{N_T}} \mathbf{d} \mathbf{H}_{n_r} \mathbf{g} \quad (5.8)$$

with

$$\mathbf{d} = \left[1 \quad \exp\left\{-j2\pi\frac{s}{2\bar{N}+1}\right\} \quad \exp\left\{-j2\pi\frac{2s}{2\bar{N}+1}\right\} \quad \dots \quad \exp\left\{-j2\pi\frac{(L_{\text{eq}}-1)s}{2\bar{N}+1}\right\} \right]. \quad (5.9)$$

Finally, the SNR of DFE with infinite-length FFFs can be easily calculated to

$$\text{SNR}_{\text{DFE-NU}}(\mathbf{h}, \mathbf{g}) = \frac{\sigma_b^2 E_s}{\sigma_n^2 N_T} \left\{ \prod_{s=-\bar{N}}^{\bar{N}} \left[\frac{\sigma_n^2 N_T}{\sigma_b^2 E_s} + \mathbf{g}^H \left(\sum_{n_r=1}^{N_R} \mathbf{H}_{n_r}^H \mathbf{d}^H \mathbf{d} \mathbf{H}_{n_r} \right) \mathbf{g} \right] \right\}^{\frac{1}{2\bar{N}+1}} \quad (5.10)$$

where the subscript, NU, stands for numerical.

5.2 SNR for LE

According to [27], the output noise variance of LE with infinite-length FFFs and multiple receive antennas is

$$\sigma^2(\mathbf{h}, \mathbf{g}) = T \sigma_b^2 \int_{-1/2T}^{1/2T} \frac{\sigma_n^2}{\sigma_b^2 \sum_{n_r=1}^{N_R} |H_{n_r}^{\text{eq}}(e^{j2\pi f T})|^2 + \sigma_n^2} df. \quad (5.11)$$

The SNR depending on \mathbf{h} and \mathbf{g} can be written as

$$\begin{aligned} \text{SNR}_{\text{LE}}(\mathbf{h}, \mathbf{g}) &= \frac{\sigma_b^2}{\sigma^2(\mathbf{h}, \mathbf{g})} \\ &= \frac{1}{\int_{-1/2}^{1/2} \frac{\sigma_n^2}{\sigma_b^2 \sum_{n_r=1}^{N_R} |H_{n_r}^{\text{eq}}(e^{j2\pi x})|^2 + \sigma_n^2} dx}. \end{aligned} \quad (5.12)$$

Again, a closed-form solution to the above expression does not seem to be possible. Therefore, the same numerical method as used in the DFE case is used to approximate the SNR expression. We again use $2\bar{N} + 1$ points

to evaluate the above integral in the interval $[-1/2, 1/2]$. The SNR can be approximated by

$$\begin{aligned} \text{SNR}_{\text{LE-NU}}(\mathbf{h}, \mathbf{g}) &= \left(\frac{1}{2\bar{N} + 1} \sum_{s=-\bar{N}}^{\bar{N}} \frac{\sigma_n^2}{\sigma_b^2 \sum_{n_r=1}^{N_R} |H_{n_r}^{\text{eq}}(e^{j2\pi \frac{s}{2\bar{N}+1}})|^2 + \sigma_n^2} \right)^{-1} \\ &= \left(\frac{1}{2\bar{N} + 1} \sum_{s=-\bar{N}}^{\bar{N}} \frac{1}{\frac{\sigma_b^2}{\sigma_n^2} \sum_{n_r=1}^{N_R} |H_{n_r}^{\text{eq}}(e^{j2\pi \frac{s}{2\bar{N}+1}})|^2 + 1} \right)^{-1} \end{aligned} \quad (5.13)$$

Substituting (5.8) into (5.13), the SNR of LE with infinite-length FFFs can be easily calculated from

$$\text{SNR}_{\text{LE-NU}}(\mathbf{h}, \mathbf{g}) = \left(\frac{1}{2\bar{N} + 1} \sum_{s=-\bar{N}}^{\bar{N}} \frac{1}{\frac{\sigma_b^2 E_s}{\sigma_n^2 N_T} \mathbf{g}^H \left(\sum_{n_r=1}^{N_R} \mathbf{H}_{n_r}^H \mathbf{d}^H \mathbf{d} \mathbf{H}_{n_r} \right) \mathbf{g} + 1} \right)^{-1} \quad (5.14)$$

5.3 Pairwise Error Probability

The SNRs obtained in (5.3) and (5.12) from the last two sections are both biased [47]. The biased and unbiased output SNRs are related by

$$\text{SNR}_U = \text{SNR}_B - 1, \quad (5.15)$$

where SNR_U and SNR_B stand for the biased and unbiased output SNR, respectively. To calculate the PEP of both DFE and LE, we assume that the error term, $e[k]$, in Figures 4.1 and 4.2 are both Gaussian distributed, which is a good approximation in practice. With this assumption, the PEP for two adjacent signal points of DFE and LE can be calculated by

$$\text{PEP} = Q \left(\sqrt{\frac{d_{\min}^2 \text{SNR}_U}{2}} \right), \quad (5.16)$$

where $Q(\cdot)$ is the complementary Gaussian error integral defined in (2.23) and d_{\min}^2 is the squared minimum Euclidean distance between two adjacent

signal points and thus depends on the modulation scheme. For an M -PSK modulation scheme, d_{\min}^2 can be calculated by using the following equation:

$$d_{\min}^2 = [2\sin(\pi/M)]^2. \quad (5.17)$$

Therefore, for 2-PSK symbols, $d_{\min}^2 = 4$ while for 8-PSK symbols, $d_{\min}^2 = 0.5859$. It should be noted that the nearest neighbor signal points are considered and therefore, the PEP presented above is the worst-case PEP.

Since the SNR_U of both DFE and LE depends on the overall channel \mathbf{h} , and DD filters \mathbf{g} , the PEPs of DFE and LE are both channel and DD filters dependent as well. Therefore, the worst-case PEP for DFE and LE can be finally written as

$$\text{PEP}_{\text{DFE}}(\mathbf{h}, \mathbf{g}) = Q \left(\sqrt{\frac{d_{\min}^2 (\text{SNR}_{\text{DFE}}(\mathbf{h}, \mathbf{g}) - 1)}{2}} \right) \quad (5.18)$$

and

$$\text{PEP}_{\text{LE}}(\mathbf{h}, \mathbf{g}) = Q \left(\sqrt{\frac{d_{\min}^2 (\text{SNR}_{\text{LE}}(\mathbf{h}, \mathbf{g}) - 1)}{2}} \right), \quad (5.19)$$

respectively.

The above expressions only give the worst-case PEPs for a specific equivalent channel and since mobile channels are random, the expectation operator is applied to both equations to arrive at the approximate average BER. This will guarantee that the final ODD filter coefficients obtained are optimized for the average of the channels and not only to a specific one. Therefore, the average PEPs of DFE and LE are

$$\mathcal{E} \{ \text{PEP}_{\text{DFE}}(\mathbf{h}, \mathbf{g}) \} = \mathcal{E} \left\{ Q \left(\sqrt{\frac{d_{\min}^2 (\text{SNR}_{\text{DFE}}(\mathbf{h}, \mathbf{g}) - 1)}{2}} \right) \right\} \quad (5.20)$$

and

$$\mathcal{E} \{ \text{PEP}_{\text{LE}}(\mathbf{h}, \mathbf{g}) \} = \mathcal{E} \left\{ Q \left(\sqrt{\frac{d_{\min}^2 (\text{SNR}_{\text{LE}}(\mathbf{h}, \mathbf{g}) - 1)}{2}} \right) \right\}, \quad (5.21)$$

respectively, where the expectation is with respect to the CIR vector \mathbf{h} .

Our goal is to minimize (5.20) and (5.21) with respect to the DD filter coefficients, \mathbf{g} . However, a closed-form solution to the minimization problem is not feasible. In the next chapter, a stochastic gradient algorithm for optimization of the ODD filter coefficients is proposed.

Chapter 6

Stochastic Gradient Algorithm

In this chapter, a stochastic gradient algorithm for optimization of the ODD filters for DFE and LE will be derived. Since we cannot carry out the expectation operation of both (5.20) and (5.21), we first calculate the gradient vectors of (5.18) and (5.19) for a fixed channel, \mathbf{h} . As we will see later in this chapter, a closed-form solution to the gradient vectors is not feasible and therefore, we have to rely on numerical methods to approximate the gradient vectors. We will then present the stochastic gradient algorithm to obtain the DD filter coefficients and perform the averaging over the statistics of the channel. We refer the filters optimized by the proposed algorithm as DFE-ODD and LE-ODD, respectively. At the end of this chapter, some of the issues which affect the convergence behaviour of the stochastic gradient algorithm for the two novel ODD schemes will be discussed.

6.1 Gradient Vector

Since both (5.18) and (5.19) involve the Q -function and their only difference is the argument in the square root, for convenience, we introduce

$$y_x = \alpha(\text{SNR}_x(\mathbf{h}, \mathbf{g}) - 1), \quad (6.1)$$

where the subscript “x” stands for “DFE” and “LE”, respectively, and

$$\alpha = \frac{d_{\min}^2}{2}. \quad (6.2)$$

It should be noted that y_x depends on both \mathbf{h} and \mathbf{g} , but we use y_x instead of $y_x(\mathbf{h}, \mathbf{g})$ for convenience. Now the general $\text{PEP}_x(\mathbf{h}, \mathbf{g})$ expression can be written as

$$\text{PEP}_x(\mathbf{h}, \mathbf{g}) = Q(\sqrt{y_x}). \quad (6.3)$$

The following expression results when the above expression is differentiated with respect to \mathbf{g}^* :

$$\begin{aligned} \frac{\partial}{\partial \mathbf{g}^*} \text{PEP}_x(\mathbf{h}, \mathbf{g}) &= \frac{\partial}{\partial \mathbf{g}^*} Q(\sqrt{y_x}) \\ &= \frac{\partial}{\partial \mathbf{g}^*} \left(\frac{1}{\sqrt{2\pi}} \int_{\sqrt{y_x}}^{\infty} e^{-t^2/2} dt \right) \\ &= \frac{\partial}{\partial \mathbf{g}^*} \left(\frac{1}{\sqrt{2\pi}} \int_{y_x}^{\infty} \frac{e^{-u/2}}{2\sqrt{u}} du \right) \\ &= \left(\frac{-1}{\sqrt{8\pi}} \frac{e^{-y_x/2}}{\sqrt{y_x}} \right) \frac{\partial}{\partial \mathbf{g}^*} y_x. \end{aligned} \quad (6.4)$$

The fundamental theorem of calculus [49],

$$\frac{d}{dx} \int_a^{g(x)} f(t) dt = f(g(x)) \frac{d}{dx} g(x), \quad (6.5)$$

was used for the last equality in (6.4).

Finally, an expression that can in principle be used for the optimization of the DFE-ODD filters and LE-ODD filters is obtained by substituting (6.1) back into (6.4).

6.2 Gradient Vector for DFE-ODD

The gradient vector for (5.18) can be obtained by substituting (6.1) into (6.4) and completing the resulting derivative. In the following derivation, the dependence of the SNR on \mathbf{h} and \mathbf{g} is dropped for convenience. This leads to

the following equation:

$$\begin{aligned}
\frac{\partial}{\partial \mathbf{g}^*} \text{PEP}_{\text{DFE}}(\mathbf{h}, \mathbf{g}) &= \left(\frac{-1}{\sqrt{8\pi}} \frac{\exp(-\alpha(\text{SNR}_{\text{DFE}} - 1)/2)}{\sqrt{\alpha(\text{SNR}_{\text{DFE}} - 1)}} \right) \frac{\partial}{\partial \mathbf{g}^*} y_{\text{DFE}} \\
&= \left(\frac{-1}{\sqrt{8\pi}} \frac{\exp(-\alpha(\text{SNR}_{\text{DFE}} - 1)/2) \alpha \text{SNR}_{\text{DFE}}}{\sqrt{\alpha(\text{SNR}_{\text{DFE}} - 1)}} \right) \\
&\quad \times \frac{\partial}{\partial \mathbf{g}^*} \left(\int_{-1/2}^{1/2} \ln \left[\frac{\sigma_n^2}{\sigma_b^2} + \sum_{n_r=1}^{N_R} |H_{n_r}^{\text{eq}}(e^{j2\pi x})|^2 \right] dx \right) \\
&= \left(\frac{-1}{\sqrt{8\pi}} \frac{\exp(-\alpha(\text{SNR}_{\text{DFE}} - 1)/2) \alpha \text{SNR}_{\text{DFE}}}{\sqrt{\alpha(\text{SNR}_{\text{DFE}} - 1)}} \right) \\
&\quad \times \int_{-1/2}^{1/2} \frac{\frac{\partial}{\partial \mathbf{g}^*} \sum_{n_r=1}^{N_R} |H_{n_r}^{\text{eq}}(e^{j2\pi x})|^2}{\left[\frac{\sigma_n^2}{\sigma_b^2} + \sum_{n_r=1}^{N_R} |H_{n_r}^{\text{eq}}(e^{j2\pi x})|^2 \right]} dx. \tag{6.6}
\end{aligned}$$

At this point it should be clear that a closed-form solution to the above expression is not feasible because both SNR_{DFE} and the integral in the above expression cannot be computed in closed-form. To compute (6.6) numerically, SNR_{DFE} can be approximated by (5.10) and the integral can be approximated by using the same approach as in Section 5.1. The resulting gradient vector becomes

$$\begin{aligned}
\frac{\partial}{\partial \mathbf{g}^*} \text{PEP}_{\text{DFE}}(\mathbf{h}, \mathbf{g}) &\approx \left(\frac{-1}{\sqrt{8\pi}} \frac{\exp(-\alpha(\text{SNR}_{\text{DFE-NU}} - 1)/2) \alpha \text{SNR}_{\text{DFE-NU}}}{(2\bar{N} + 1) \sqrt{\alpha(\text{SNR}_{\text{DFE-NU}} - 1)}} \right) \\
&\quad \times \sum_{s=-\bar{N}}^{\bar{N}} \frac{\left(\sum_{n_r=1}^{N_R} \mathbf{H}_{n_r}^H \mathbf{d}^H \mathbf{d} \mathbf{H}_{n_r} \right) \mathbf{g}}{\left[\frac{\sigma_n^2 N_T}{\sigma_b^2 E_s} + \mathbf{g}^H \left(\sum_{n_r=1}^{N_R} \mathbf{H}_{n_r}^H \mathbf{d}^H \mathbf{d} \mathbf{H}_{n_r} \right) \mathbf{g} \right]}. \tag{6.7}
\end{aligned}$$

6.3 Gradient Vector for LE-ODD

The gradient vector for (5.19) can be computed in a similar way as for DFE by substituting (6.1) into (6.4) and completing the resulting derivative. Again, the dependence of the SNR on \mathbf{h} and \mathbf{g} is dropped in the following derivation

for convenience. The following expression results:

$$\begin{aligned}
\frac{\partial}{\partial \mathbf{g}^*} \text{PEP}_{\text{LE}}(\mathbf{h}, \mathbf{g}) &= \left(\frac{-1}{\sqrt{8\pi}} \frac{\exp(-\alpha(\text{SNR}_{\text{LE}} - 1)/2)}{\sqrt{\alpha(\text{SNR}_{\text{LE}} - 1)}} \right) \frac{\partial}{\partial \mathbf{g}^*} y_{\text{LE}} \\
&= \left(\frac{-\alpha}{\sqrt{8\pi}} \frac{\exp(-\alpha(\text{SNR}_{\text{LE}} - 1)/2)}{\sqrt{\alpha(\text{SNR}_{\text{LE}} - 1)}} \right) \\
&\quad \times \frac{\partial}{\partial \mathbf{g}^*} \left(\int_{-1/2}^{1/2} \frac{\sigma_n^2}{\sigma_b^2 \sum_{n_r=1}^{N_R} |H_{n_r}^{\text{eq}}(e^{j2\pi x})|^2 + 1} dx \right)^{-1} \\
&= \left(\frac{-\alpha}{\sqrt{8\pi}} \frac{\exp(-\alpha(\text{SNR}_{\text{LE}} - 1)/2)}{\sqrt{\alpha(\text{SNR}_{\text{LE}} - 1)}} \right) \\
&\quad \times - \int_{-1/2}^{1/2} \frac{\partial}{\partial \mathbf{g}^*} \left(\frac{1}{\frac{\sigma_b^2}{\sigma_n^2} \sum_{n_r=1}^{N_R} |H_{n_r}^{\text{eq}}(e^{j2\pi x})|^2 + 1} \right) dx \\
&\quad \times \left[\int_{-1/2}^{1/2} \frac{1}{\frac{\sigma_b^2}{\sigma_n^2} \sum_{n_r=1}^{N_R} |H_{n_r}^{\text{eq}}(e^{j2\pi x})|^2 + 1} dx \right]^{-2} \\
&= \left(\frac{-\alpha(\text{SNR}_{\text{LE}})^2 \exp(-\alpha(\text{SNR}_{\text{LE}} - 1)/2)}{\sqrt{8\pi} \sqrt{\alpha(\text{SNR}_{\text{LE}} - 1)}} \right) \\
&\quad \times \int_{-1/2}^{1/2} \left(\frac{\frac{\partial}{\partial \mathbf{g}^*} \left(\frac{\sigma_b^2}{\sigma_n^2} \sum_{n_r=1}^{N_R} |H_{n_r}^{\text{eq}}(e^{j2\pi x})|^2 + 1 \right)}{\left(\frac{\sigma_b^2}{\sigma_n^2} \sum_{n_r=1}^{N_R} |H_{n_r}^{\text{eq}}(e^{j2\pi x})|^2 + 1 \right)^2} \right) dx. \quad (6.8)
\end{aligned}$$

Again a closed-form solution to the above expression is not possible and therefore, a numerical method is used to approximate (6.8). SNR_{LE} can be approximated by (5.13) and the integral can be approximated by using a similar approach as used in Section 5.1. The resulting gradient vector is

$$\begin{aligned}
\frac{\partial}{\partial \mathbf{g}^*} \text{PEP}_{\text{LE}}(\mathbf{h}, \mathbf{g}) &= \left(\frac{-\alpha(\text{SNR}_{\text{LE-NU}})^2 \exp(-\alpha(\text{SNR}_{\text{LE-NU}} - 1)/2)}{(2\bar{N} + 1) \sqrt{8\pi} \sqrt{\alpha(\text{SNR}_{\text{LE-NU}} - 1)}} \right) \\
&\quad \times \sum_{s=-\bar{N}}^{\bar{N}} \left(\frac{\frac{\partial}{\partial \mathbf{g}^*} \left(\frac{\sigma_b^2 E_s}{\sigma_n^2 N_T} \mathbf{g}^H \left(\sum_{n_r=1}^{N_R} \mathbf{H}_{n_r}^H \mathbf{d}^H \mathbf{d} \mathbf{H}_{n_r} \right) \mathbf{g} + 1 \right)}{\left(\frac{\sigma_b^2 E_s}{\sigma_n^2 N_T} \mathbf{g}^H \left(\sum_{n_r=1}^{N_R} \mathbf{H}_{n_r}^H \mathbf{d}^H \mathbf{d} \mathbf{H}_{n_r} \right) \mathbf{g} + 1 \right)^2} \right)
\end{aligned}$$

$$\begin{aligned}
&= \left(\frac{-\alpha(\text{SNR}_{\text{LE-NU}})^2 \exp(-\alpha(\text{SNR}_{\text{LE-NU}} - 1)/2)}{(2\bar{N} + 1) \sqrt{8\pi} \sqrt{\alpha(\text{SNR}_{\text{LE-NU}} - 1)}} \right) \\
&\quad \times \sum_{s=-\bar{N}}^{\bar{N}} \left(\frac{\frac{\sigma_s^2 E_s}{\sigma_n^2 N_T} \left(\sum_{n_r=1}^{N_R} \mathbf{H}_{n_r}^H \mathbf{d}^H \mathbf{d} \mathbf{H}_{n_r} \right) \mathbf{g}}{\left(\frac{\sigma_s^2 E_s}{\sigma_n^2 N_T} \mathbf{g}^H \left(\sum_{n_r=1}^{N_R} \mathbf{H}_{n_r}^H \mathbf{d}^H \mathbf{d} \mathbf{H}_{n_r} \right) \mathbf{g} + 1 \right)^2} \right) \quad (6.9)
\end{aligned}$$

6.4 Adaptive Algorithm

If the equivalent channel \mathbf{h} is fixed, we can use the steepest descent algorithm to optimize the ODD filters. However, since wireless channels are random, we have to use a stochastic gradient algorithm to perform the filter search. A brief review of the steepest descent algorithm will be given first. Then we will describe the stochastic gradient algorithm, which is used in this work. The following two equations describe the steepest descent algorithm

$$\mathbf{g}_0[i+1] = \mathbf{g}[i] - \delta \left[\frac{\partial}{\partial \mathbf{g}^*} \text{PEP}_x(\mathbf{h}, \mathbf{g}[i]) \right], \quad (6.10)$$

$$\mathbf{g}[i+1] = \sqrt{\frac{N_T}{\mathbf{g}_0^H[i+1] \mathbf{g}_0[i+1]}} \mathbf{g}_0[i+1]. \quad (6.11)$$

The algorithm runs for a pre-defined number of iterations with a pre-defined step size, δ . Eq. (6.10) describes the operation of the algorithm for each iteration i . The negative sign in (6.10) refers to a minimization problem. A time index i is introduced to the vector \mathbf{g} to indicate that a new vector containing the ODD filter coefficients is obtained at the end of each iteration. At the end of each iteration, the new vector $\mathbf{g}[i+1]$ is normalized to ensure that the new vector has an energy of N_T . This is mathematically shown in (6.11).

The stochastic gradient algorithm is similar to the steepest descent algorithm explained above except that the fixed channel condition is removed. In other words, the equivalent channel \mathbf{h} is allowed to change for each iteration. In fact, for each iteration a new channel is generated according to the statistical properties of the wireless channel described in Chapter 2. This allows the

algorithm to adapt to the statistics of the wireless channel rather than to a specific one. In this way, the averaging over the statistics of the channel is done implicitly. The resulting stochastic gradient algorithm is given by,

$$\mathbf{g}_0[i+1] = \mathbf{g}[i] - \delta \left[\frac{\partial}{\partial \mathbf{g}^*} \text{PEP}_x(\mathbf{h}[i], \mathbf{g}[i]) \right], \quad (6.12)$$

$$\mathbf{g}[i+1] = \sqrt{\frac{N_T}{\mathbf{g}_0^H[i+1]\mathbf{g}_0[i+1]}} \mathbf{g}_0[i+1]. \quad (6.13)$$

The new notation $\mathbf{h}[i]$ is introduced to indicate that a new channel is used for each iteration. The number of channels that are used for the results in this work is 100,000. These channel samples are generated by a program taken from the previous work [1, 2].

6.5 Convergence of the ODD Schemes

The proposed stochastic gradient algorithm runs for a certain numbers of iterations before it converges. Ideally, the shorter the time it takes the algorithm to produce the filters with good performance, the better. There are a few factors which affect the convergence time of the algorithm and the performance of the resulting ODD filters, e.g., the number of iterations that shall be performed, the initial filter coefficients, N , \bar{N} , and δ . However, convergence time is not very crucial here because in practice, the ODD filters have to be optimized only once for each base station, since we consider transmissions in the downlink direction and the channel statistics for a given base station do not significantly change with time. Nonetheless, it is still desirable to choose the right parameters such that the resulting algorithm does not take too long to converge yet providing good performance.

Because of the relatively involved nature it seems to be difficult to provide a convergence proof for the proposed stochastic gradient algorithm. However, our simulation results suggest that the stochastic gradient algorithm always converges if the parameters such as \bar{N} and δ are chosen properly. The various factors that affect the convergence behaviour of the algorithm and the

performance of the resulting ODD filters will be discussed in the following sections.

6.6 The Influence of δ

An appropriate step size δ has to be chosen before running the proposed algorithm. It is found that although δ affects the convergence time, it does not affect the performance of the converged ODD filters. In Figure 6.1, the $\mathcal{E}\{\text{PEP}_{\text{DFE}}(\mathbf{h}, \mathbf{g})\}$ vs. the iteration number i of the stochastic gradient algorithm for 2-PSK transmission over an EQ profile with $L = 7$, $N_T = 2$, $N_R = 2$, $\boldsymbol{\rho}_t = [0.5]$, and $\boldsymbol{\rho}_r = [0.7]$ is shown. The filters were optimized for $10\log_{10}(E_b/N_0) = 10$ dB. $\mathcal{E}\{\text{PEP}_{\text{DFE}}(\mathbf{h}, \mathbf{g})\}$ was calculated over 100,000 channel samples using (5.10) and (5.20) at 10 dB. For the results in this section, we use $\bar{N} = 10$ and we initialize the algorithm with GDD filters with $N = 3$. In other words,

$$\mathbf{g}[0] = \begin{bmatrix} 1 & 0 & 0 & 0 & 0 & 1 \end{bmatrix}^T \quad (6.14)$$

for this case. The influence of \bar{N} , initial filter coefficients, and N will be discussed in each of the subsequent sections, respectively.

For the step size of the algorithm we adopted $\delta = 2$, $\delta = 4$, and $\delta = 10$. If δ is chosen properly, it is expected that $\mathcal{E}\{\text{PEP}_{\text{DFE}}(\mathbf{h}, \mathbf{g})\}$ decreases with increasing number of iterations. When $\delta = 2$ is used, the number of iterations required for the algorithm to converge is about 40,000. On the other hand, if $\delta = 10$ is used instead, only about 10,000 iterations are required for the algorithm to converge.

In Figure 6.2, we consider the EQ profile with 8-PSK modulation, $N_T = 2$, $N_R = 1$, $N = 3$, $\bar{N} = 10$, $\boldsymbol{\rho}_t = [0.5]$, and DFE employed at the receiver. The filters were optimized for $10\log_{10}(E_b/N_0) = 15$ dB and $\mathcal{E}\{\text{PEP}_{\text{DFE}}(\mathbf{h}, \mathbf{g})\}$ at 15 dB is shown in the figure. For the step size, we adopted $\delta = 0.1$, 0.2 , and 2 . The same observation as in the previous case is made, i.e., convergence time decreases with increasing δ . It is also noted that for the $\delta = 2$ curve, there are

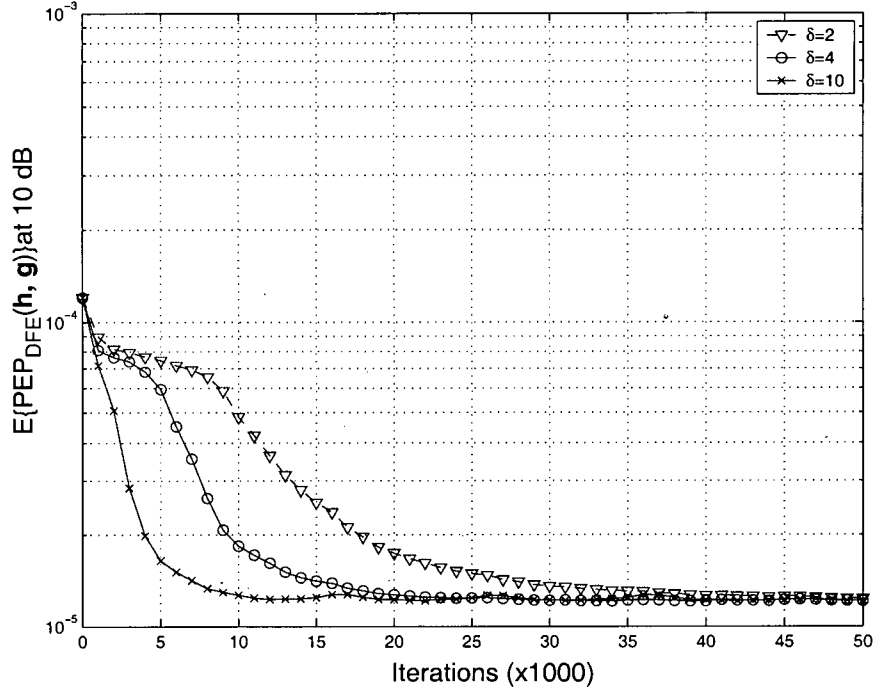


Figure 6.1: $\mathcal{E}\{\text{PEP}_{\text{DFE}}(\mathbf{h}, \mathbf{g})\}$ vs. number of iterations for 2-PSK transmission over EQ channel with $L = 7$, $N_T = N_R = 2$, $N = 3$, $\bar{N} = 10$, $\rho_t = [0.5]$, $\rho_r = [0.7]$, and DFE at the receiver.

ripples at iteration $i = 6000, 11000, 16000, 26000,$ and 36000 . This behaviour is inherited from our stochastic gradient algorithm because a new channel is used for each iteration and as a result, the algorithm will not converge to a specific value if a relatively large δ is used. Consequently, a large δ results in larger ripples. This is evidenced in this figure where the smaller δ s, i.e., $\delta = 0.1$ and 0.2 , do not result in noticeable ripples. It should be noted that the algorithm may not even converge if δ is too large.

The same observation can be made for the LE-ODD scheme. Figures 6.3 and 6.4 use exactly the same setup in Figures 6.1 and 6.2, however, with LE employed at the receiver and the filters were optimized for $10\log_{10}(E_b/N_0) = 15$ dB and $10\log_{10}(E_b/N_0) = 20$ dB, respectively. $\mathcal{E}\{\text{PEP}_{\text{DFE}}(\mathbf{h}, \mathbf{g})\}$ at 15 dB and 20 dB is shown in Figures 6.3 and 6.4, respectively. One can see that δ affects the convergence time and the amount of ripple after convergence in the same

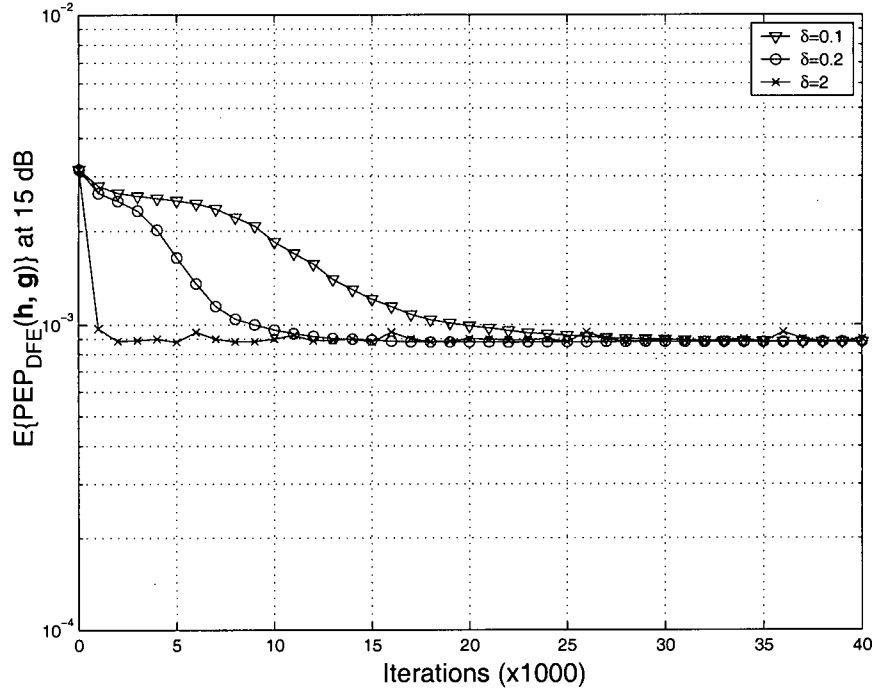


Figure 6.2: $\mathcal{E}\{\text{PEP}_{\text{DFE}}(\mathbf{h}, \mathbf{g})\}$ vs. number of iterations for 8-PSK transmission over EQ channel with $L=7$, $N_T = 2$, $N_R = 1$, $N = 3$, $\bar{N} = 10$, $\rho_t = [0.5]$, and DFE at the receiver.

way that it does for the DFE cases.

6.7 The Influence of \bar{N}

In order to compute (5.10), (5.14), (6.7) and (6.9), a suitable value for \bar{N} has to be chosen. In theory, one would want to choose \bar{N} as large as possible because a larger \bar{N} gives a more accurate approximation of the integrals. However, a larger \bar{N} also translates into a higher complexity since more points need to be evaluated for the integral. As we have already mentioned, convergence time is not very important because, in practice, the ODD filters have to be optimized only once for each base station. Nevertheless, it is still desirable to choose a value for \bar{N} such that the resulting expressions are not too complex to evaluate yet providing accurate result. It is the goal of this section to investigate the

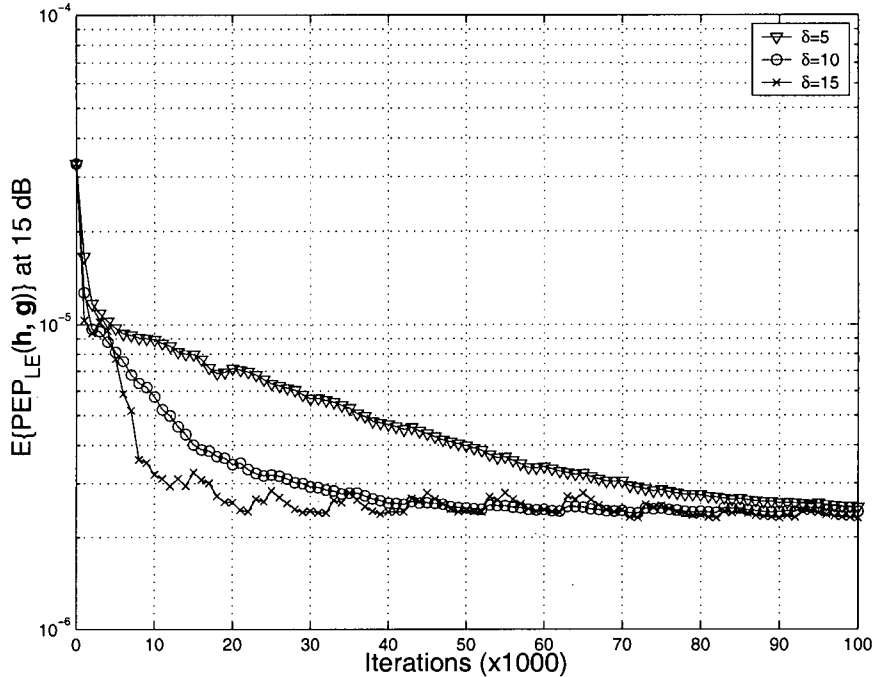


Figure 6.3: $\mathcal{E}\{\text{PEP}_{\text{LE}}(\mathbf{h}, \mathbf{g})\}$ vs. number of iterations for 2-PSK transmission over EQ channel with $L = 7$, $N_T = N_R = 2$, $N = 3$, $\bar{N} = 10$, $\rho_t = [0.5]$, $\rho_r = [0.7]$, and LE at the receiver.

influence of \bar{N} on the performance of the resulting ODD filters.

To do this, different \bar{N} s were used to generate the ODD filters for a specific channel setups. We show the average simulated BERs of the ODD schemes with $N = 3$ and different values of \bar{N} for different power delay profiles. The ODD filters were optimized for $10\log_{10}(E_b/N_0) = 10$ dB and 15 dB for DFE and LE, respectively. We use the channel model described in Chapter 2 and at least 10000 CIRs have been randomly generated in accordance with the respective power delay profile for each $10\log_{10}(E_b/N_0)$ value simulated. The BER vs. \bar{N} results are shown in Figure 6.5. The top graph shows the BER simulation results for 2-PSK transmission over EQ, TU, and HT with DFE employed at the receiver, respectively. In all cases, two transmit antennas and one receive antenna are used. The correlation factors used for EQ, TU, and HT are 0.5, 0.5, and 0.7, respectively. The graph plots the average simulated

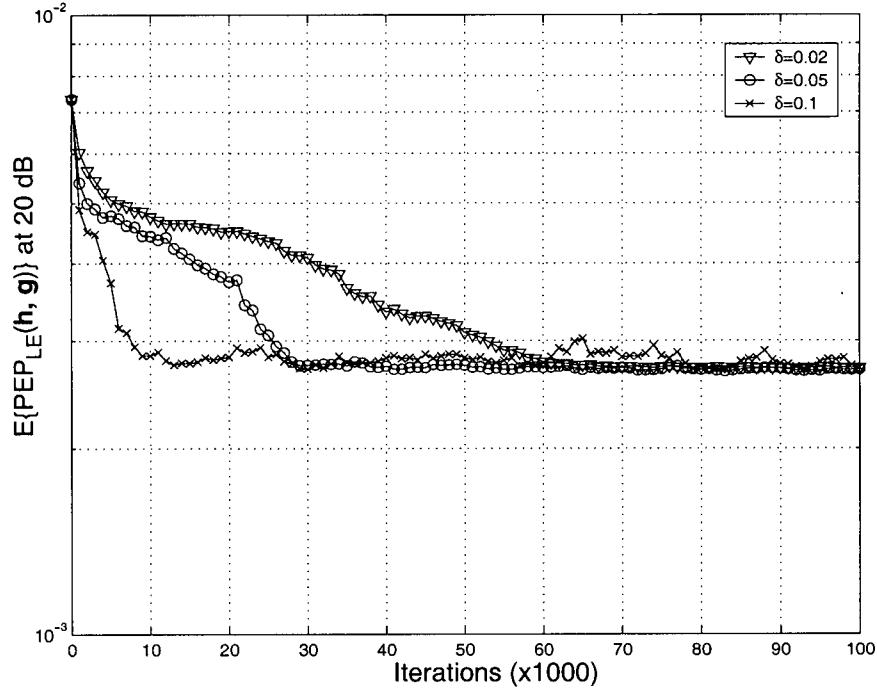


Figure 6.4: $\mathcal{E}\{\text{PEP}_{\text{LE}}(\mathbf{h}, \mathbf{g})\}$ vs. number of iterations for 8-PSK transmission over EQ channel with $L = 7$, $N_T = 2$, $N_R = 1$, $N = 3$, $\bar{N} = 10$, $\boldsymbol{\rho}_t = [0.5]$, and LE at the receiver.

BER at $10\log_{10}(E_b/N_0) = 10$ dB for all three cases. It is noticed that different values of \bar{N} do not result in a big difference in the BER except for the EQ profile where $\bar{N} = 1$ yields inferior performance.

The bottom graph shows the BER at 15 dB vs. \bar{N} results for LE with the same channels used in the DFE cases. It can be seen that also in this case, \bar{N} does not affect the BER except for the EQ profile, where $\bar{N} = 1, 2, 3$, and 4 suffer from a performance penalty. Therefore, a relatively small value of \bar{N} can be used. This is desirable because a small \bar{N} speeds up the optimization process.

It is interesting to find out that a small \bar{N} yields comparable result to a large \bar{N} . The main reason to this is that we consider $\mathcal{E}\{\text{PEP}_x(\mathbf{h}, \mathbf{g})\}$ instead of $\text{PEP}_x(\mathbf{h}, \mathbf{g})$ for a specific channel. To illustrate this, we consider the EQ profile with 8-PSK, $N_T = 2$, $N_R = 1$, $N = 3$, $\boldsymbol{\rho}_t = [0.5]$, and DFE employed at the

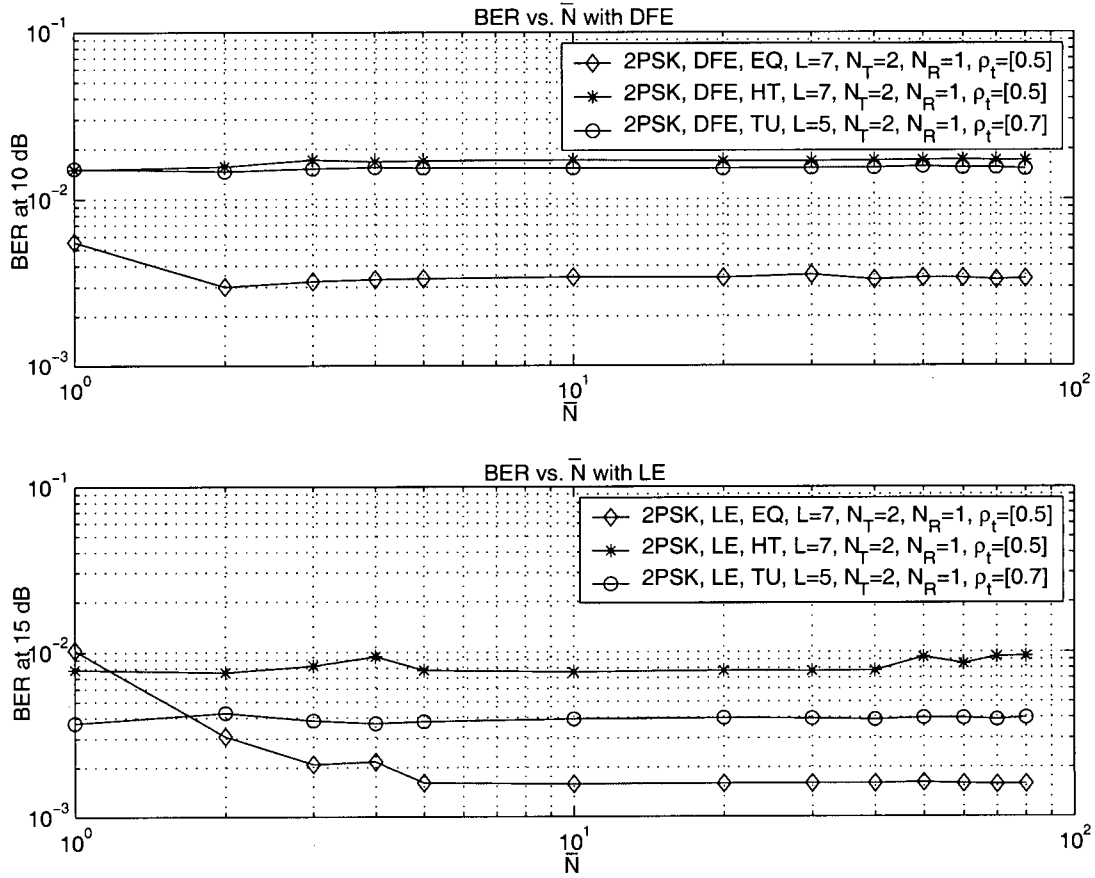


Figure 6.5: Simulated BER vs. \bar{N} for DFE and LE.

receiver. We evaluate $\text{PEP}_{\text{DFE}}(\mathbf{h}[i], \mathbf{g})$ according to (5.18) at $10\log_{10}(E_b/N_0) = 15$ dB with $\mathbf{g} = [1, 0, 0, 0, 0, 1]$ for 50 independent channels, i.e., $i = 1, \dots, 50$, using $\bar{N} = 5$ and 100, respectively. The result is shown in Figure 6.6.

It can be seen that different \bar{N} s indeed give different $\text{PEP}_{\text{DFE}}(\mathbf{h}[i], \mathbf{g})$ values. Obviously, $\text{PEP}_{\text{DFE}}(\mathbf{h}[i], \mathbf{g})$ calculated using $\bar{N} = 100$ is more accurate than the one calculated using $\bar{N} = 5$. However, if we use the same \bar{N} s to compute $\mathcal{E}\{\text{PEP}_{\text{DFE}}(\mathbf{h}, \mathbf{g})\}$ over 100,000 samples, their values are

$$\mathcal{E}\{\text{PEP}_{\text{DFE}}(\mathbf{h}, \mathbf{g})\}_{\bar{N}=5} = 0.00323044820091, \quad (6.15)$$

and

$$\mathcal{E}\{\text{PEP}_{\text{DFE}}(\mathbf{h}, \mathbf{g})\}_{\bar{N}=100} = 0.00314907825794, \quad (6.16)$$

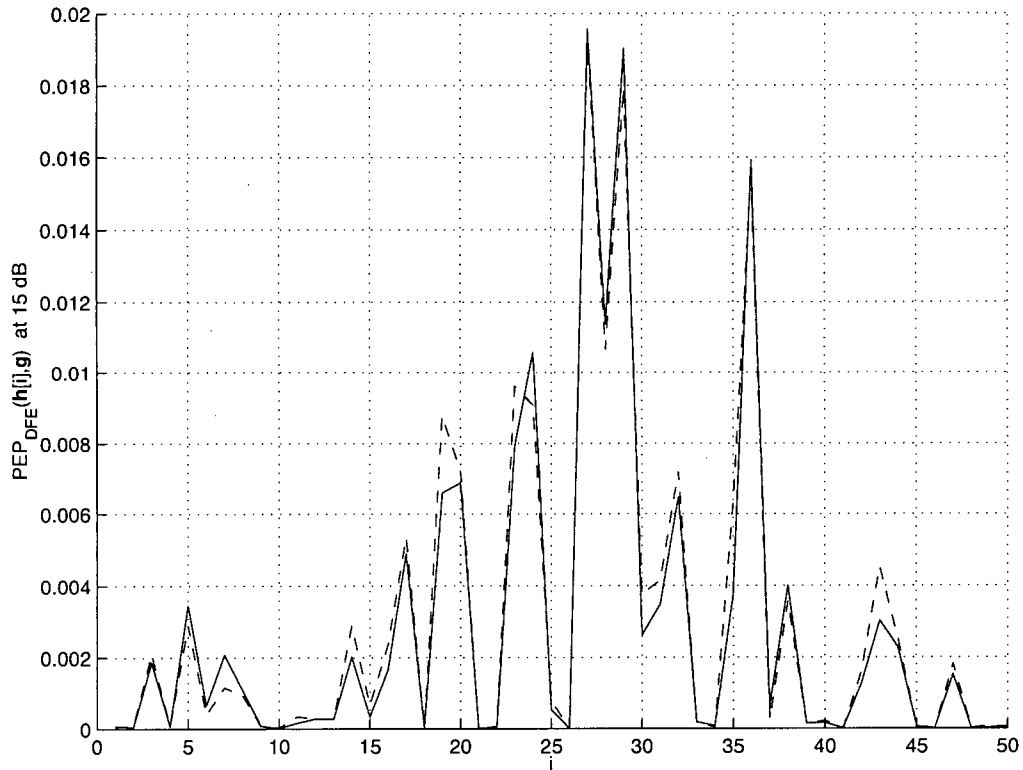


Figure 6.6: $\text{PEP}_{\text{DFE}}(\mathbf{h}[i], \mathbf{g})$ vs. i for 8-PSK transmission over EQ profile with $N_T = 2$, $N_R = 1$, $N = 3$, $\rho_t = [0.5]$, and DFE employed at receiver. Solid line: $\bar{N} = 5$. Dashed line: $\bar{N} = 100$.

respectively. The difference is less than 2.6%. Therefore, we conclude that although it may not be a good idea to use a small \bar{N} to evaluate $\text{PEP}_x(\mathbf{h}, \mathbf{g})$, it is acceptable to use a relatively small \bar{N} to run the stochastic gradient algorithm and evaluate $\mathcal{E}\{\text{PEP}_x(\mathbf{h}, \mathbf{g})\}$ because the averaging compensates for the error which a small \bar{N} causes. In the following, we use $\bar{N} = 10$.

6.8 The Influence of the Initial ODD Filter Coefficients

The proposed gradient search method requires an initial filter vector $\mathbf{g}[0]$ to start from. The initial filter coefficients may affect the performance of the re-

sulting ODD filters and the convergence time of the algorithm. By randomly choosing some initial filter vector and comparing the performance of the resulting final filter coefficients, it is found that the initial filter vector chosen does not play a big role in the performance of the resulting ODD filters. Also, the initial filter vector chosen does not affect the convergence time significantly. Therefore, the GDD filter is always used as the initial filter vector in this work for convenience. For example, in a $N_T = 3$ and $N = 3$ case, the initial filter vector would be set to

$$\mathbf{g}[0] = \begin{bmatrix} 1 & 0 & 0 & 0 & 1 & 0 & 0 & 0 & 1 \end{bmatrix}^T. \quad (6.17)$$

To illustrate the point, we initialize the algorithm with two different $\mathbf{g}[0]$ s and evaluate $\mathcal{E}\{\text{PEP}_{\text{DFE}}(\mathbf{h}, \mathbf{g})\}$ at 10 dB for every 1000 iterations for the EQ profile with 2-PSK, $N_T = 2$, $N_R = 2$, $N = 3$, $\boldsymbol{\rho}_t = [0.5]$, $\boldsymbol{\rho}_r = [0.7]$, and DFE employed at the receiver. $\delta = 10$ was used to optimize the ODD filters. The two initial filter vectors considered are

$$\mathbf{g}[0] = \frac{1}{\sqrt{3}} \begin{bmatrix} 1 & 1 & 1 & 1 & 1 & 1 \end{bmatrix}^T, \quad (6.18)$$

and

$$\mathbf{g}[0] = \begin{bmatrix} 1 & 0 & 0 & 0 & 0 & 1 \end{bmatrix}^T. \quad (6.19)$$

The filters were optimized for $10\log_{10}(E_b/N_0) = 10$ dB and the results are shown in Figure 6.7.

It is seen that the algorithm converges to the same $\mathcal{E}\{\text{PEP}_{\text{DFE}}(\mathbf{h}, \mathbf{g})\}$ value independent of the $\mathbf{g}[0]$ s used. In other words, the resulting performance of the ODD filters optimized with different $\mathbf{g}[0]$ s are essentially the same. It is also noted in the graph that although the algorithm converges faster with initial filter vector set to

$$\mathbf{g}[0] = \frac{1}{\sqrt{3}} \begin{bmatrix} 1 & 1 & 1 & 1 & 1 & 1 \end{bmatrix}^T, \quad (6.20)$$

the improvement is not significant.

In Figure 6.8, we consider the EQ profile with 8-PSK modulation, $N_T = 2$, $N_R = 1$, $N = 3$, $\boldsymbol{\rho}_t = [0.5]$, and DFE employed at the receiver. The filters were

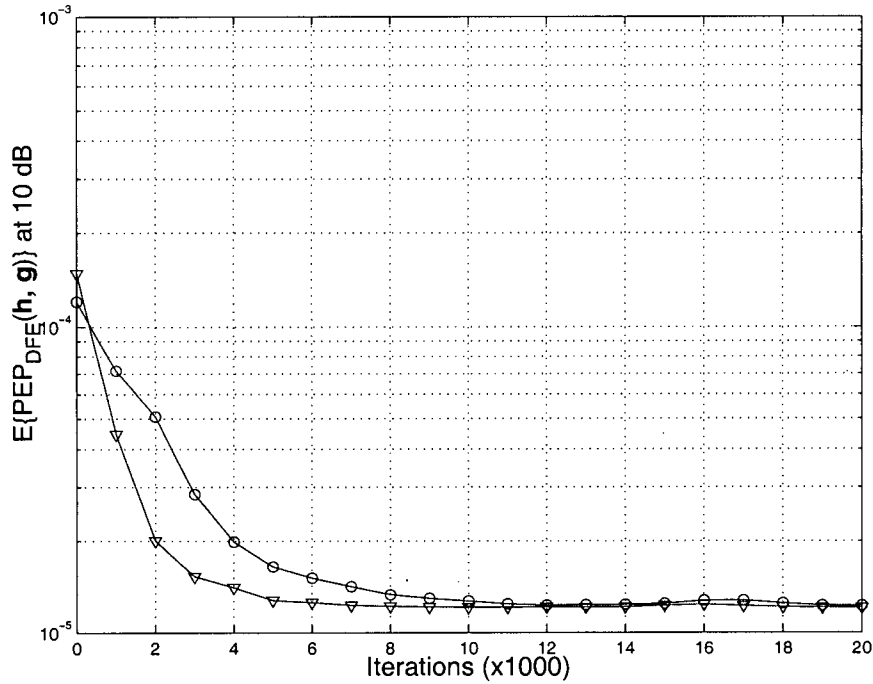


Figure 6.7: $\mathcal{E}\{\text{PEP}_{\text{DFE}}(\mathbf{h}, \mathbf{g})\}$ vs. number of iterations for 2-PSK transmission over EQ channel with $L = 7$, $N_T = N_R = 2$, $N = 3$, $\delta = 10$, $\boldsymbol{\rho}_t = [0.5]$, $\boldsymbol{\rho}_r = [0.7]$, and DFE at the receiver. Circles: $\mathbf{g}[0] = [1 \ 0 \ 0 \ 0 \ 0 \ 1]^T$. Triangles: $\mathbf{g}[0] = 1/\sqrt{3}[1 \ 1 \ 1 \ 1 \ 1]^T$.

optimized for $10\log_{10}(E_b/N_0) = 15$ dB with $\delta = 0.1$. We initialize the algorithm with the filter coefficients defined in (6.18) and (6.19). Again, ODD filters optimized with different $\mathbf{g}[0]$ s yield almost exactly the same $\mathcal{E}\{\text{PEP}_{\text{DFE}}(\mathbf{h}, \mathbf{g})\}$ after convergence. Also for this case, the algorithm initialized with (6.18) converges faster than the one initialized with (6.19).

Similar observations can be made for the LE-ODD scheme. Figures 6.9 and 6.10 again show the $\mathcal{E}\{\text{PEP}_{\text{LE}}(\mathbf{h}, \mathbf{g})\}$ as a function of the iteration number, i . The same system parameters as used in Figures 6.3 and 6.4 are valid for Figures 6.9 and 6.10, respectively, however, with LE employed at the receiver. The ODD filters of Figure 6.9 were optimized for $10\log_{10}(E_b/N_0) = 15$ dB with $\delta = 10$ while those of Figure 6.10 were optimized for $10\log_{10}(E_b/N_0) = 20$ dB with $\delta = 0.05$. In both figures, one can see that although $\mathbf{g}[0]$ affects

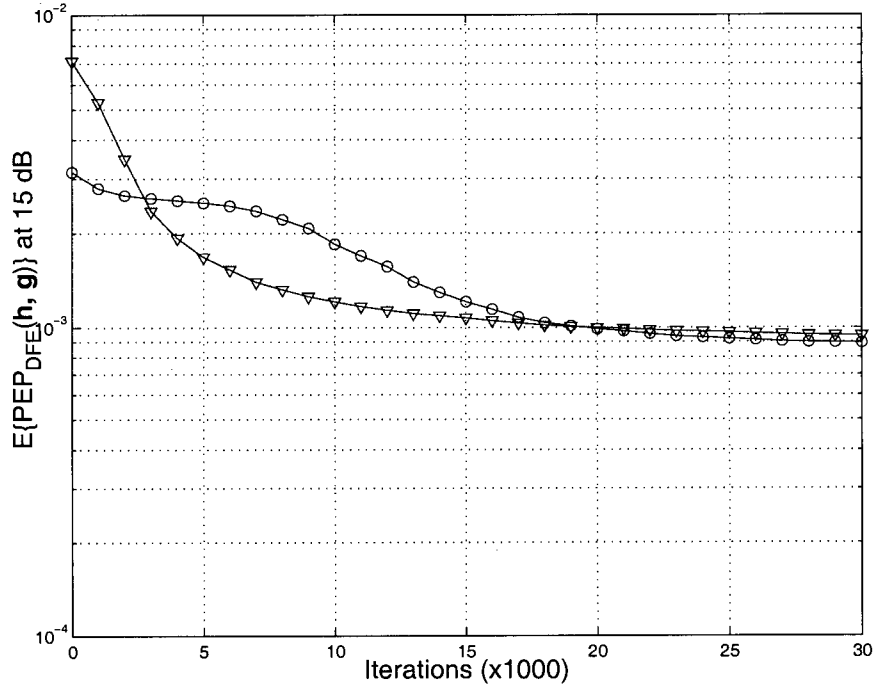


Figure 6.8: $\mathcal{E}\{\text{PEP}_{\text{DFE}}(\mathbf{h}, \mathbf{g})\}$ vs. number of iterations for 8-PSK transmission over EQ channel with $L = 7$, $N_T = 2$, $N_R = 1$, $N = 3$, $\delta = 0.1$, $\rho_t = [0.5]$, and DFE at the receiver. Circles: $\mathbf{g}[0] = [1 \ 0 \ 0 \ 0 \ 0 \ 1]^T$. Triangles: $\mathbf{g}[0] = 1/\sqrt{3}[1 \ 1 \ 1 \ 1 \ 1 \ 1]^T$.

the convergence time, the resulting ODD filters initialized with different $\mathbf{g}[0]$ s always yield similar performance after the filters converge.

It is worth mentioning that the converged ODD filters do not necessarily have to be the same filters even though they yield similar $\mathcal{E}\{\text{PEP}_{\text{DFE}}(\mathbf{h}, \mathbf{g})\}$ values. In fact, it can be inferred from (5.10), (5.14), (5.18), and (5.19) that for a given vector \mathbf{x} of length NN_T , $\mathbf{g} = e^{j\theta}\mathbf{x}$ yields the same average BER for any phase θ . Since we are mostly interested in the performance of the ODD filters and we can be sure that the algorithm converges in less than 100,000 iterations as long as we choose a proper δ , we always use the GDD filters to initialize the algorithm in this work for convenience.

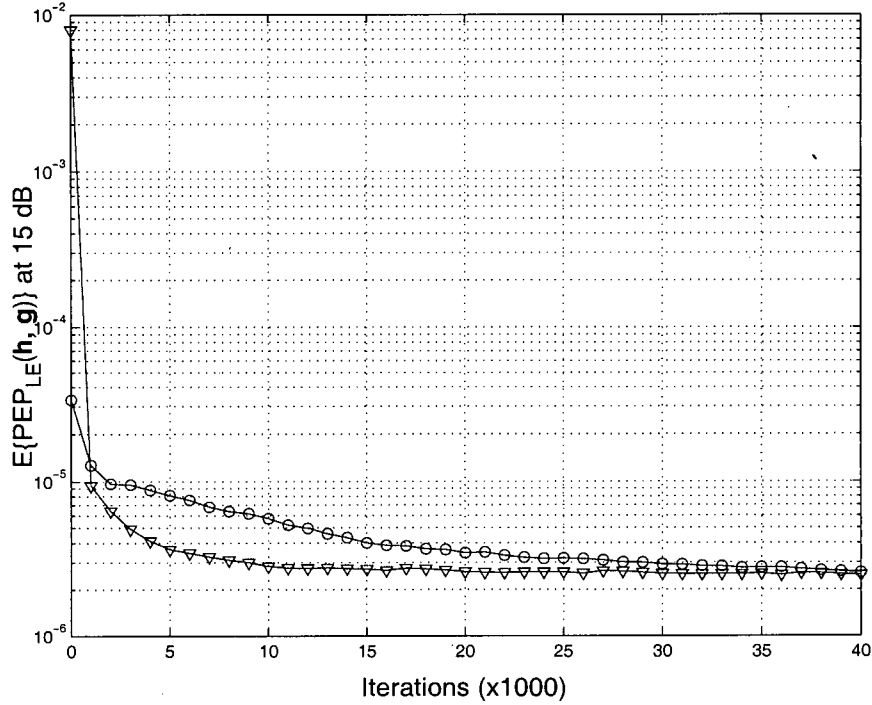


Figure 6.9: $\mathcal{E}\{\text{PEP}_{\text{LE}}(\mathbf{h}, \mathbf{g})\}$ vs. number of iterations for 8-PSK transmission over EQ channel with $L = 7$, $N_T = N_R = 2$, $N = 3$, $\delta = 10$, $\boldsymbol{\rho}_t = [0.5]$, $\boldsymbol{\rho}_r = [0.7]$, and LE at the receiver. Circles: $\mathbf{g}[0] = [1 \ 0 \ 0 \ 0 \ 1]^T$. Triangles: $\mathbf{g}[0] = 1/\sqrt{3}[1 \ 1 \ 1 \ 1 \ 1]^T$.

6.9 The Influence of N

Until now only filters of length $N = 3$ have been considered. It is interesting to compare the performance of the various ODD schemes using filters of different lengths. Figure 6.11 and 6.12 show the average simulated BERs vs. the filter length N with DFE and LE employed at the receiver, respectively. We consider 2-PSK transmission over the EQ profile with $N_T = 2$, $N_R = 1$, and $\boldsymbol{\rho}_t = [0.5]$ for both cases.

The DFE-ODD filters of Figure 6.11 were optimized for $10\log_{10}(E_b/N_0) = 10$ dB, while the LE-ODD filters of Figure 6.12 were optimized for $10\log_{10}(E_b/N_0) = 15$ dB. The average BERs at 10 dB and 15 dB are shown in Figure 6.11 and 6.12, respectively. For the DFE-ODD case shown in Figure 6.11, increasing the

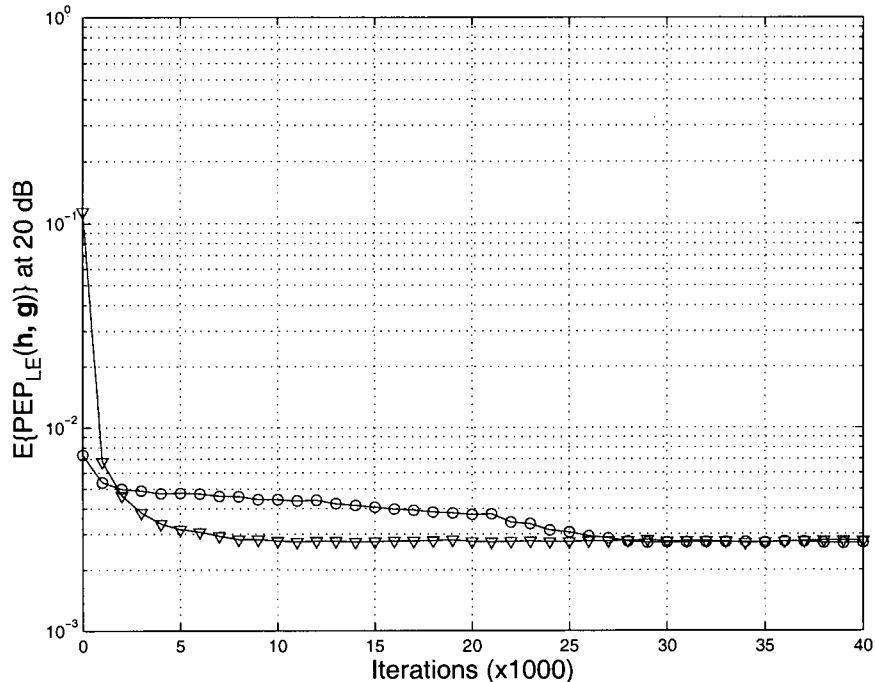


Figure 6.10: $\mathcal{E}\{\text{PEP}_{\text{LE}}(\mathbf{h}, \mathbf{g})\}$ vs. number of iterations for 8-PSK transmission over EQ channel with $L = 7$, $N_T = 2$, $N_R = 1$, $N = 3$, $\delta = 0.05$, $\boldsymbol{\rho}_t = [0.5]$, and LE at the receiver. Circles: $\mathbf{g}[0] = [1 \ 0 \ 0 \ 0 \ 0 \ 1]^T$. Triangles: $\mathbf{g}[0] = 1/\sqrt{3}[1 \ 1 \ 1 \ 1 \ 1 \ 1]^T$.

DFE-ODD filter length does not improve the performance of the filter. The filter with a length of 7 yields almost exactly the same result as the filter with a length of 1. We will see why the performance of the filter does not improve with N in the next chapter when we examine the filter coefficients. For the LE result shown in Figure 6.12, the performance of the LE-ODD filters improves with increasing N .

In general, longer DFE-ODD and LE-ODD filters achieve a better performance. However, they also increase the required computational complexity at the receiver, since larger N s correspond to longer equivalent CIRs which in turn require longer equalizer filters. The results also suggest that the DFE-ODD and LE-ODD filters of length $N > 1$ perform better than both the MLSE-ODD and GDD filters with longer lengths when DFE or LE are employed at

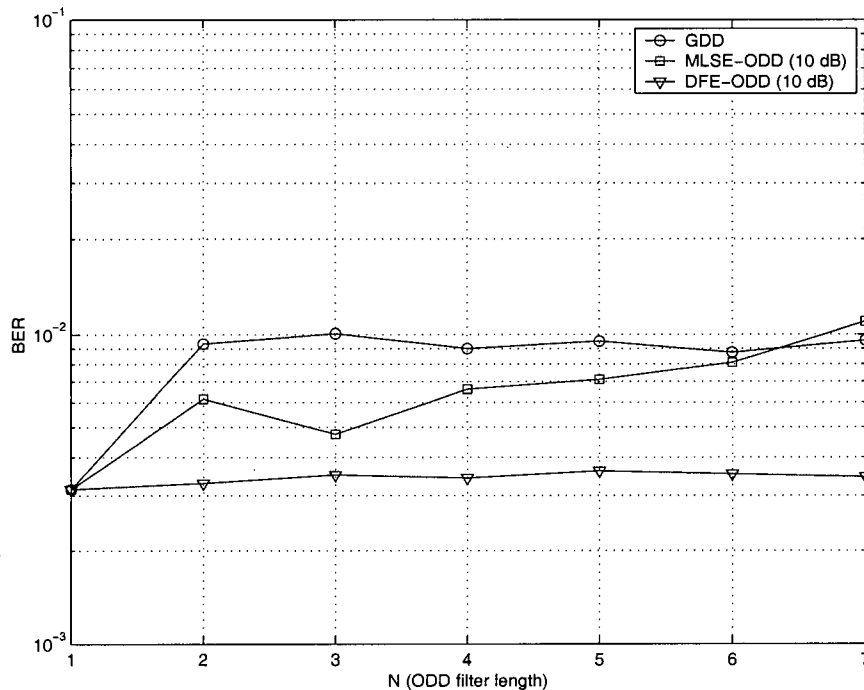


Figure 6.11: Simulated BER of DFE vs. N for 2-PSK transmission over EQ channel with $L = 7$, $N_T = 2$, $N_R = 1$ and $\rho_t = [0.5]$.

the receiver. This is desirable because the complexity of the receiver decreases with decreasing N . It is also interesting to note that the performance degrades when long MLSE-ODD or GDD filters are used. In fact, both GDD and MLSE-ODD filters achieve a better performance with $N = 1$ than with $N = 7$ for both DFE and LE. This shows the importance of an appropriate optimization of the DD filters for different equalization strategies.

Appendix A tabulates the DFE-ODD and LE-ODD filters for several different practically interesting channel profiles with different number of antennas and correlation factors.

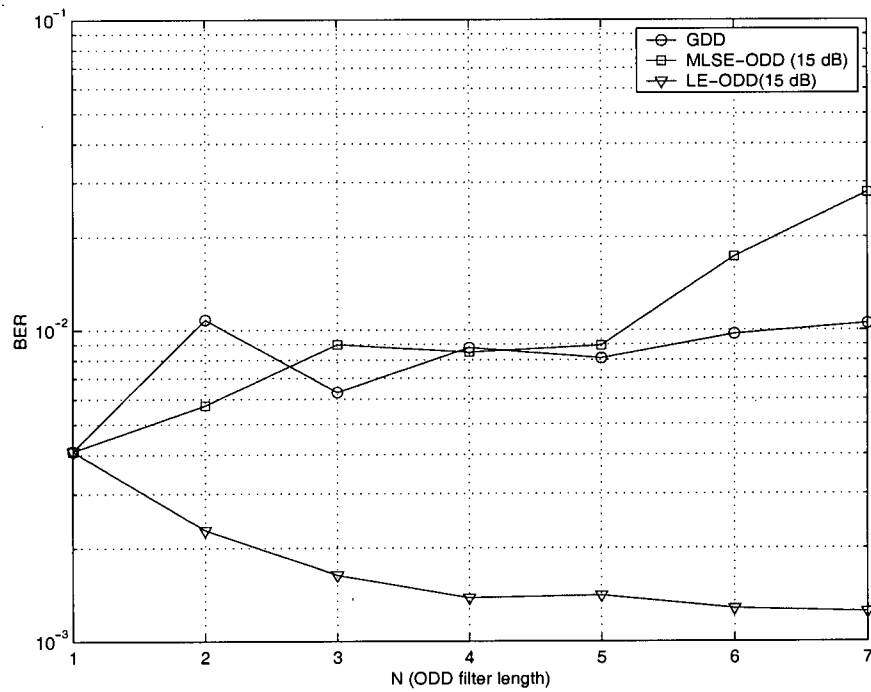


Figure 6.12: Simulated BER of LE vs. N for 2-PSK transmission over EQ channel with $L = 7$, $N_T = 2$, $N_R = 1$ and $\rho_t = [0.5]$.

Chapter 7

Simulation Results

In this chapter, we present some simulation results for the proposed DFE-ODD and LE-ODD schemes. The DFE-ODD and LE-ODD filter coefficients are obtained by using the stochastic gradient algorithm described in Chapter 6. The DFE-ODD and LE-ODD filters will be compared with the MLSE-ODD filters obtained in [1, 2] and the GDD filters proposed in [4]. Correlated MIMO frequency-selective Rayleigh fading channels presented in Chapter 2 are considered and simulations are carried out with a program taken from the previous work [1, 2]. The program was enhanced by introducing receive antenna correlation and LE at the receiver and by extending DFE to the case of multiple receive antennas. Suboptimum equalization strategies, DFE and LE, are used at the receiver. The DD filters in this chapter have a length of $N = 3$, since in general, larger N s do not improve performance significantly.

7.1 Decision-Feedback Equalization

Figures 7.1 and 7.2 show the 2-PSK simulation results when DFE is employed at the receiver with different power delay profiles and different numbers of antennas. Settings with up to three transmit antennas and two receive antennas are considered. Practical antenna correlations are considered where the receive antenna correlation factor is equal to or greater than the transmit an-

tenna correlation factor due to the smaller size of the mobile receiver. For each simulation result, the case with no transmit diversity ($N_T = 1$) is shown as dashed line as well for reference. The ODD filters were optimized for a certain E_b/N_0 value. The results show that the DFE-ODD filters perform better than both the GDD and MLSE-ODD filters at the E_b/N_0 for which the filters were optimized. Usually, we optimize the filters for $10\log_{10}(E_b/N_0) = 10$ dB unless for simulations with poor BER performance at 10 dB, where we optimize the filters for a higher SNR ratio. The E_b/N_0 value for which the filters were optimized is indicated in parenthesis in the legend of each graph.

The achieved gain by the DFE-ODD filters compared to the MLSE-ODD and GDD filters in most of cases is small. A relatively large gain is obtained for the EQ profile with $N_T = 2$ and $N_R = 2$. The gain that the DFE-ODD filters achieve over the MLSE-ODD filters is about 1 dB at $\text{BER} = 10^{-4}$. The results suggest that for 2-PSK transmission, the performance advantage of MLSE-ODD over GDD is not only preserved for DFE, but its performance is indeed close to that of the DFE-ODD scheme.

A careful look at the filter coefficients of the different ODD schemes indicates that the ODD filters are practically identical among the different transmit antennas for both MLSE-ODD and DFE-ODD schemes. As an example, the MLSE-ODD and DFE-ODD filter coefficients for 2-PSK transmission over the EQ profile with $N_T = 2$, $N_R = 1$, and $\rho_t = [0.5]$ are tabulated in Table 7.1. Both ODD filters were optimized for $10\log_{10}(E_b/N_0) = 10$ dB. One can see that the filter coefficients of both transmit antennas are almost identical for MLSE-ODD and DFE-ODD schemes, respectively. According to (2.30), the equivalent channel with the DFE-ODD filters shown in Table 7.1 is

$$h_{nr}^{\text{eq}}[k] = \sqrt{\frac{E_s}{N_T}} \{h_{11}[k] * g_1[k] + h_{12}[k] * g_2[k]\}. \quad (7.1)$$

This is very different from the equivalent channel resulted from the GDD filters where the equivalent channel is simply the sum of channel $h_{11}[k]$ and delayed version of $h_{12}[k]$. It is clear from Figures 7.1 and 7.2 that the DFE-ODD

Table 7.1: MLSE-ODD and DFE-ODD comparison: 2-PSK, EQ, $L = 7$, $N_T = 2$, $N_R = 1$, and $\rho_t = [0.5]$.

ODD filters	Tx	$g_i[0]$	$g_i[1]$	$g_i[2]$
MLSE	$i = 1$	0.77439	0.61059	-0.16582
	$i = 2$	0.77340	0.61412	-0.15718
DFE	$i = 1$	-0.21956+0.04205i	0.82452-0.14587i	0.49187-0.08346i
	$i = 2$	-0.23189+0.03666i	0.81385-0.15536i	0.49833-0.10027i

filters yield much better performance than the GDD filters. The MLSE-ODD filters obtained are different from the DFE-ODD filters, however, like the DFE-ODD filters, the MLSE-ODD filters are essentially identical for both transmit antennas. This explains why MLSE-ODD yields better performance than GDD as well. It has been already pointed out in Section 6.8 that different filters can yield the same average BER.

It is also interesting to look at the filter coefficients optimized for 2-PSK transmission over the EQ profile with $N_T = 2$, $N_R = 2$, $\rho_t = [0.5]$, and $\rho_r = [0.7]$. The filters were optimized for $10\log_{10}(E_b/N_0) = 10$ dB and the filter coefficients are shown in Table 7.2. It is noted that the energy is concentrated in the last taps of the ODD transmit filters. With those filter coefficients and using (2.30), one can see that the resulting equivalent channel, $h_{n_r}^{\text{eq}}[k]$, is almost simply the addition of the two overall channels, $h_{n_r,1}[k]$ and $h_{n_r,2}[k]$ with the $\sqrt{\frac{E_s}{N_T}}$ normalizing term multiplied to the result. It can be inferred that $N = 1$ would give almost the same results as $N = 3$. This explains why increasing the filter length, N , does not improve the performance of the resulting ODD filters for some setups such as the one shown in Figure 6.11.

For the ODD filters shown in Table 7.2, we should expect their performance to be similar to the no diversity case where there is only one transmit and two receive antennas. However, the simulation result depicted in Figure 7.2 shows that the DFE-ODD filters tabulated in Table 7.2 perform much better than the no diversity case. This is due to the fact that, in addition to the diversity

Table 7.2: DFE-ODD filter coefficients: 2-PSK, EQ, $L = 7$, $N_T = 2$, $N_R = 2$, $\rho_t = [0.5]$, and $\rho_r = [0.7]$.

ODD Filters	Tx	$g_i[0]$	$g_i[1]$	$g_i[2]$
DFE	$i = 1$	-0.09381-0.00623i	0.17003+0.00522i	0.97966+0.04984i
	$i = 2$	-0.08377-0.00061i	0.19674+0.01227i	0.97534+0.05329i

gain the ODD filters achieve, there is also a power gain due to the positive correlation factor, $\rho_t = [0.5]$, used between the two transmit antennas. This is shown mathematically as follows:

$$\begin{aligned}
 \mathcal{E} \left\{ |h_{n_r}^{\text{eq}}[k]|^2 \right\} &= \mathcal{E} \left\{ \left| \sqrt{\frac{E_s}{N_T}} (h_{n_r,1}[k] + h_{n_r,2}[k]) \right|^2 \right\} \\
 &= \frac{E_s}{N_T} \left\{ \mathcal{E} \left\{ |h_{n_r,1}[k]|^2 \right\} + \mathcal{E} \left\{ 2\text{Re} \left\{ h_{n_r,1}[k] h_{n_r,2}^*[k] \right\} \right\} \right. \\
 &\quad \left. + \mathcal{E} \left\{ |h_{n_r,2}[k]|^2 \right\} \right\} \\
 &= \frac{E_s}{N_T} \left\{ \sigma_{h_{n_r,1}[k]}^2 + 2\text{Re} \left\{ \rho_{12}^t \sqrt{\sigma_{h_{n_r,1}[k]}^2 \sigma_{h_{n_r,2}[k]}^2} \right\} + \sigma_{h_{n_r,2}[k]}^2 \right\} \quad (7.2)
 \end{aligned}$$

where

$$\mathcal{E} \left\{ |h_{n_r,n_t}[k]|^2 \right\} = \sigma_{h_{n_r,n_t}[k]}^2, \quad (7.3)$$

and the correlation factor ρ_{12}^t was defined in (2.12).

By looking at (7.2), one can immediately see that in addition to the energy contributed by the two overall channels, $\mathcal{E} \left\{ |h_{n_r,1}[k]|^2 \right\}$ and $\mathcal{E} \left\{ |h_{n_r,2}[k]|^2 \right\}$, there is also an extra term, $2\text{Re} \left\{ \rho_{12}^t \sqrt{\sigma_{h_{n_r,1}[k]}^2 \sigma_{h_{n_r,2}[k]}^2} \right\}$. If the correlation factor ρ_{12}^t is zero, the resulting power will be the same as the one where there is no diversity. On the other hand, if ρ_{12}^t is a positive number, there will be a power gain and in contrast, if ρ_{12}^t is negative, a power loss results. This explains why although the DFE-ODD filters have their energy concentrated in one tap, it achieves a relatively large gain over the no diversity case.

Figures 7.3 and 7.4 show the 8-PSK simulation results with the same system parameters as used for Figures 7.1 and 7.2, respectively. The results again indicate that the DFE-ODD filters perform better than both the GDD and the MLSE-ODD filters at the E_b/N_0 values for which the filters were optimized.

Table 7.3: MLSE-ODD and DFE-ODD comparison: 8-PSK, EQ, $L = 7$, $N_T = 3$, $N_R = 2$, $\rho_t = [0.5, 0.7, 0.5]$, and $\rho_r = [0.7]$.

ODD Filters	Tx	$g_i[0]$	$g_i[1]$	$g_i[2]$
MLSE	$i = 1$	-0.13491	0.63120	0.76379
	$i = 2$	-0.12665	0.63319	0.76357
	$i = 3$	-0.13160	0.63274	0.76310
DFE	$i = 1$	0.01288+0.00187i	0.04592-0.00349i	0.99885+0.00019i
	$i = 2$	-0.05947-0.00141i	0.08640+0.00613i	0.99446+0.00043i
	$i = 3$	-0.02954+0.00119i	0.05766-0.00481i	0.99788-0.00288i

The gain is minimal for the $N_R = 1$ cases except for the EQ profile. The figures for the EQ profile with one receive antenna indicate that the gain increases with SNR.

The DFE-ODD filters achieve a 1.7 dB gain over the GDD filters at 10^{-4} for the EQ profile with $N_T = 2$ and $N_R = 2$. It is also noted that the MLSE-ODD filters are inferior to the GDD filters for this setup and some other setups. The DFE-ODD filters have a 2 dB advantage at $\text{BER} = 10^{-3}$ over the MLSE-ODD filters for the EQ profile with $N_T = 3$ and $N_R = 2$. Although the DFE-ODD filters are better than the other filters for the TU profiles with two receive antennas, the gain is negligible.

We have also compared the MLSE-ODD and DFE-ODD filters for the 8-PSK modulation scheme. Similar to the 2-PSK modulation scheme, the coefficients of the ODD filters are practically identical for all the EQ profiles and for the other profiles if the filters were optimized for a low SNR ratio. This is true for both MLSE-ODD and DFE-ODD schemes. This is not surprising because the PEP depends only on d_{\min}^2 and SNR of the equalizer. As an example, the DFE-ODD filters optimized for EQ profile with $N_T = 3$, $N_R = 2$, $\rho_t = [0.5, 0.7, 0.5]$, and $\rho_r = [0.7]$ for $10\log_{10}(E_b/N_0) = 10$ dB is considered. Table 7.3 summarizes the result.

7.2 Linear Equalization

Figures 7.5 and 7.6 show the simulation results for 2-PSK and LE-ODD with different numbers of antennas and power delay profiles. The LE-ODD filters perform better than both the MLSE-ODD and GDD filters for all examples considered. The gains that the LE-ODD filters achieve over the MLSE-ODD and GDD filters are quite significant in some cases. For example, for 2-PSK simulation over the EQ profile with $N_T = 3$, $N_R = 1$, and $\boldsymbol{\rho}_t = [0.5, 0.5, 0.5]$, the LE-ODD filters provide a 6 dB gain over the GDD filters at $\text{BER} = 10^{-3}$. Similar gains are achieved for the two receive antennas cases. For example, for the 2-PSK simulation of the EQ profile with $N_T = 3$, $N_R = 2$, $\boldsymbol{\rho}_t = [0.5, 0.7, 0.5]$, and $\boldsymbol{\rho}_r = [0.7]$, a gain of almost 7 dB is achieved by the LE-ODD filters over the GDD filters at $\text{BER} = 10^{-3}$. It is also noted that the MLSE-ODD filters perform badly when LE is employed at the receiver and in many cases, their performance is worse than that of the GDD filters. For example, in Figure 7.6, the GDD filters are 5 dB better than the MLSE-ODD filters at $\text{BER} = 10^{-2}$ for 2-PSK transmission over the HT profile with $N_T = 2$, $N_R = 2$, $\boldsymbol{\rho}_t = [0.5]$, and $\boldsymbol{\rho}_r = [0.7]$.

We examine again the filter coefficients similar to the DFE-ODD case. For all the EQ profiles considered and some other profiles, the ODD filters for the transmit antennas are practically identical and with the energy concentrated in one tap. For instance, the LE-ODD filters optimized for $10\log_{10}(E_b/N_0) = 15$ dB for 2-PSK transmission over the EQ profile with $N_T = 2$, $N_R = 1$, and $\boldsymbol{\rho}_t = [0.5]$ are shown in Table 7.4. There are cases where the filter coefficients are different among the antennas. For example, the LE-ODD filters optimized for $10\log_{10}(E_b/N_0) = 15$ dB for 2-PSK and the HT profile with $N_T = 3$, $N_R = 1$, and $\boldsymbol{\rho}_t = [0.2, 0.5, 0.2]$ are shown in Table 7.5.

For Figures 7.7 and 7.8, the same system parameters as for Figures 7.5 and 7.6 were used but with the 8-PSK modulation scheme. It can again be observed that the LE-ODD filters perform better than the MLSE-ODD and GDD filters.

Table 7.4: LE-ODD filter coefficients: 2-PSK, EQ, $L = 7$, $N_T = 2$, $N_R = 1$, $\rho_t = [0.5]$.

ODD Filters	Tx	$g_i[0]$	$g_i[1]$	$g_i[2]$
LE	$i = 1$	0.06807+0.03627i	-0.21697-0.08106i	0.881049+0.40516i
	$i = 2$	0.06011+0.02640i	-0.22893-0.11567i	0.883002+0.38756i

Table 7.5: LE-ODD filter coefficients: 2-PSK, HT, $L = 7$, $N_T = 3$, $N_R = 1$, $\rho_t = [0.2, 0.5, 0.2]$.

ODD Filters	Tx	$g_i[0]$	$g_i[1]$	$g_i[2]$
LE	$i = 1$	0.17537-0.19031i	-0.41813+0.28345i	0.47755-0.67067i
	$i = 2$	-0.47094+0.63133i	-0.31984+0.43845i	0.23695-0.17017i
	$i = 3$	0.06916-0.24311i	-0.21881+0.28746i	0.58868-0.67753i

However, even though the LE-ODD filters achieve a considerable gain over the other two schemes, the performance is still unacceptable for the one receive antenna case. For example, the BER the LE-ODD filters achieve for the 8-PSK simulation of the HT profile with $N_T = 2$, $N_R = 1$, and $\rho_t = [0.7]$ at $10\log_{10}(E_b/N_0) = 25$ dB is 4×10^{-2} . This is because wireless channels usually contain zeros close to the unit circle of the z-transform of the equivalent CIR and therefore, LE does not perform very well in wireless channels. The performance is even worse if higher modulation schemes, such as 8-PSK, are employed. However, the performance of LE can be significantly improved by using multiple receive antennas [50]. For example, the BER achievable with LE-ODD for the 8-PSK and the HT profile with $N_T = 2$, $N_R = 2$, $\rho_t = [0.5]$, and $\rho_t = [0.7]$ at $10\log_{10}(E_b/N_0) = 25$ dB is 1×10^{-3} .

Similar to the 2-PSK case, the MLSE-ODD filters also perform badly for 8-PSK if LE is employed at the receiver. Moreover, it is also noted that the setups with no transmit diversity yield better results than those with multiple transmit antennas and MLSE-ODD filters employed in most cases.

7.3 Future Work

In the BER simulations, the assumption that the receiver has perfect channel state information (CSI) is made. In practice, a least sum of squared errors (LSSE) channel estimation algorithm can be used to estimate the CSI from a known training sequences [51]. However, the impact of the channel estimation errors on the BER performance is unknown. Therefore, channel estimation errors can be taken into account in the future work. Also, we assume MMSE-DFE and MMSE-LE at the receiver, it will be interesting to compare their performance with ZF-DFE and ZF-LE where the ISI is completely eliminated in these two schemes. Finally, it is brought to the author's attention that the Kiefer-Wolfowitz finite-difference stochastic approximation algorithm and the simultaneous perturbation stochastic approximation (SPSA) algorithm can be used for the optimization problem. Interested readers are referred to [52] for an introductory treatment of the two algorithms.

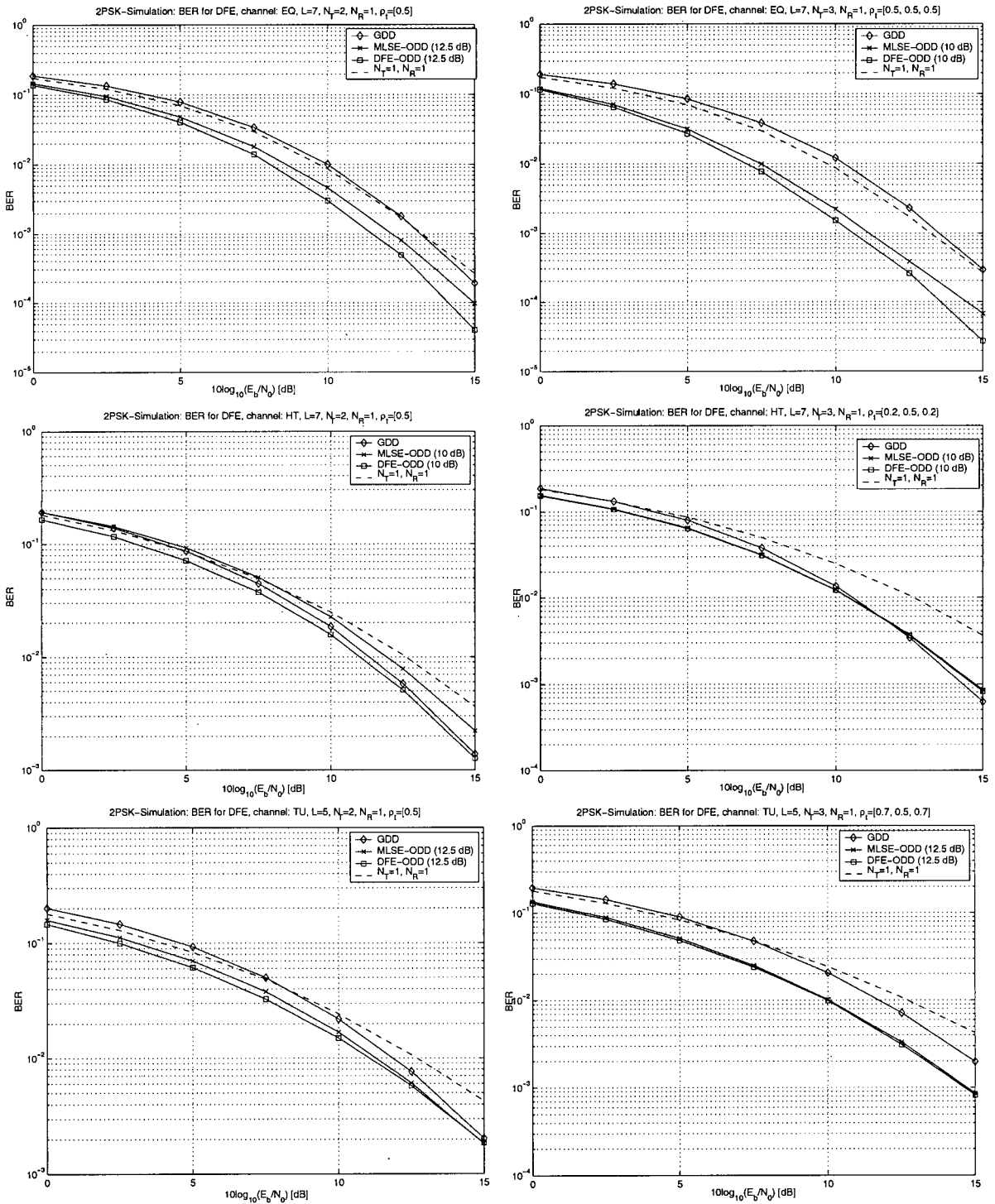


Figure 7.1: 2-PSK simulations for GDD, MLSE-ODD, and DFE-ODD filters.

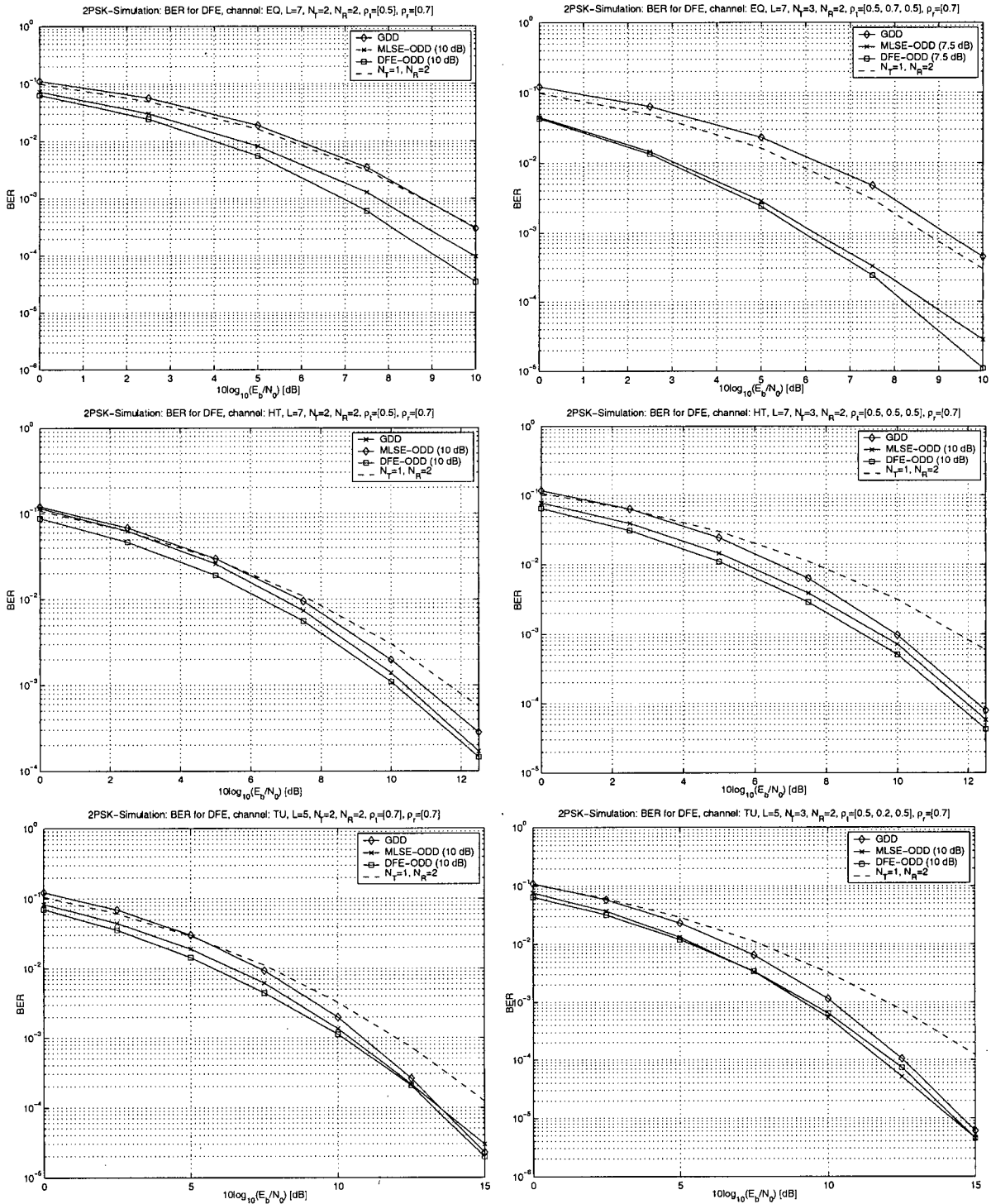


Figure 7.2: 2-PSK simulations for GDD, MLSE-ODD, and DFE-ODD filters.

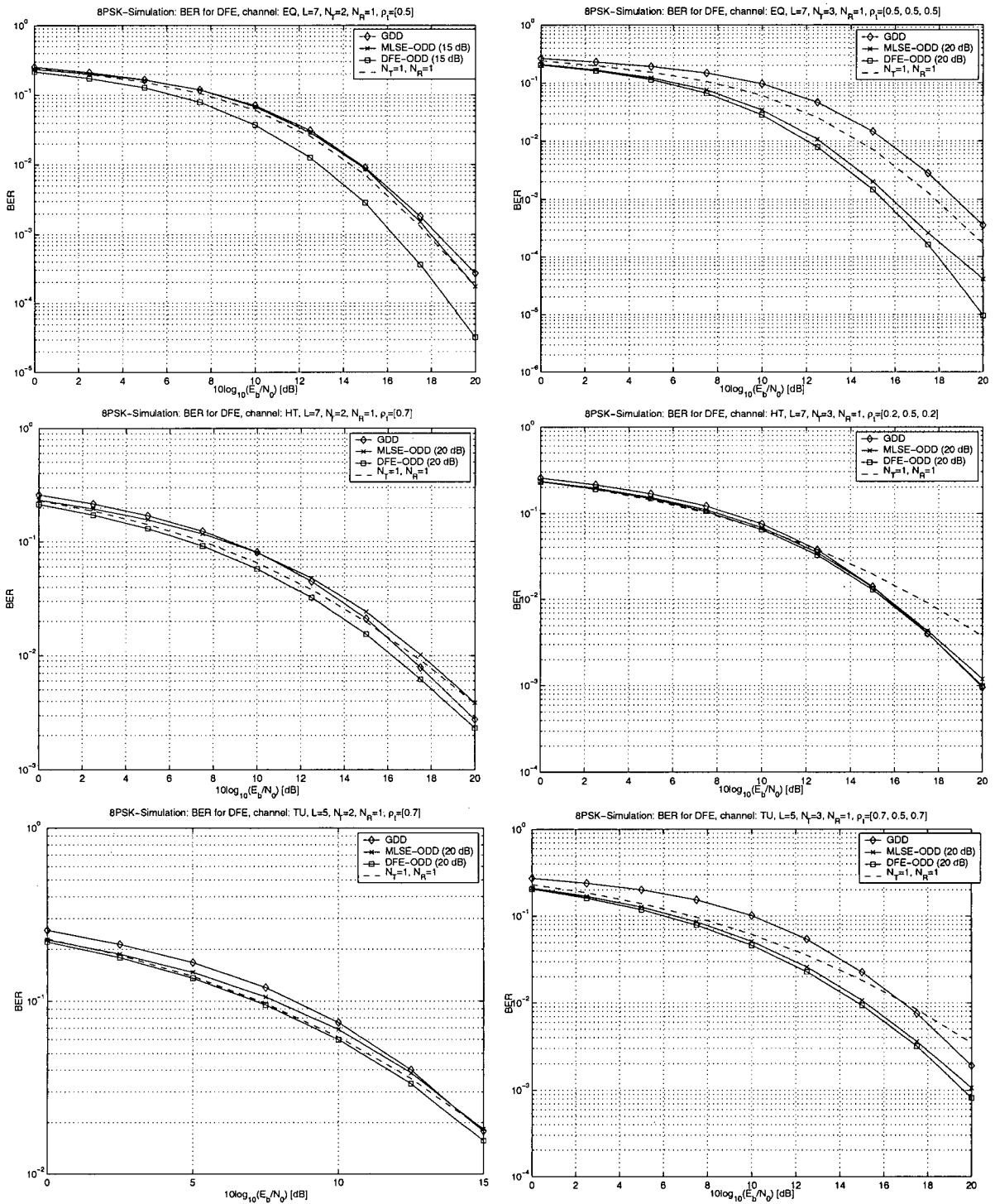


Figure 7.3: 8-PSK simulations for GDD, MLSE-ODD, and DFE-ODD filters.

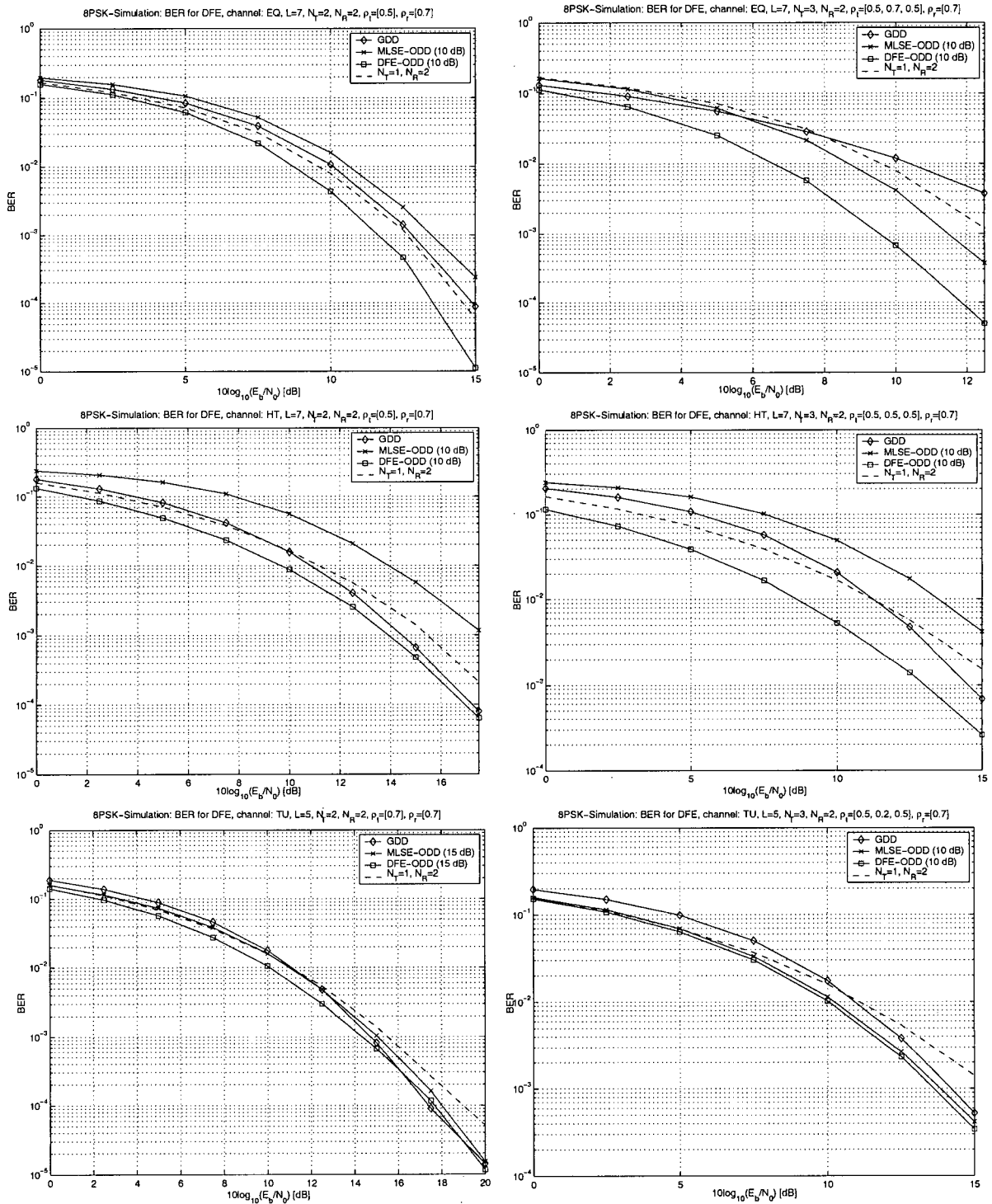


Figure 7.4: 8-PSK simulations for GDD, MLSE-ODD, and DFE-ODD filters.

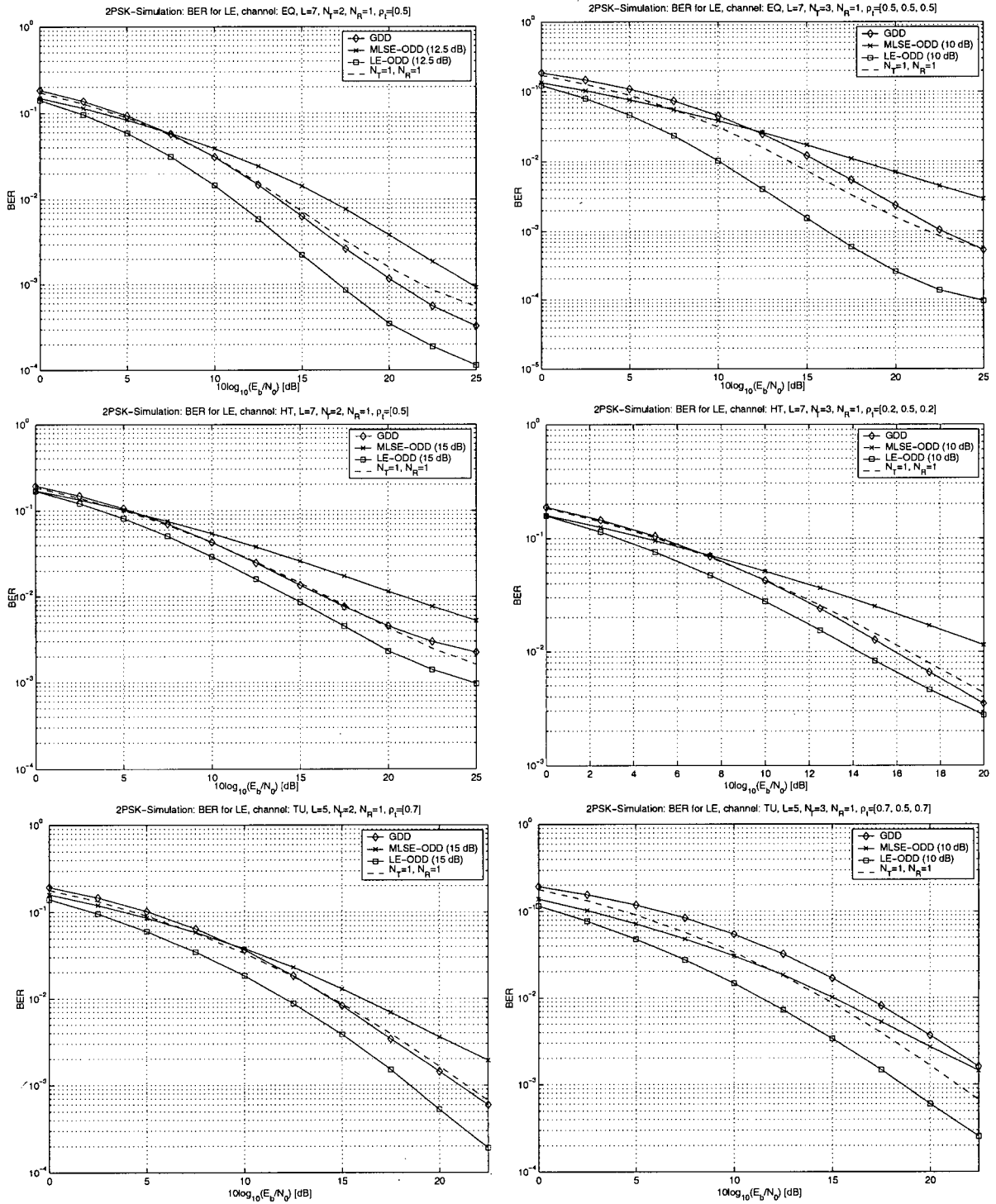


Figure 7.5: 2-PSK simulations for GDD, MLSE-ODD, and LE-ODD filters.

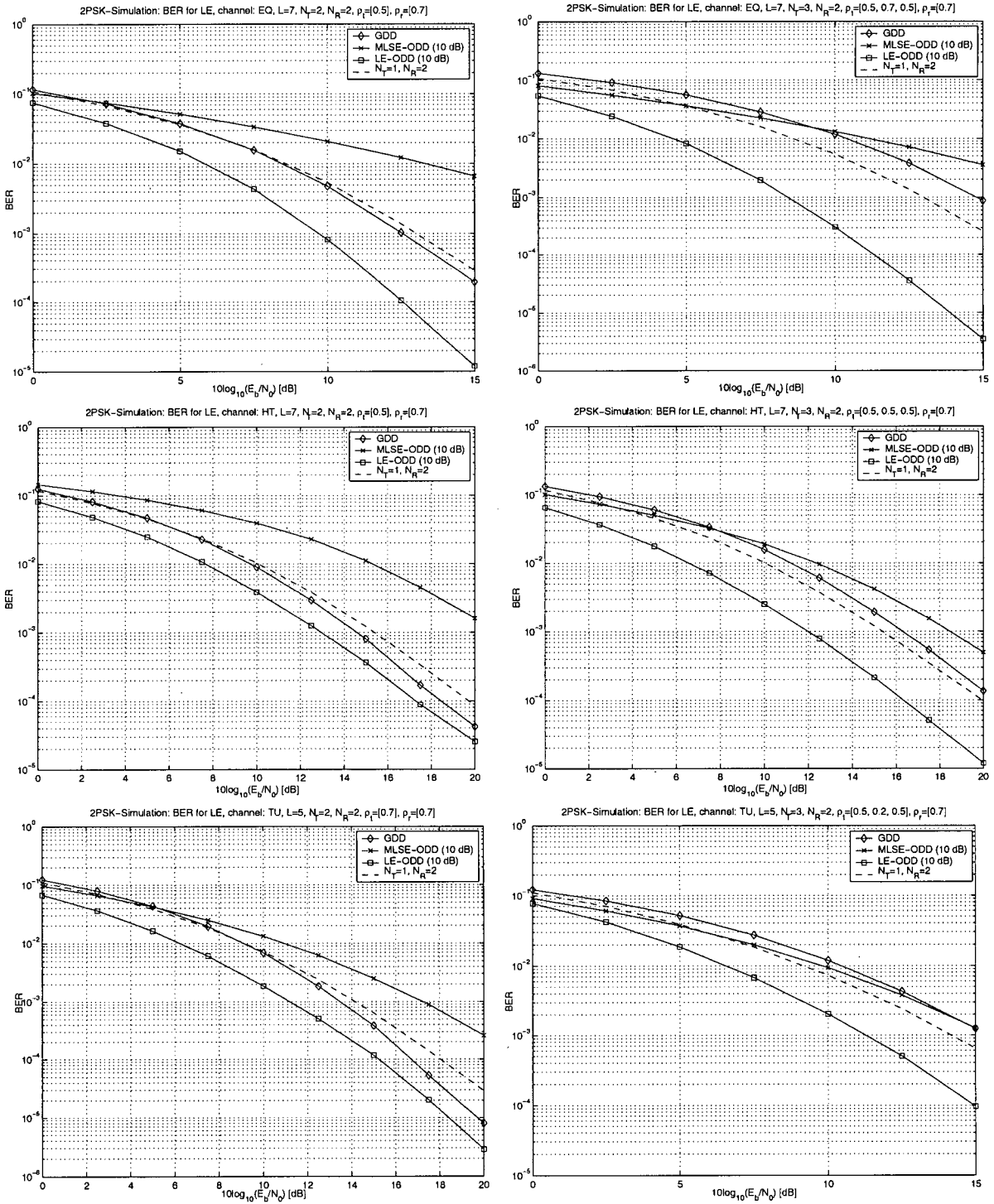


Figure 7.6: 2-PSK simulations for GDD, MLSE-ODD, and LE-ODD filters.

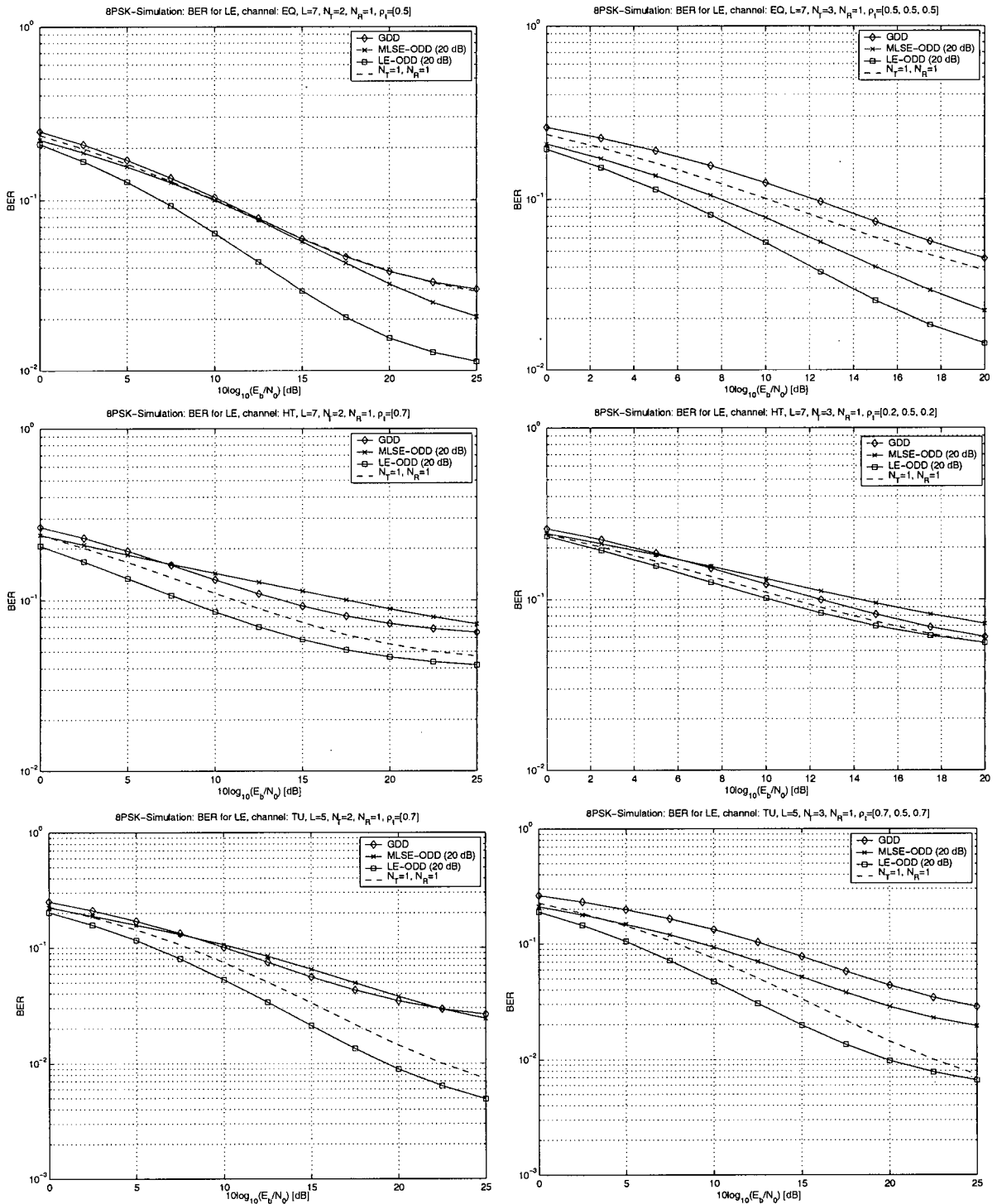


Figure 7.7: 8-PSK simulations for GDD, MLSE-ODD, and LE-ODD filters.

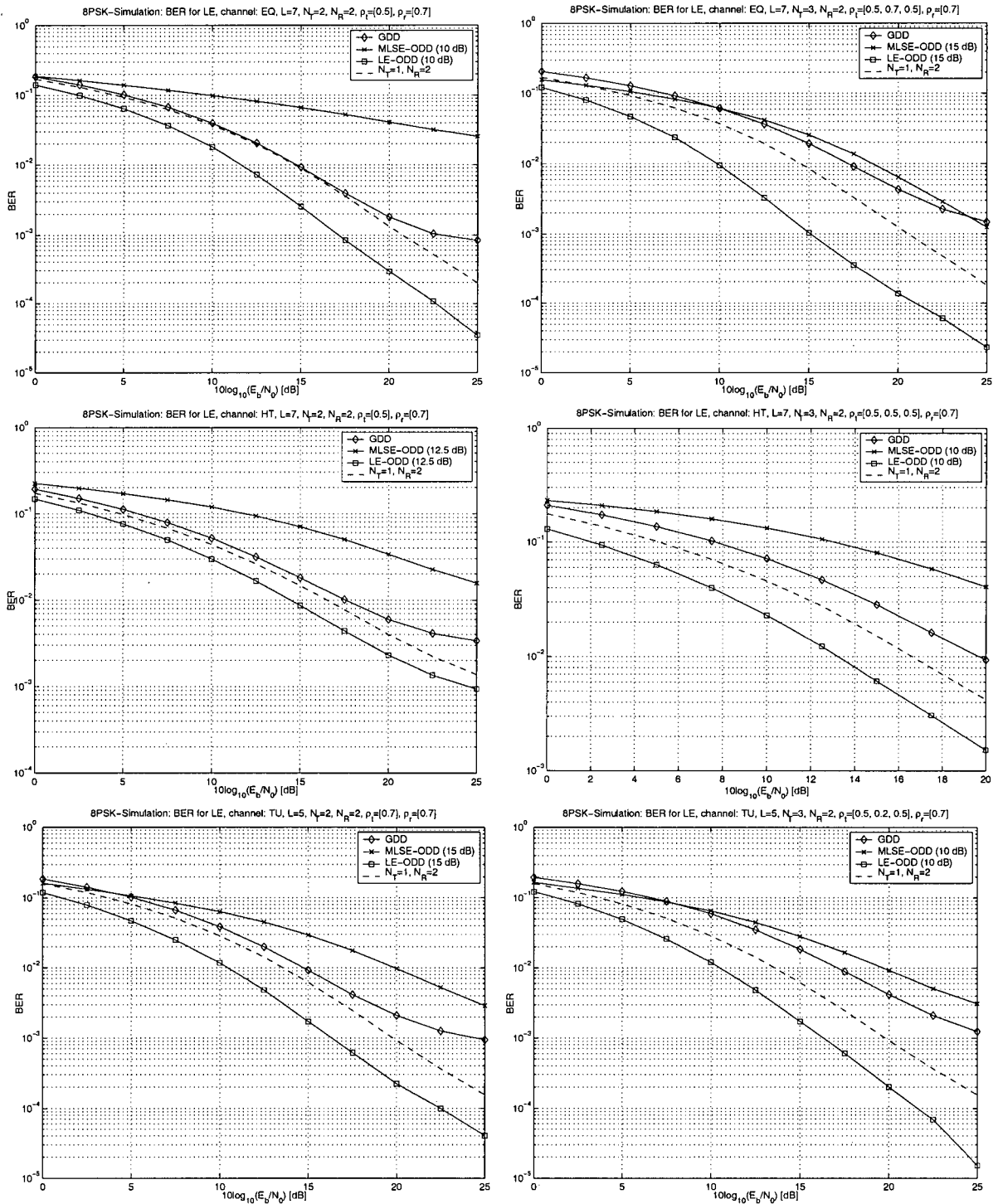


Figure 7.8: 8-PSK simulations for GDD, MLSE-ODD, and LE-ODD filters.

Chapter 8

Conclusions

In this work, DD filters have been optimized for Rayleigh fading frequency-selective correlated MIMO channels with LE and DFE at the receiver. A discrete-time correlated MIMO channel was developed for optimization purposes. The optimization takes into account the statistical properties of the overall CIR, which includes the influence of transmit pulse shaping and analog receive filtering. Based on the variance of DFE and LE, we have designed a stochastic gradient algorithm to calculate the DFE-ODD and LE-ODD filters, which minimizes the expected worst-case PEP of DFE and LE, respectively. All the integrals in this work are approximated by numerical methods as they cannot be computed in closed-form. It was shown that the proposed algorithm is not sensitive to the approximation error due to the numerical methods even with a relatively small \bar{N} . Furthermore, it was shown that although the resulting ODD filters may be different, the proposed stochastic gradient algorithm always converges regardless of the choice of the initial filters $\mathbf{g}[0]$ if the step size δ is chosen properly. We also investigate the effect of the DD filter length N on the performance. It was found that while in general, the performances of the DFE-ODD and LE-ODD filters improve as N increases, this is not necessarily true for suboptimum GDD and MLSE-ODD filters. Simulation results for the GSM/EDGE system have shown that the proposed DFE-ODD and LE-ODD filters outperform previously proposed GDD and MLSE-ODD filters if DFE

and LE are used at the receiver. Please refer to [11, 12] for a summary of this work.

Bibliography

- [1] T. Hehn. Optimized (space time) delay diversity codes for frequency selective fading channels. Master's thesis, Department of Electrical and Computer Engineering, University of Erlangen–Nürnberg, 2003.
- [2] R. Schober, T. Hehn, and W. H. Gerstacker. Optimized delay diversity for frequency-selective fading channels. Accepted for presentation at IEEE International Conference on Communications (ICC), Paris, France, June 2004.
- [3] G. D. Forney. Maximum-likelihood sequence estimation of digital sequences in the presence of intersymbol interference. *IEEE Transactions on Information Theory*, IT-18:363–378, May 1972.
- [4] D. Gore, S. Sandhu, and A. Paulraj. Delay diversity codes for frequency selective channels. In *Proceedings of the IEEE International Conference on Communications (ICC)*, pages 1949–1953, New York, May 2002.
- [5] C.A. Belfiore and J.H. Park. Decision-feedback equalization. *Proceedings of the IEEE*, 67:1143–1156, August 1979.
- [6] R. W. Lucky, J. Salz Jr., and E. J. Weldon. *Principles of Data Communication*. McGraw-Hill, New York, 1968.
- [7] Propagation conditions. GSM Recommendation 05.05, Vers. 5.3.0, Release, 1996.

- [8] 3GPP. Digital cellular communications system (phase 2+). Technical Specifications 3GPP TS 05.01-05, 2001.
- [9] A. Furuskar, S. Mazur, F. Muller, and H. Olofsson. Edge: Enhanced data rates for GSM and TDMA/136 evolution. *IEEE Personal Communications Magazine*, 6:56–66, June 1999.
- [10] R. van Nobelen, N. Seshadri, J. Whitehead, and S. Timiri. An adaptive radio link protocol with enhanced data rates for GSM evolution. *IEEE Personal Communications Magazine*, 6:54–63, February 1999.
- [11] S. Yiu, R. Schober, and W. Gerstacker. Optimization of delay diversity for decision-feedback equalization. Submitted for the 15th IEEE International Symposium on Personal, Indoor and Mobile Radio Communications (PIMRC), Barcelona, Spain, September 2004.
- [12] S. Yiu, R. Schober, and W. Gerstacker. Optimization of delay diversity for linear equalization. Submitted for the the IEEE Global Telecommunications Conference (GLOBECOM), Dallas, Texas, December 2004.
- [13] D. Gesbert, M. Shafi, Da-Shan Shiu, P. J. Smith, and A. Naguib. From theory to practice: An overview of MIMO space-time coded wireless systems. *IEEE Journal on Selected Areas in Communications*, 21(3):281–302, April 2003.
- [14] I. E. Telatar. Capacity of multi-antenna Gaussian channels. *European Transactions on Telecommunications*, 10(6):585–595, November-December 1999.
- [15] G. J. Foschini and M. J. Gans. On limits of wireless communications in a fading environment when using multiple antennas. *Wireless Personal Communications*, 6:311–335, 1998.
- [16] V. Tarokh, N. Seshadri, and A. R. Calderbank. Space-time codes for high data rate wireless communication: Performance criterion and code

- construction. *IEEE Transactions on Information Theory*, 44:744–765, March 1998.
- [17] S. M. Alamouti. A simple transmit diversity technique for wireless communications. *Journal of Selective Areas of Communications*, 16, October 1998.
- [18] V. Tarokh, H. Jafarkhani, and A. R. Calderbank. Space-time block codes from orthogonal designs. *IEEE Transactions on Information Theory*, 45:1456–1467, July 1999.
- [19] Y. Gong and K. B. Letaief. Performance evaluation and analysis of space-time coding in unequalized multipath fading links. *IEEE Transactions on Communications*, 48(11):1778–1782, November 2000.
- [20] E. Lindskog and A. Paulraj. A transmit diversity scheme for channels with intersymbol interference. In *Proceedings of the IEEE International Conference on Communications (ICC)*, pages 307–311, New Orleans, Louisiana, June 2002.
- [21] Y. Li, J. C. Chung, and N. R. Sollenberger. Transmit diversity for OFDM systems and its impact on high-rate data wireless networks. *IEEE Journal on Selected Areas in Communications*, SAC-17:1233–1243, July 1999.
- [22] H. Bolcskei and A. J. Paulraj. Space-frequency coded for broadband OFDM systems. In *IEEE Wireless Communications and Networking Conference (WCNC)*, pages 1–6, Chicago (IL), September 2000.
- [23] N. Al-Dhahir. Single-carrier frequency-domain equalization for space-time block-coded transmission over frequency-selective fading channels. *IEEE Communications Letters*, 5:304–306, July 2001.
- [24] S. Zhou and G. B. Giannakis. Single-carrier space-time block-coded transmission over frequency-selective fading channels. *IEEE Transactions on Information Theory*, IT-49:164–179, January 2003.

- [25] A. Wittneben. A new bandwidth efficient transmit antenna modulation diversity scheme for linear digital modulation. In *Proceedings of the IEEE International Conference on Communications (ICC)*, pages 1630–1634, Geneva, May 1993.
- [26] W. Van Etten. Maximum-likelihood receiver for multiple channel transmission systems. *IEEE Transactions on Communications*, pages 276–283, February 1976.
- [27] J. G. Proakis. *Digital Communications*. McGraw-Hill, New York, 4th edition, 2001.
- [28] E. J. Borowski and J. M. Borwein. *The Harper Collins Dictionary of Mathematics*. McGraw-Hill, New York, 1968.
- [29] T. S. Rappaport. *Wireless Communications*. Prentice-Hall, Englewood Cliffs, NJ, 1996.
- [30] H. Bolcskei and A. J. Paulraj. Performance of space-time codes in the presence of spatial fading correlation. In *Conf. Rec. of the 34th Asilomar Conference on Signals, Systems and Computers*, volume 1, pages 686–693, 2000.
- [31] D. Chizhik, J. Ling, P. Wolniansky, R. Valenzuela, N. Costa, and K. Huber. Multiple input multiple output measurements and modeling in Manhattan. In *Proceedings IEEE Vehicular Technology Conference (VTC)*, pages 107–110, Vancouver, BC, October 2002.
- [32] David S. Watkins. *Fundamentals of Matrix Computations*. John Wiley & Sons, Inc., New York, 2nd edition, 2002.
- [33] W. H. Gerstacker and R. Schober. Equalization concepts for EDGE. *IEEE Transactions on Wireless Communications*, 1(1):190–199, January 2002.
- [34] Tdoc SMG2 WPB 325/98. ETSI, November 1998.

- [35] P. Jung. Laurent's representation of binary digital continuous phase modulated signals with modulation index $1/2$ revisited. *IEEE Transactions on Communications*, 42:221–224, February-April 1994.
- [36] C. Luschi, M. Sandell, P. Strauch, and R.-H Yan. Adaptive channel memory truncation for TDMA digital mobile radio. In *Proceedings IEEE International Workshop Intelligent Signal Processing and Communication Systems*, pages 665–669, Melbourne, Australia, November 1998.
- [37] N. Seshadri and J. H. Winters. Two signaling schemes for improving the error performance of frequency-division-duplex (FDD) transmission system using transmitter antenna diversity. In *Proceedings 43rd IEEE Vehicular Technology Conference (VTC)*, pages 508–511, Secaucus, NJ, USA, May 1993.
- [38] P. E. Mogensen. GSM base-station antenna diversity using soft decision combining on up-link and delayed-signal transmission on down-link. In *Proceedings 43rd IEEE Vehicular Technology Conference (VTC)*, pages 611–616, Secaucus, NJ, USA, May 1993.
- [39] P. E. Ostling. Performance of MMSE linear equalizer and decision feedback equalizer in single-frequency simulcast environment. In *Proceedings 43rd IEEE Vehicular Technology Conference (VTC)*, pages 629–632, Secaucus, NJ, USA, May 1993.
- [40] J. H. Winters. The diversity gain of transmit diversity in wireless systems with rayleigh fading. *IEEE Transactions on Vehicular Technology*, 47(1):119–123, February 1998.
- [41] S. Haykin. *Adaptive Filter Theory*. Prentice-Hall, Upper Saddle River, New Jersey, 3rd edition, 1996.
- [42] A. Duel-Hallen and C. Heegard. Delayed decision-feedback sequence estimation. *IEEE Transactions on Communications*, 37:428–436, May 1989.

- [43] G. D. Forney. The Viterbi algorithm. *IEEE Proceedings*, 61:268–278, 1973.
- [44] Shahid U. H. Qureshi. Adaptive equalization. *Proceedings of the IEEE*, 73(9):1349–1387, September 1985.
- [45] N. Al-Dhahir and Ali H. Sayed. The finite-length multi-input multi-output MMSE-DFE. *IEEE Transactions on Signal Processing*, 48(10):2921–2936, October 2000.
- [46] R. Schober and W. H. Gerstacker. On the distribution of zeros of mobile channels with applications on GSM/EDGE. *IEEE Journal on Selected Areas in Communications*, 19(7):1289–1299, July 2001.
- [47] K. E. Baddour and P. J. McLane. Analysis of optimum diversity combining and decision feedback equalization in dispersive rayleigh fading. In *IEEE International Conference on Communications (ICC), Communications Theory Mini-Conference*, pages 21–26, Vancouver, B.C., June 6-10 1999.
- [48] Alan V. Oppenheim and Ronald W. Schaffer with John R. Buck. *Discrete-Time Signal Processing*. Prentice-Hall, Upper Saddle River, New Jersey, 2nd edition, 1999.
- [49] Robert A. Adams. *Single-Variable Calculus*. Addison-Wesley, 3rd edition, 1995.
- [50] M. V. Clark, L. J. Greenstein, W. K. Kennedy, and M. Shafi. Optimum linear diversity receivers for mobile communications. *IEEE Transactions on Vehicular Technology*, 43:47–56, February 1994.
- [51] S. N. Crozier, D. D. Falconer, and S. A. Mahmoud. Least sum of squared errors (LSSE) channel estimation. *IEE Proceedings-F*, 138:371–378, issue: 4, August 1991.

- [52] James C. Spall. Stochastic optimization and the simulations perturbation method. In *Proceedings of the 1999 Winter Simulation Conference (WSC)*, pages 101–109, 1999.

Appendix A

Optimized Filters

Various LE-ODD and DFE-ODD filters are given in this appendix. The filters are optimized for the three common Rayleigh fading setups: Hilly Terrain (HT), Typical Urban (TU) and the Equalizer Test channel (EQ) [7]. The filters are optimized for different E_b/N_0 values for the 2-PSK modulation scheme used in GSM and the 8-PSK modulation scheme used in EDGE. Antenna correlations are assumed at both the transmit and receive antennas.

A.1 Filters for 2-PSK

A.1.1 DFE, EQ, $L = 7$, $N_T = 2$, $N_R = 1$, $\rho_t = [0.5]$

$10 \log_{10}(E_b/N_0)$	Tx	$g_i[0]$	$g_i[1]$	$g_i[2]$
7.5	$i = 1$	-0.17227+0.03835i	0.44370-0.09334i	0.85510-0.17909i
	$i = 2$	-0.18714+0.03547i	0.43638-0.09639i	0.85406-0.18596i
10	$i = 1$	-0.21956+0.04205i	0.82452-0.14587i	0.49187-0.08346i
	$i = 2$	-0.23189+0.03666i	0.81385-0.15536i	0.49833-0.10027i
12.5	$i = 1$	-0.11420+0.17268i	0.56998-0.69853i	0.24788-0.28789i
	$i = 2$	-0.14172+0.14803i	0.52646-0.71232i	0.23800-0.34177i

A.1.2 LE, EQ, $L = 7$, $N_T = 2$, $N_R = 1$, $\rho_t = [0.5]$

$10 \log_{10}(E_b/N_0)$	Tx	$g_i[0]$	$g_i[1]$	$g_i[2]$
10	$i = 1$	0.13958+0.12510i	0.17690-0.94905i	0.13626+0.11960i
	$i = 2$	0.13181+0.12072i	0.16817-0.95304i	0.13471+0.11552i
12.5	$i = 1$	0.08382+0.11826i	0.32925-0.92205i	0.08516+0.11469i
	$i = 2$	0.08208+0.12016i	0.32388-0.92428i	0.08304+0.11286i
15	$i = 1$	0.06807+0.03627i	-0.21697-0.08106i	0.881049+0.40516i
	$i = 2$	0.06011+0.02640i	-0.22893-0.11567i	0.883002+0.38756i

A.1.3 DFE, HT, $L = 7$, $N_T = 2$, $N_R = 1$, $\rho_t = [0.5]$

$10 \log_{10}(E_b/N_0)$	Tx	$g_i[0]$	$g_i[1]$	$g_i[2]$
7.5	$i = 1$	-0.23616-0.02688i	-0.29269+0.59417i	-0.17127+0.68954i
	$i = 2$	0.29971-0.20668i	-0.03195+0.50253i	-0.27415+0.73399i
10	$i = 1$	0.05315-0.40275i	0.24078-0.20371i	0.84750+0.13127i
	$i = 2$	-0.61674+0.21735i	-0.17647+0.21828i	0.60406+0.35876i
12.5	$i = 1$	0.04554-0.80935i	-0.15888-0.42513i	-0.35625-0.09993i
	$i = 2$	0.13123-0.71911i	0.20828-0.04093i	0.27554+0.58709i

A.1.4 LE, HT, $L = 7$, $N_T = 2$, $N_R = 1$, $\rho_t = [0.5]$

$10 \log_{10}(E_b/N_0)$	Tx	$g_i[0]$	$g_i[1]$	$g_i[2]$
10	$i = 1$	-0.05905+0.026747i	-0.76465+0.62301i	0.13389-0.07104i
	$i = 2$	-0.03780+0.06107i	-0.76883+0.60626i	0.13764-0.13135i
12.5	$i = 1$	0.04949-0.19029i	-0.60830-0.66190i	0.38983+0.03528i
	$i = 2$	-0.20620+0.04030i	-0.68391-0.58904i	0.04236+0.37331i
15	$i = 1$	-0.31806+0.41997i	-0.00510-0.79143i	-0.13277-0.28009i
	$i = 2$	0.25904+0.62643i	0.30438-0.59883i	0.28877+0.07646i

A.1.5 DFE, TU, $L = 5$, $N_T = 2$, $N_R = 1$, $\rho_t = [0.7]$

$10 \log_{10}(E_b/N_0)$	Tx	$g_i[0]$	$g_i[1]$	$g_i[2]$
7.5	$i = 1$	0.76994+0.12108i	0.59542+0.09465i	-0.16521-0.04191i
	$i = 2$	0.76110+0.12696i	0.61000+0.10757i	-0.14418-0.01223i
10	$i = 1$	0.71985-0.41982i	0.48179-0.24766i	-0.04784+0.09910i
	$i = 2$	0.71075-0.36802i	0.45808-0.25187i	-0.28076+0.08544i
12.5	$i = 1$	0.42193-0.16657i	-0.12618-0.28206i	-0.62005-0.56061i
	$i = 2$	-0.00949+0.49943i	-0.29810-0.00489i	-0.67871-0.44826i

A.1.6 LE, TU, $L = 5$, $N_T = 2$, $N_R = 1$, $\rho_t = [0.7]$

$10 \log_{10}(E_b/N_0)$	Tx	$g_i[0]$	$g_i[1]$	$g_i[2]$
10	$i = 1$	-0.07229-0.05087i	-0.74224-0.63929i	0.13795+0.11637i
	$i = 2$	-0.06676-0.07136i	-0.74057-0.64293i	0.12771+0.11112i
12.5	$i = 1$	-0.03636-0.02420i	0.37261+0.91917i	-0.09051-0.07866i
	$i = 2$	-0.05605+0.02594i	0.35846+0.92642i	-0.06135-0.07540i
15	$i = 1$	0.17111+0.24026i	-0.12231-0.04661i	0.75062+0.57657i
	$i = 2$	-0.12510-0.20391i	-0.15448-0.14633i	0.76405+0.56010i

A.1.7 DFE, EQ, $L = 7, N_T = 2, N_R = 2, \rho_t = [0.5], \rho_r = [0.7]$

$10 \log_{10}(E_b/N_0)$	Tx	$g_i[0]$	$g_i[1]$	$g_i[2]$
5	$i = 1$	-0.18350-0.04081i	0.43106+0.07100i	0.86755+0.14550i
	$i = 2$	-0.18441-0.03003i	0.41947+0.07719i	0.87060+0.15886i
7.5	$i = 1$	-0.12613-0.00603i	0.26142+0.00620i	0.95647+0.02910i
	$i = 2$	-0.12224-0.00216i	0.26487+0.01053i	0.95584+0.03388i
10	$i = 1$	-0.09381-0.00623i	0.17003+0.00522i	0.97966+0.04984i
	$i = 2$	-0.08377-0.00061i	0.19674+0.01227i	0.97534+0.05329i

A.1.8 LE, EQ, $L = 7, N_T = 2, N_R = 2, \rho_t = [0.5], \rho_r = [0.7]$

$10 \log_{10}(E_b/N_0)$	Tx	$g_i[0]$	$g_i[1]$	$g_i[2]$
7.5	$i = 1$	0.23496+0.03957i	-0.63086+0.69887i	0.23554+0.03671i
	$i = 2$	0.22771+0.04220i	-0.62872+0.70367i	0.23196+0.04608i
10	$i = 1$	0.08454+0.00583i	-0.27241-0.02271i	0.95523+0.07501i
	$i = 2$	0.08571+0.00750i	-0.27012-0.01695i	0.95616+0.07142i
12.5	$i = 1$	0.10868+0.00018i	-0.30941-0.01468i	0.94385+0.03725i
	$i = 2$	0.10785+0.00832i	-0.30764-0.00180i	0.94511+0.02050i

A.1.9 DFE, HT, $L = 7$, $N_T = 2$, $N_R = 2$, $\rho_t = [0.5]$, $\rho_r = [0.7]$

$10 \log_{10}(E_b/N_0)$	Tx	$g_i[0]$	$g_i[1]$	$g_i[2]$
7.5	$i = 1$	0.73151+0.28678i	0.30871+0.06391i	-0.43947-0.30023i
	$i = 2$	0.71030+0.29291i	0.55522+0.28103i	0.04665+0.14233i
10	$i = 1$	-0.41407+0.46663i	0.04899+0.06622i	0.66014-0.41016i
	$i = 2$	0.07640-0.22484i	0.34835-0.30388i	0.71759-0.46367i
12.5	$i = 1$	0.73812-0.09951i	-0.17331-0.07247i	-0.63046-0.11180i
	$i = 2$	0.90202-0.06247i	0.33367+0.04851i	0.23366+0.11906i

A.1.10 LE, HT, $L = 7$, $N_T = 2$, $N_R = 2$, $\rho_t = [0.5]$, $\rho_r = [0.7]$

$10 \log_{10}(E_b/N_0)$	Tx	$g_i[0]$	$g_i[1]$	$g_i[2]$
7.5	$i = 1$	0.13690-0.05755i	-0.17800+0.96191i	0.12069-0.08019i
	$i = 2$	0.10397-0.06593i	-0.19638+0.96415i	0.12090-0.04555i
10	$i = 1$	0.16582+0.14273i	0.03294-0.93139i	0.20881+0.19990i
	$i = 2$	0.15478+0.05308i	0.07847-0.97557i	0.10873+0.05932i
12.5	$i = 1$	-0.21810+0.05372i	-0.63839-0.63517i	-0.09900+0.35883i
	$i = 2$	0.15072-0.05811i	-0.36357-0.70939i	0.50002+0.29745i

A.1.11 DFE, TU, $L = 5$, $N_T = 2$, $N_R = 2$, $\rho_t = [0.7]$,

$$\rho_r = [0.7]$$

$10 \log_{10}(E_b/N_0)$	Tx	$g_i[0]$	$g_i[1]$	$g_i[2]$
7.5	$i = 1$	-0.21454+0.04096i	0.55464-0.12424i	0.77307-0.17772i
	$i = 2$	-0.20364+0.05122i	0.56560-0.12428i	0.76986-0.16696i
10	$i = 1$	0.27431-0.77981i	0.12590-0.30033i	-0.05967+0.45501i
	$i = 2$	0.28051-0.87383i	0.10035-0.37223i	-0.05004-0.08124i
12.5	$i = 1$	-0.29542+0.33421i	-0.21820-0.06972i	-0.31669-0.80515i
	$i = 2$	0.43391+0.05076i	0.12376-0.23683i	-0.18298-0.83920i

A.1.12 LE, TU, $L = 5$, $N_T = 2$, $N_R = 2$, $\rho_t = [0.7]$, $\rho_r =$

$$[0.7]$$

$10 \log_{10}(E_b/N_0)$	Tx	$g_i[0]$	$g_i[1]$	$g_i[2]$
7.5	$i = 1$	0.96408-0.22426i	-0.13927+0.02874i	0.00476+0.00402i
	$i = 2$	0.96514-0.19055i	-0.17396+0.03315i	0.02610-0.01255i
10	$i = 1$	0.17634-0.08452i	-0.11122+0.95596i	0.17458-0.07111i
	$i = 2$	0.16957-0.07461i	-0.11628+0.95689i	0.16961-0.08806i
12.5	$i = 1$	0.94250+0.14928i	-0.26990-0.02592i	-0.11373+0.05440i
	$i = 2$	0.94614+0.15800i	-0.17607-0.03374i	0.21601-0.03249i

A.1.13 DFE, EQ, $L = 7, N_T = 3, N_R = 1, \rho_t = [0.5, 0.5, 0.5]$

$10 \log_{10}(E_b/N_0)$	Tx	$g_i[0]$	$g_i[1]$	$g_i[2]$
7.5	$i = 1$	-0.23974+0.00142i	0.78495-0.00801i	0.57121+0.00526i
	$i = 2$	-0.23186-0.00050i	0.78371-0.00135i	0.57607-0.01365i
	$i = 3$	-0.24163+0.00392i	0.77692-0.01066i	0.58125-0.00486i
10	$i = 1$	-0.21781-0.03046i	0.85938+0.12754i	0.43695+0.07683i
	$i = 2$	-0.21300-0.03218i	0.85819+0.13335i	0.44363+0.05014i
	$i = 3$	-0.22881-0.03858i	0.85207+0.12592i	0.44590+0.07384i
12.5	$i = 1$	-0.18390-0.08864i	0.75949+0.49572i	0.27235+0.24816i
	$i = 2$	-0.14673-0.08439i	0.76758+0.50154i	0.33671+0.13137i
	$i = 3$	-0.18510-0.15730i	0.78577+0.44837i	0.30212+0.17679i

A.1.14 LE, EQ, $L = 7, N_T = 3, N_R = 1, \rho_t = [0.5, 0.5, 0.5]$

$10 \log_{10}(E_b/N_0)$	Tx	$g_i[0]$	$g_i[1]$	$g_i[2]$
7.5	$i = 1$	0.11021-0.07524i	0.04591+0.98228i	0.07679-0.09652i
	$i = 2$	0.08844-0.07898i	0.04052+0.98239i	0.11871-0.07156i
	$i = 3$	0.12773-0.10245i	0.05729+0.97406i	0.11009-0.09481i
10	$i = 1$	0.16379-0.12804i	0.17315+0.94270i	0.13275-0.14312i
	$i = 2$	0.14484-0.13580i	0.17416+0.93710i	0.18458-0.13426i
	$i = 3$	0.17107-0.15537i	0.19397+0.92990i	0.15555-0.14161i
12.5	$i = 1$	0.11021-0.07524i	0.04591+0.98228i	0.07679-0.09652i
	$i = 2$	0.08844-0.07898i	0.04052+0.98239i	0.11871-0.07156i
	$i = 3$	0.12773-0.10245i	0.05729+0.97406i	0.11009-0.09481i

A.1.15 DFE, HT, $L = 7$, $N_T = 3$, $N_R = 1$, $\rho_t = [0.2, 0.5, 0.2]$

$10 \log_{10}(E_b/N_0)$	Tx	$g_i[0]$	$g_i[1]$	$g_i[2]$
7.5	$i = 1$	0.77743-0.31386i	0.35059-0.16708i	-0.36774+0.10503i
	$i = 2$	0.27931-0.14547i	0.65393-0.16086i	0.66319-0.08663i
	$i = 3$	0.77888-0.30980i	0.31808-0.16603i	-0.39691+0.10532i
10	$i = 1$	0.48941-0.18505i	-0.17272+0.01104i	-0.81429+0.18224i
	$i = 2$	-0.52011+0.32493i	-0.54858+0.26297i	-0.48095+0.15000i
	$i = 3$	0.52886-0.19294i	-0.17474+0.00514i	-0.78329+0.19740i
12.5	$i = 1$	0.37376+0.01367i	0.060962-0.01622i	-0.73651-0.56008i
	$i = 2$	-0.33054+0.59334i	-0.44017+0.28713i	-0.50895+0.05889i
	$i = 3$	0.642386+0.13415i	-0.20026-0.33440i	-0.55359-0.33309i

A.1.16 LE, HT, $L = 7$, $N_T = 3$, $N_R = 1$, $\rho_t = [0.2, 0.5, 0.2]$

$10 \log_{10}(E_b/N_0)$	Tx	$g_i[0]$	$g_i[1]$	$g_i[2]$
10	$i = 1$	-0.26091-0.68386i	0.04811+0.62810i	-0.09214+0.24279i
	$i = 2$	0.13860-0.75424i	0.39578+0.02826i	0.40134-0.30561i
	$i = 3$	-0.29347-0.66315i	0.03370+0.64160i	-0.08595+0.23223i
12.5	$i = 1$	-0.18965+0.80146i	0.19846-0.50888i	0.14242+0.05527i
	$i = 2$	-0.27347+0.10642i	-0.04924-0.59433i	-0.32562-0.67247i
	$i = 3$	-0.13472+0.80492i	0.21602-0.51304i	0.12141+0.09662i
15	$i = 1$	0.17537-0.19031i	-0.41813+0.28345i	0.47755-0.67067i
	$i = 2$	-0.47094+0.63133i	-0.31984+0.43845i	0.23695-0.17017i
	$i = 3$	0.06916-0.24311i	-0.21881+0.28746i	0.58868-0.67753i

A.1.17 DFE, TU, $L = 5$, $N_T = 3$, $N_R = 1$, $\rho_t = [0.7, 0.5, 0.7]$

$10 \log_{10}(E_b/N_0)$	Tx	$g_i[0]$	$g_i[1]$	$g_i[2]$
7.5	$i = 1$	-0.07380+0.37627i	0.50537+0.11104i	0.76324-0.05198i
	$i = 2$	-0.22630+0.03233i	0.49522-0.02762i	0.83399-0.07866i
	$i = 3$	-0.32411-0.34911i	0.40691-0.19547i	0.75164-0.06577i
10	$i = 1$	-0.16557-0.68118i	0.19601-0.07134i	0.55384+0.39791i
	$i = 2$	-0.25526-0.22631i	0.21731+0.18726i	0.68304+0.57861i
	$i = 3$	-0.20991+0.34070i	0.19010+0.40397i	0.54726+0.58399i
12.5	$i = 1$	-0.16447-0.76864i	0.07085-0.16586i	0.45629+0.37604i
	$i = 2$	-0.26690-0.30450i	0.06959+0.08760i	0.61048+0.67145i
	$i = 3$	-0.16556+0.31825i	0.10983+0.34126i	0.46982+0.72253i

A.1.18 LE, TU, $L = 5$, $N_T = 3$, $N_R = 1$, $\rho_t = [0.7, 0.5, 0.7]$

$10 \log_{10}(E_b/N_0)$	Tx	$g_i[0]$	$g_i[1]$	$g_i[2]$
10	$i = 1$	0.16271-0.01436i	-0.98007+0.10960i	-0.02450+0.01304i
	$i = 2$	0.15016-0.02612i	-0.98203+0.10551i	-0.02845+0.02103i
	$i = 3$	0.08946+0.00122i	-0.99191+0.07279i	-0.05013-0.01725i
12.5	$i = 1$	-0.11555+0.08092i	0.55515-0.79174i	-0.18728+0.09988i
	$i = 2$	-0.07097-0.00537i	0.55436-0.81833i	-0.12631+0.04464i
	$i = 3$	-0.06099-0.13352i	0.56938-0.80593i	-0.06433-0.02436i
15	$i = 1$	0.52660+0.08515i	0.05008-0.19959i	0.19722+0.79637i
	$i = 2$	0.05422+0.04557i	-0.07646-0.26915i	0.26961+0.91870i
	$i = 3$	-0.50239-0.00589i	-0.16116-0.23306i	0.17854+0.79712i

A.1.19 DFE, EQ, $L = 7, N_T = 3, N_R = 2, \rho_t = [0.5, 0.7, 0.5]$,

$$\rho_r = [0.7]$$

$10 \log_{10}(E_b/N_0)$	Tx	$g_i[0]$	$g_i[1]$	$g_i[2]$
2.5	$i = 1$	-0.19801+0.00868i	0.60710-0.03063i	0.76876-0.01460i
	$i = 2$	-0.25260-0.00535i	0.58305+0.00760i	0.77195-0.01583i
	$i = 3$	-0.22208+0.00705i	0.60295-0.02143i	0.76585-0.01029i
5	$i = 1$	-0.19474-0.00497i	0.84338+ 0.00917i	0.50066+0.00361i
	$i = 2$	-0.22473-0.00401i	0.84835+0.00953i	0.47922+0.00644i
	$i = 3$	-0.21241-0.00503i	0.84719+0.00381i	0.48692+0.00429i
7.5	$i = 1$	0.04988-0.00864i	0.32847+0.02012i	0.94294+0.00215i
	$i = 2$	-0.20375-0.01680i	0.46259+0.01033i	0.86246+0.01636i
	$i = 3$	-0.12224-0.01483i	0.35576+0.00714i	0.92634+0.01057i

A.1.20 LE, EQ, $L = 7, N_T = 3, N_R = 2, \rho_t = [0.5, 0.7, 0.5]$,

$$\rho_r = [0.7]$$

$10 \log_{10}(E_b/N_0)$	Tx	$g_i[0]$	$g_i[1]$	$g_i[2]$
2.5	$i = 1$	0.03731+0.01196i	-0.13236+0.00929i	0.98680-0.08416i
	$i = 2$	-0.01066-0.01267i	-0.17974+0.00316i	0.98184-0.05841i
	$i = 3$	0.00862-0.00640i	-0.13947+0.01163i	0.98709-0.07709i
5	$i = 1$	0.19943+0.00017i	-0.30472-0.00403i	0.93115+0.01754i
	$i = 2$	-0.08390+0.00305i	0.00723-0.00127i	0.99631+0.01608i
	$i = 3$	0.01911+0.00072i	-0.22720-0.00334i	0.97356+0.01340i
7.5	$i = 1$	0.08284+0.00308i	-0.25056-0.00250i	0.96452+0.00657i
	$i = 2$	0.07586-0.00230i	-0.26996+0.00777i	0.95974+0.01420i
	$i = 3$	0.07581+0.00181i	-0.26132-0.00600i	0.96224+0.00449i

A.1.21 DFE, HT, $L = 7, N_T = 3, N_R = 2, \rho_t = [0.5, 0.5, 0.5]$,

$$\rho_r = [0.7]$$

$10 \log_{10}(E_b/N_0)$	Tx	$g_i[0]$	$g_i[1]$	$g_i[2]$
5	$i = 1$	-0.18139-0.06826i	0.55671+0.19758i	0.71808+0.31279i
	$i = 2$	-0.15954-0.04358i	0.57525+0.23273i	0.72520+0.24831i
	$i = 3$	-0.17035-0.08724i	0.55347+0.20652i	0.72902+0.28795i
7.5	$i = 1$	-0.03245+0.04722i	0.52247+0.32323i	0.61241+0.49418i
	$i = 2$	-0.44941-0.03879i	0.31895+0.36094i	0.62971+0.40985i
	$i = 3$	-0.07328-0.37803i	0.45937+0.19233i	0.63360+0.44973i
10	$i = 1$	0.21172+0.05055i	0.38404+0.11407i	0.80053+0.38894i
	$i = 2$	-0.38911+0.12181i	0.10392+0.25045i	0.79600+0.35584i
	$i = 3$	-0.24423-0.39886i	0.13585-0.11011i	0.76585+0.40516i

A.1.22 LE, HT, $L = 7, N_T = 3, N_R = 2, \rho_t = [0.5, 0.5, 0.5]$,

$$\rho_r = [0.7]$$

$10 \log_{10}(E_b/N_0)$	Tx	$g_i[0]$	$g_i[1]$	$g_i[2]$
5	$i = 1$	0.00370+0.00688i	-0.14947+0.02359i	0.97099-0.18496i
	$i = 2$	0.00055-0.00569i	-0.13047+0.03084i	0.97338-0.18580i
	$i = 3$	0.00704-0.00219i	-0.14291+0.02611i	0.97176-0.18580i
7.5	$i = 1$	0.17019-0.13767i	0.08738+0.96396i	0.09601-0.07758i
	$i = 2$	0.12896-0.08807i	0.10359+0.95615i	0.16747-0.15037i
	$i = 3$	0.12487-0.10205i	0.09338+0.96187i	0.16990-0.10585i
10	$i = 1$	0.04755+0.02787i	-0.26237+0.07367i	0.86635-0.41489i
	$i = 2$	0.07303-0.04608i	-0.08218+0.13423i	0.87808-0.44356i
	$i = 3$	0.01357-0.04741i	-0.22070+0.08006i	0.86050-0.44943i

A.1.23 DFE, TU, $L = 5, N_T = 3, N_R = 2, \rho_t = [0.5, 0.2, 0.5]$,

$$\rho_r = [0.7]$$

$10 \log_{10}(E_b/N_0)$	Tx	$g_i[0]$	$g_i[1]$	$g_i[2]$
7.5	$i = 1$	0.51407-0.64071i	0.16865+0.00539i	-0.02593+0.54414i
	$i = 2$	0.09847-0.35249i	-0.05767+0.27400i	-0.19989+0.86470i
	$i = 3$	-0.38296+0.07315i	-0.25797+0.36465i	-0.29111+0.75082i
10	$i = 1$	0.17036-0.47001i	0.26527-0.14546i	0.81149+0.00421i
	$i = 2$	-0.40610-0.09202i	0.14758+0.05268i	0.86370+0.23683i
	$i = 3$	-0.75652+0.34594i	-0.10397+0.17833i	0.42749+0.28747i
12.5	$i = 1$	0.13501-0.70466i	0.09940-0.25821i	0.61544+0.17294i
	$i = 2$	-0.27531-0.20073i	0.10123+0.18158i	0.72354+0.56318i
	$i = 3$	-0.56974+0.37882i	-0.06275+0.13787i	0.40215+0.58926i

A.1.24 LE, TU, $L = 5, N_T = 3, N_R = 2, \rho_t = [0.5, 0.2, 0.5]$,

$$\rho_r = [0.7]$$

$10 \log_{10}(E_b/N_0)$	Tx	$g_i[0]$	$g_i[1]$	$g_i[2]$
7.5	$i = 1$	0.36811-0.13581i	0.82641+0.24173i	-0.08705-0.31156i
	$i = 2$	0.16612+0.04909i	0.85057+0.33306i	-0.33818-0.14569i
	$i = 3$	-0.14912+0.19391i	0.66592+0.33485i	-0.62013+0.00507i
10	$i = 1$	0.27097-0.66299i	-0.13068+0.43108i	-0.04284+0.53130i
	$i = 2$	0.37652-0.83892i	-0.15969+0.35148i	0.02069-0.07053i
	$i = 3$	0.29993-0.69771i	-0.05778+0.13252i	0.10637-0.62533i
12.5	$i = 1$	0.65385-0.45705i	-0.14783+0.13047i	0.47703-0.31168i
	$i = 2$	0.15155-0.09325i	-0.29422+0.17940i	0.78727-0.47937i
	$i = 3$	-0.39497+0.28155i	-0.29692+0.22183i	0.64691-0.45702i

A.2 Filters for 8-PSK

A.2.1 DFE, EQ, $L = 7$, $N_T = 2$, $N_R = 1$, $\rho_t = [0.5]$

$10 \log_{10}(E_b/N_0)$	Tx	$g_i[0]$	$g_i[1]$	$g_i[2]$
10	$i = 1$	0.77307+0.12397i	0.57891+0.09718i	-0.20113-0.04429i
	$i = 2$	0.78021+0.13694i	0.56487+0.09781i	-0.20756-0.02805i
15	$i = 1$	-0.09967-0.00538i	0.21515+0.01119i	0.96923+0.06493i
	$i = 2$	-0.10562-0.00354i	0.23502+0.02224i	0.96343+0.07009i
20	$i = 1$	0.11964-0.00744i	0.18609+0.00153i	0.96992-0.10130i
	$i = 2$	-0.30671+0.07724i	-0.01180+0.01749i	0.94552-0.07429i

A.2.2 LE, EQ, $L = 7$, $N_T = 2$, $N_R = 1$, $\rho_t = [0.5]$

$10 \log_{10}(E_b/N_0)$	Tx	$g_i[0]$	$g_i[1]$	$g_i[2]$
10	$i = 1$	0.99127-0.08721i	-0.09677+0.00676i	-0.01936-0.00165i
	$i = 2$	0.99101-0.08424i	-0.10159+0.01174i	-0.01806+0.00333i
15	$i = 1$	0.21053+0.00561i	-0.47997-0.82343i	0.21734-0.00037i
	$i = 2$	0.22096+0.00091i	-0.46845-0.82852i	0.21278+0.00207i
20	$i = 1$	0.07514+0.03982i	-0.23317-0.10755i	0.88291+0.38380i
	$i = 2$	0.07467+0.02283i	-0.24275-0.09689i	0.87897+0.39114i

A.2.3 DFE, HT, $L = 7$, $N_T = 2$, $N_R = 1$, $\rho_t = [0.5]$

$10 \log_{10}(E_b/N_0)$	Tx	$g_i[0]$	$g_i[1]$	$g_i[2]$
10	$i = 1$	0.75875+0.05593i	0.63604+0.04753i	-0.11951-0.0089i
	$i = 2$	0.75519+0.05223i	0.64149+0.04140i	-0.11686-0.00944i
15	$i = 1$	0.81519-0.09895i	0.40567-0.13183i	-0.34955-0.14676i
	$i = 2$	0.80263-0.12213i	0.54729-0.00110i	-0.03242+0.20073i
20	$i = 1$	0.64057-0.58920i	-0.03681-0.28644i	-0.28053-0.28357i
	$i = 2$	0.69377-0.45026i	0.13703+0.20258i	-0.02245+0.50560i

A.2.4 LE, HT, $L = 7$, $N_T = 2$, $N_R = 1$, $\rho_t = [0.5]$

$10 \log_{10}(E_b/N_0)$	Tx	$g_i[0]$	$g_i[1]$	$g_i[2]$
10	$i = 1$	0.99539-0.07229i	-0.03823+0.00026i	-0.05003+0.00408i
	$i = 2$	0.99575-0.06771i	-0.03969+0.00456i	-0.04796+0.00307i
15	$i = 1$	-0.04035-0.08208i	-0.63778+0.75666i	-0.03008-0.10691i
	$i = 2$	-0.00603-0.10935i	-0.59718+0.78890i	-0.00347-0.09495i
20	$i = 1$	0.28542-0.06199i	-0.59977-0.68502i	0.29276+0.00244i
	$i = 2$	0.26139-0.02829i	-0.59290-0.70928i	0.26506-0.07748i

A.2.5 DFE, TU, $L = 5$, $N_T = 2$, $N_R = 1$, $\rho_t = [0.7]$

$10 \log_{10}(E_b/N_0)$	Tx	$g_i[0]$	$g_i[1]$	$g_i[2]$
10	$i = 1$	-0.15337+0.00539i	0.61899-0.02253i	0.76946-0.02692i
	$i = 2$	-0.13894+0.00081i	0.62560-0.01139i	0.76743-0.01550i
15	$i = 1$	-0.06814+0.29184i	0.40449+0.20080i	0.81635+0.19956i
	$i = 2$	-0.43424-0.41026i	0.20380-0.08765i	0.76019+0.12656i
20	$i = 1$	0.14704+0.28166i	0.24739+0.06094i	0.90522-0.12128i
	$i = 2$	-0.69983-0.18671i	-0.18906-0.11101i	0.62266-0.19898i

A.2.6 LE, TU, $L = 5$, $N_T = 2$, $N_R = 1$, $\rho_t = [0.7]$

$10 \log_{10}(E_b/N_0)$	Tx	$g_i[0]$	$g_i[1]$	$g_i[2]$
10	$i = 1$	-0.05875+0.00496i	-0.01919+0.00076i	0.99716-0.04281i
	$i = 2$	-0.05438+0.00154i	-0.01883-0.00102i	0.99700-0.05178i
15	$i = 1$	-0.00025-0.01333i	-0.09612+0.01798i	0.98379-0.14975i
	$i = 2$	-0.00359+0.01525i	-0.10046+0.00409i	0.98507-0.13883i
20	$i = 1$	-0.27960+0.20792i	-0.07632+0.28261i	0.03602-0.88972i
	$i = 2$	0.30032-0.31258i	0.054411+0.16027i	0.07548-0.88191i

A.2.7 DFE, EQ, $L = 7, N_T = 2, N_R = 2, \rho_t = [0.5], \rho_r = [0.7]$

$10 \log_{10}(E_b/N_0)$	Tx	$g_i[0]$	$g_i[1]$	$g_i[2]$
5	$i = 1$	-0.13228+0.09978i	0.50446-0.33889i	0.64513-0.43246i
	$i = 2$	-0.15324+0.09152i	0.49823-0.34310i	0.64376-0.43333i
7.5	$i = 1$	-0.16983+0.12964i	0.47578-0.32329i	0.65298-0.44393i
	$i = 2$	-0.19122+0.11773i	0.46686-0.32852i	0.65291-0.44430i
10	$i = 1$	-0.14288+0.19545i	0.48178-0.63251i	0.34074-0.43943i
	$i = 2$	-0.15245+0.19354i	0.47894-0.63011i	0.33591-0.44726i

A.2.8 LE, EQ, $L = 7, N_T = 2, N_R = 2, \rho_t = [0.5], \rho_r = [0.7]$

$10 \log_{10}(E_b/N_0)$	Tx	$g_i[0]$	$g_i[1]$	$g_i[2]$
5	$i = 1$	0.13228+0.23208i	-0.41366-0.83953i	-0.09813-0.20755i
	$i = 2$	0.10961+0.25710i	-0.41160-0.84130i	-0.09359-0.18955i
7.5	$i = 1$	0.08253+0.10897i	-0.56487-0.81374i	0.00577+0.00590i
	$i = 2$	0.07335+0.11903i	-0.55963-0.81679i	0.00285+0.01058i
10	$i = 1$	0.21458-0.00291i	-0.50618-0.80927i	0.20691+0.00194i
	$i = 2$	0.19977+0.00813i	-0.50008-0.81721i	0.20509+0.00741i

A.2.9 DFE, HT, $L = 7, N_T = 2, N_R = 2, \rho_t = [0.5], \rho_r = [0.7]$

$10 \log_{10}(E_b/N_0)$	Tx	$g_i[0]$	$g_i[1]$	$g_i[2]$
7.5	$i = 1$	-0.14443-0.02017i	0.60840+0.13182i	0.75406+0.15031i
	$i = 2$	-0.13579-0.03421i	0.61694+0.11327i	0.75172+0.14786i
10	$i = 1$	0.01059+0.10282i	-0.49808+0.84440i	0.16767+0.00975i
	$i = 2$	-0.05536-0.18889i	-0.52766+0.67873i	0.05457-0.46817i
12.5	$i = 1$	0.11270+0.15151i	0.43013+0.29455i	0.73224+0.39547i
	$i = 2$	-0.48927-0.39234i	0.14103+0.00762i	0.67821+0.35603i

A.2.10 LE, HT, $L = 7, N_T = 2, N_R = 2, \rho_t = [0.5], \rho_r = [0.7]$

$10 \log_{10}(E_b/N_0)$	Tx	$g_i[0]$	$g_i[1]$	$g_i[2]$
7.5	$i = 1$	-0.02930-0.00380i	-0.09165-0.01035i	0.98352+0.15267i
	$i = 2$	-0.03216-0.00614i	-0.08790-0.01762i	0.98349+0.15372i
10	$i = 1$	0.05977-0.04460i	-0.39632+0.91044i	0.05686-0.07239i
	$i = 2$	0.03777-0.05610i	-0.41048+0.90612i	0.05318-0.05522i
12.5	$i = 1$	0.51814+0.05356i	-0.45558+0.69859i	0.16604+0.07418i
	$i = 2$	0.16422+0.08400i	-0.45670+0.71140i	0.49407+0.08489i

A.2.11 DFE, TU, $L = 5, N_T = 2, N_R = 2, \rho_t = [0.7],$

$$\rho_r = [0.7]$$

$10 \log_{10}(E_b/N_0)$	Tx	$g_i[0]$	$g_i[1]$	$g_i[2]$
10	$i = 1$	0.76507+0.18314i	0.56595+0.12647i	-0.20289-0.06060i
	$i = 2$	0.76139+0.19114i	0.56844+0.15248i	-0.19033-0.03390i
12.5	$i = 1$	0.52613-0.60181i	0.33748-0.42785i	-0.19634+0.15974i
	$i = 2$	0.53733-0.58138i	0.40986-0.39454i	-0.11538+0.19055i
15	$i = 1$	-0.05937-0.3007i	0.27731-0.15674i	0.88224-0.16196i
	$i = 2$	-0.33861+0.34410i	0.18392+0.08958i	0.85099-0.03017i

A.2.12 LE, TU, $L = 5, N_T = 2, N_R = 2, \rho_t = [0.7], \rho_r =$

$$[0.7]$$

$10 \log_{10}(E_b/N_0)$	Tx	$g_i[0]$	$g_i[1]$	$g_i[2]$
10	$i = 1$	0.94954+0.27921i	-0.13587-0.04430i	0.00160+0.00011i
	$i = 2$	0.94824+0.28757i	-0.13067-0.03164i	0.00760+0.00354i
12.5	$i = 1$	0.96856+0.16783i	-0.17778-0.03783i	0.02558+0.00500i
	$i = 2$	0.96651+0.18539i	-0.17268-0.02361i	0.03259+0.00725i
15	$i = 1$	0.97927-0.02942i	-0.19543+0.00274i	0.04440+0.00105i
	$i = 2$	0.97535-0.01354i	-0.21483+0.00882i	0.04772-0.00219i

A.2.13 DFE, EQ, $L = 7, N_T = 3, N_R = 1, \rho_t = [0.5, 0.5, 0.5]$

$10 \log_{10}(E_b/N_0)$	Tx	$g_i[0]$	$g_i[1]$	$g_i[2]$
10	$i = 1$	-0.23518+0.01855i	0.70488-0.06084i	0.66406-0.05300i
	$i = 2$	-0.23829+0.02169i	0.70444-0.05708i	0.66345-0.05555i
	$i = 3$	-0.23440+0.02107i	0.70405-0.06098i	0.66457-0.05961i
15	$i = 1$	-0.16852+0.10660i	0.73745-0.50949i	0.33545-0.21049i
	$i = 2$	-0.19469+0.11813i	0.73265-0.49401i	0.34197-0.22446i
	$i = 3$	-0.15215+0.13356i	0.73227-0.52249i	0.30517-0.23805i
20	$i = 1$	-0.24368+0.00730i	0.72977-0.56783i	0.28725-0.05534i
	$i = 2$	-0.25426+0.05202i	0.70395-0.52642i	0.32290-0.23603i
	$i = 3$	0.02353+0.30396i	0.65121-0.61533i	0.09297-0.30937i

A.2.14 LE, EQ, $L = 7, N_T = 3, N_R = 1, \rho_t = [0.5, 0.5, 0.5]$

$10 \log_{10}(E_b/N_0)$	Tx	$g_i[0]$	$g_i[1]$	$g_i[2]$
10	$i = 1$	0.99133-0.02959i	-0.12781+0.00155i	0.00545+0.00402i
	$i = 2$	0.99042-0.02721i	-0.13519+0.00608i	0.00027-0.00430i
	$i = 3$	0.99069-0.03586i	-0.13124+0.00424i	0.00083+0.00085i
15	$i = 1$	0.97491+0.02556i	-0.21329-0.01178i	0.05685+0.00639i
	$i = 2$	0.97303+0.03013i	-0.22171+0.00285i	0.05528-0.00950i
	$i = 3$	0.97363+0.01117i	-0.21973-0.00574i	0.05955+0.00718i
20	$i = 1$	0.04311+0.05075i	-0.23088-0.16349i	0.80090+0.52354i
	$i = 2$	0.03345+0.00051i	-0.30530-0.16776i	0.78051+0.51801i
	$i = 3$	0.14186+0.09607i	-0.14755-0.12429i	0.82173+0.50813i

A.2.15 DFE, HT, $L = 7, N_T = 3, N_R = 1, \rho_t = [0.2, 0.5, 0.2]$

$10 \log_{10}(E_b/N_0)$	Tx	$g_i[0]$	$g_i[1]$	$g_i[2]$
10	$i = 1$	0.64442-0.31570i	0.57160-0.36763i	0.04423-0.14568i
	$i = 2$	0.48989-0.34235i	0.01163+0.15438i	-0.52776+0.58336i
	$i = 3$	0.63790-0.35444i	0.57163-0.36393i	0.03542-0.08361i
15	$i = 1$	-0.42434-0.29951i	-0.07818+0.09268i	0.64297+0.54966i
	$i = 2$	0.61840+0.04696i	0.56302+0.15275i	0.45455+0.26163i
	$i = 3$	-0.50253-0.27729i	0.16244+0.13198i	0.56124+0.55837i
20	$i = 1$	-0.17177-0.54650i	0.33685+0.19246i	0.70395+0.16056i
	$i = 2$	0.01659+0.73367i	0.20285+0.26403i	0.51450+0.29304i
	$i = 3$	-0.22102-0.27016i	-0.26244-0.37736i	0.74948+0.32431i

A.2.16 LE, HT, $L = 7, N_T = 3, N_R = 1, \rho_t = [0.2, 0.5, 0.2]$

$10 \log_{10}(E_b/N_0)$	Tx	$g_i[0]$	$g_i[1]$	$g_i[2]$
10	$i = 1$	-0.19980+0.00191i	-0.24956-0.01608i	0.93194+0.17035i
	$i = 2$	0.28912-0.02927i	0.23860+0.01404i	0.91106+0.16853i
	$i = 3$	-0.18967+0.00097i	-0.24265-0.02056i	0.93830+0.15592i
15	$i = 1$	0.78604+0.15619i	-0.57050+0.02639i	-0.08672+0.15509i
	$i = 2$	0.37433-0.34267i	-0.42391-0.43766i	-0.07604-0.60450i
	$i = 3$	0.77873+0.15857i	-0.58023+0.05607i	-0.10110+0.13565i
20	$i = 1$	0.45928-0.20142i	-0.83664+0.13278i	0.09743+0.14631i
	$i = 2$	0.91225-0.27274i	0.26467+0.03874i	0.14702+0.01563i
	$i = 3$	0.51371-0.19236i	-0.78103+0.12652i	0.01306-0.27002i

A.2.17 DFE, TU, $L = 5$, $N_T = 3$, $N_R = 1$, $\rho_t = [0.7, 0.5, 0.7]$

$10 \log_{10}(E_b/N_0)$	Tx	$g_i[0]$	$g_i[1]$	$g_i[2]$
10	$i = 1$	0.48839+0.61000i	0.37969+0.44818i	-0.14194-0.15557i
	$i = 2$	0.50972+0.60487i	0.39644+0.43526i	-0.08510-0.14304i
	$i = 3$	0.48991+0.58541i	0.36640+0.51695i	-0.09290-0.08457i
15	$i = 1$	0.24413-0.57565i	0.31920-0.08739i	0.48996+0.50936i
	$i = 2$	-0.11639-0.27560i	0.077810+0.24238i	0.47499+0.78745i
	$i = 3$	-0.55752+0.03484i	-0.10728+0.21485i	0.22881+0.76022i
20	$i = 1$	0.29537-0.07458i	0.17315-0.11670i	0.92346-0.10396i
	$i = 2$	-0.36629+0.02504i	0.03099+0.06879i	0.92449-0.06949i
	$i = 3$	-0.83773+0.03746i	-0.33215-0.01507i	0.43067-0.02777i

A.2.18 LE, TU, $L = 5$, $N_T = 3$, $N_R = 1$, $\rho_t = [0.7, 0.5, 0.7]$

$10 \log_{10}(E_b/N_0)$	Tx	$g_i[0]$	$g_i[1]$	$g_i[2]$
10	$i = 1$	0.11198+0.14658i	0.61493+0.73294i	-0.15052-0.16727i
	$i = 2$	0.12386+0.14094i	0.62632+0.71835i	-0.15095-0.18358i
	$i = 3$	0.12044+0.13066i	0.62266+0.72936i	-0.14418-0.16721i
15	$i = 1$	-0.01608-0.13367i	-0.03668+0.98881i	0.00690-0.05229i
	$i = 2$	0.06816-0.08365i	-0.01635+0.98532i	0.12817-0.02828i
	$i = 3$	0.14720-0.13250i	-0.05042+0.97674i	0.03691+0.05332i
20	$i = 1$	0.62912-0.06913i	-0.11445+0.12288i	0.66212-0.36447i
	$i = 2$	0.06738-0.03834i	-0.23381+0.15257i	0.81818-0.49661i
	$i = 3$	-0.48364+0.03519i	-0.30093+0.13016i	0.68239-0.43783i

A.2.19 DFE, EQ, $L = 7, N_T = 3, N_R = 2, \rho_t = [0.5, 0.7, 0.5]$,

$$\rho_r = [0.7]$$

$10 \log_{10}(E_b/N_0)$	Tx	$g_i[0]$	$g_i[1]$	$g_i[2]$
5	$i = 1$	-0.06041+0.00059i	0.11577+0.00085i	0.99142+0.00588i
	$i = 2$	-0.06627-0.00088i	0.10956+0.00082i	0.99175+0.00641i
	$i = 3$	-0.06473-0.00011i	0.11350-0.00147i	0.99142+0.00184i
7.5	$i = 1$	0.06153+0.00029i	0.06647-0.00262i	0.99579+0.01406i
	$i = 2$	-0.08841+0.00194i	0.18056+0.00075i	0.97952+0.01110i
	$i = 3$	-0.04205+0.00042i	0.09331-0.00137i	0.99470+0.00983i
10	$i = 1$	0.01288+0.00187i	0.04592-0.00349i	0.99885+0.00019i
	$i = 2$	-0.05947-0.00141i	0.08640+0.00613i	0.99446+0.00043i
	$i = 3$	-0.02954+0.00119i	0.05766-0.00481i	0.99788-0.00288i

A.2.20 LE, EQ, $L = 7, N_T = 3, N_R = 2, \rho_t = [0.5, 0.7, 0.5]$,

$$\rho_r = [0.7]$$

$10 \log_{10}(E_b/N_0)$	Tx	$g_i[0]$	$g_i[1]$	$g_i[2]$
7.5	$i = 1$	0.13800+0.00575i	-0.31196-0.00297i	0.93999+0.00492i
	$i = 2$	0.14483-0.00229i	-0.33265+0.00377i	0.93173+0.01498i
	$i = 3$	0.13577+0.00527i	-0.32250-0.00376i	0.93672+0.00848i
10	$i = 1$	0.15181+0.01950i	-0.32291-0.02298i	0.93194+0.05707i
	$i = 2$	0.16659+0.00120i	-0.36423-0.01653i	0.91264+0.07999i
	$i = 3$	0.15271+0.01635i	-0.34491-0.02608i	0.92282+0.07193i
15	$i = 1$	0.18068+0.09159i	-0.29846-0.14428i	0.84432+0.36904i
	$i = 2$	0.17588+0.06350i	-0.46342-0.20018i	0.74761+0.38895i
	$i = 3$	0.21857+0.06145i	-0.30859-0.12590i	0.84604+0.34869i

**A.2.21 DFE, HT, $L = 7, N_T = 3, N_R = 2, \rho_t = [0.5, 0.5, 0.5],$
 $\rho_r = [0.7]$**

$10 \log_{10}(E_b/N_0)$	Tx	$g_i[0]$	$g_i[1]$	$g_i[2]$
5	$i = 1$	-0.10591-0.19576i	0.45035+0.77557i	0.18136+0.33651i
	$i = 2$	-0.10827-0.18542i	0.45340+0.78114i	0.19076+0.31897i
	$i = 3$	-0.10831-0.18642i	0.43811+0.78846i	0.18226+0.32662i
7.5	$i = 1$	-0.05584-0.19301i	0.32648+0.86795i	0.08943+0.30283i
	$i = 2$	-0.06687-0.16941i	0.32626+0.87966i	0.11839+0.26938i
	$i = 3$	-0.06244-0.17681i	0.31063+0.87979i	0.11131+0.28622i
10	$i = 1$	0.00513-0.15517i	0.25205+0.92945i	0.01216+0.21988i
	$i = 2$	-0.03731-0.09155i	0.25585+0.94269i	0.10971+0.15510i
	$i = 3$	0.00563-0.14488i	0.24046+0.92812i	0.10349+0.22146i

**A.2.22 LE, HT, $L = 7, N_T = 3, N_R = 2, \rho_t = [0.5, 0.5, 0.5],$
 $\rho_r = [0.7]$**

$10 \log_{10}(E_b/N_0)$	Tx	$g_i[0]$	$g_i[1]$	$g_i[2]$
5	$i = 1$	0.30551-0.09195i	-0.19609+0.86961i	0.30801-0.09307i
	$i = 2$	0.30019-0.15743i	-0.13390+0.88076i	0.28360-0.10486i
	$i = 3$	0.26786-0.10913i	-0.22409+0.87162i	0.30176-0.12389i
7.5	$i = 1$	0.32184-0.13966i	-0.13934+0.86741i	0.30493-0.11010i
	$i = 2$	0.30271-0.15565i	-0.10355+0.87384i	0.30460-0.13052i
	$i = 3$	0.26604-0.13865i	-0.15086+0.87578i	0.30525-0.16454i
10	$i = 1$	0.10710+0.09070i	-0.32145-0.07039i	0.93130+0.06855i
	$i = 2$	0.12956-0.01504i	-0.31410-0.00437i	0.93656+0.08461i
	$i = 3$	0.14344-0.05759i	-0.29128+0.02151i	0.93768+0.10752i

**A.2.23 DFE, TU, $L = 5, N_T = 3, N_R = 2, \rho_t = [0.5, 0.2, 0.5],$
 $\rho_r = [0.7]$**

$10 \log_{10}(E_b/N_0)$	Tx	$g_i[0]$	$g_i[1]$	$g_i[2]$
5	$i = 1$	-0.56894+0.54187i	-0.40502+0.27031i	0.16618-0.34345i
	$i = 2$	-0.56550+0.52031i	-0.45105+0.43756i	0.09856-0.06974i
	$i = 3$	-0.51810+0.44690i	-0.45879+0.53568i	-0.01133+0.18516i
7.5	$i = 1$	-0.65839-0.23858i	-0.44073-0.36952i	0.04167-0.42080i
	$i = 2$	-0.79409-0.26637i	-0.47999-0.10771i	0.21643+0.09820i
	$i = 3$	-0.67084-0.25497i	-0.33134+0.07972i	0.27294+0.54252i
10	$i = 1$	-0.77118+0.21661i	-0.47601+0.04700i	-0.34858-0.08972i
	$i = 2$	-0.82370+0.31966i	-0.26854+0.13049i	0.33609-0.13127i
	$i = 3$	-0.52721+0.19898i	0.03183+0.09013i	0.81957-0.04046i

**A.2.24 LE, TU, $L = 5, N_T = 3, N_R = 2, \rho_t = [0.5, 0.2, 0.5],$
 $\rho_r = [0.7]$**

$10 \log_{10}(E_b/N_0)$	Tx	$g_i[0]$	$g_i[1]$	$g_i[2]$
5	$i = 1$	-0.16497-0.20804i	0.609578+0.70131i	0.15653+0.20390i
	$i = 2$	-0.18409-0.22086i	0.59959+0.70341i	0.17110+0.18372i
	$i = 3$	-0.18720-0.19415i	0.59660+0.71026i	0.17646+0.18900i
7.5	$i = 1$	-0.05932-0.19817i	0.35960+0.90248i	0.00121+0.11588i
	$i = 2$	-0.07152-0.20849i	0.35481+0.90172i	0.04587+0.10163i
	$i = 3$	-0.09765-0.17547i	0.34292+0.90832i	0.08177+0.10174i
10	$i = 1$	0.04027-0.08809i	-0.89588+0.17185i	0.21508-0.33501i
	$i = 2$	-0.00621+0.00145i	-0.93839+0.28601i	0.19028-0.03709i
	$i = 3$	-0.07676+0.09515i	-0.90637+0.32579i	0.12267+0.20582i